NASA/TM—2001-211089

Large-Scale Liquid Hydrogen Testing of a Variable Density Multilayer Insulation With a Foam Substrate

J.J. Martin and L. Hastings
Marshall Space Flight Center, Marshall Space Flight Center, Alabama

June 2001

The NASA STI Program Office...in Profile

Since its founding, NASA has been dedicated to the advancement of aeronautics and space science. The NASA Scientific and Technical Information (STI) Program Office plays a key part in helping NASA maintain this important role.

The NASA STI Program Office is operated by Langley Research Center, the lead center for NASA's scientific and technical information. The NASA STI Program Office provides access to the NASA STI Database, the largest collection of aeronautical and space science STI in the world. The Program Office is also NASA's institutional mechanism for disseminating the results of its research and development activities. These results are published by NASA in the NASA STI Report Series, which includes the following report types:

- TECHNICAL PUBLICATION. Reports of completed research or a major significant phase of research that present the results of NASA programs and include extensive data or theoretical analysis. Includes compilations of significant scientific and technical data and information deemed to be of continuing reference value. NASA's counterpart of peer-reviewed formal professional papers but has less stringent limitations on manuscript length and extent of graphic presentations.

- TECHNICAL MEMORANDUM. Scientific and technical findings that are preliminary or of specialized interest, e.g., quick release reports, working papers, and bibliographies that contain minimal annotation. Does not contain extensive analysis.

- CONTRACTOR REPORT. Scientific and technical findings by NASA-sponsored contractors and grantees.

- CONFERENCE PUBLICATION. Collected papers from scientific and technical conferences, symposia, seminars, or other meetings sponsored or cosponsored by NASA.

- SPECIAL PUBLICATION. Scientific, technical, or historical information from NASA programs, projects, and mission, often concerned with subjects having substantial public interest.

- TECHNICAL TRANSLATION. English-language translations of foreign scientific and technical material pertinent to NASA's mission.

Specialized services that complement the STI Program Office's diverse offerings include creating custom thesauri, building customized databases, organizing and publishing research results...even providing videos.

For more information about the NASA STI Program Office, see the following:

- Access the NASA STI Program Home Page at ***http://www.sti.nasa.gov***

- E-mail your question via the Internet to help@sti.nasa.gov

- Fax your question to the NASA Access Help Desk at (301) 621–0134

- Telephone the NASA Access Help Desk at (301) 621–0390

- Write to:
  NASA Access Help Desk
  NASA Center for AeroSpace Information
  7121 Standard Drive
  Hanover, MD 21076–1320

NASA/TM—2001-211089

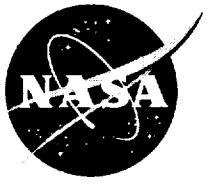

Large-Scale Liquid Hydrogen Testing of a Variable Density Multilayer Insulation With a Foam Substrate

J.J. Martin and L. Hastings
Marshall Space Flight Center, Marshall Space Flight Center, Alabama

National Aeronautics and
Space Administration

Marshall Space Flight Center • MSFC, Alabama 35812

June 2001

TRADEMARKS

Trade names and trademarks are used in this report for identification only. This usage does not constitute an official endorsement, either expressed or implied, by the National Aeronautics and Space Administration.

Available from:

NASA Center for AeroSpace Information
7121 Standard Drive
Hanover, MD 21076–1320
(301) 621–0390

National Technical Information Service
5285 Port Royal Road
Springfield, VA 22161
(703) 487–4650

TABLE OF CONTENTS

LIST OF FIGURES

LIST OF FIGURES (Continued)

LIST OF TABLES

LIST OF ACRONYMS AND SYMBOLS

ASME	American Society of Mechanical Engineers
CFM	cryogenic fluid management
CO_2	carbon dioxide
DAM	double-aluminized Mylar
FLUINT	fluid integrator
FMLI	foam multilayer insulation
GHe	gaseous helium
GN_2	gaseous nitrogen
GH_2	gaseous hydrogen
He	helium
H_2O	water
IMLEO	injected mass into low-Earth orbit
LH_2	liquid hydrogen
LN_2	liquid nitrogen
MGA	missle grade air
MHTB	multipurpose hydrogen test bed
MKS	MKS Instrument, Inc.
MLI	multilayer insulation
MSFC	Marshall Space Flight Center
N_2	nitrogen
NLS	National Launch System
O_2	oxygen
RGA	residual gas analyzer
SCIM	standard cubic inches per minute

LIST OF ACRONYMS AND SYMBOLS (Continued)

SINDA	systems improved numerical differencing analyzer
SLPM	standard liters per minute
SOFI	spray-on foam insulation
STS	Space Transportation System
TC	Titan Centaur
TCS	thermal control subsystem
TH	total hemispherical
TVS	thermodynamic vent subsystem
zero-g	zero gravity

NOMENCLATURE

A	area
h_{fg}	heat of vaporization
h	enthalpy
κ	effective conductivity
L	length
$\dot{m}$	mass flow rate
M	mass
M_{insul}	insulation mass
N	number of MLI shields
$\overline{N}$	average MLI layer density
P	MLI interstitial pressure
$\dot{Q}$	heat leak rate
q	heat leak per unit area
T	temperature
t	time
U	internal energy
ε_{TH}	total hemispherical emissivity
K	thermal conductivity
ρ	density
Δ	delta

Multipurpose hydrogen test bed.

TECHNICAL MEMORANDUM

LARGE-SCALE LIQUID HYDROGEN TESTING OF VARIABLE DENSITY MULTILAYER INSULATION WITH A FOAM SUBSTRATE

1. INTRODUCTION

1.1 Background

The development of high-energy cryogenic upper stages is essential for the efficient delivery of payloads to various destinations envisioned in future programs. A key element in such upper stages is cryogenic fluid management (CFM) advanced development/technology. Due to the cost of, and limited opportunities for, orbital experiments, ground testing must be employed to the fullest extent possible. Therefore, a system-level test bed termed the multipurpose hydrogen test bed (MHTB), which is representative in size and shape of a fully integrated space transportation vehicle liquid hydrogen (LH_2) propellant tank, was established for use at Marshall Space Flight Center (MSFC). The MHTB 18-m^3 (639-ft^3) hydrogen tank, fabricated by Martin-Marietta Corporation, Denver, CO, (now Lockheed Martin) under contract NAS8–3920, was designed to accommodate various CFM concepts as updated or alternate versions become available. The first element evaluated with the MHTB was a cryogenic thermal protection concept for ground-based upper stage. Although upper stage studies have often baselined the foam multilayer insulation (FMLI) arrangements, virtually no large-scale hardware experience with the concept existed; therefore, it was selected for MHTB testing. Multilayer insulation (MLI) technology was investigated extensively in the 1965–1973 timeframe; however, several innovative MLI features proposed by Glenn McIntosh of Cryogenic Technical Services warranted experimental verification and therefore were selected for incorporation into the MHTB program. The MLI selection and design process is documented in reference 1.

1.2 Requirements

The MHTB thermal control subsystem (TCS) baseline includes a spray-on foam insulation (SOFI) directly bonded to the tank utilizing proven materials and processes developed for the Space Shuttle external tank program. The foam was required to satisfy the requirement of retaining a fully loaded tank of LH_2 for 3 hr prior to launch. Additionally, the foam surface temperature must remain at or above –156 °C (–249°F) to preclude liquefaction of the nitrogen (N_2) purge, which has a dew point of –54 °C (–65 °F). The Saturn V acoustic environment (for vibration loads) and the Space Shuttle ascent acceleration and altitude history were assumed for ascent conditions. On-orbit conditions included an average multilayer external insulation surface temperature of 300 °C (540 °F) and an on-orbit hold time of 45 days. Prototype references and further definition of the TCS design requirements are listed in table1.

Table 1. MHTB TCS design application requirements.

MHTB Requirements	Prototype Reference
Ground hold conditions • Hold fully loaded tank for 3 hr • GN_2 purge with –54 °C dew point • Final topoff to 98% 2 min prior to liftoff • Maintain SOFI surface temp at or above –156 °C **Ascent flight conditions for design** • 3.5×10^{-6} torr 420 sec after liftoff • Vibration loads: Saturn V acoustic environment • Acceleration history Time (sec) / Acceleration (g's) 0 / 1.26 100 / 2.20 195 / 4.50 196 / 1.0 400 / 2.0 460 / 2.8 **Orbital conditions** • Average MLI external surface temperature = 300 K • Orbit hold time = 45 days	**Ground hold conditions** • External tank – Fully loaded 5 hr, 20 min before launch – Final topoff 2.5 min before liftoff – GN_2 purge dew point = –54 °C • Centaur – Fully loaded 25 to 85 min before liftoff – Final topoff 1.5 min prior to launch, 99.8% full **Ascent flight conditions** • Utilize Space Shuttle conditions **Orbital conditions: translunar injection stage** • Dual launch, 45-day mission • Maximum average surface temperature = 300 K • Minimum average surface temperature = 111 K

1.3 Objectives

The overall objective was to experimentally evaluate the SOFI/MLI combination concept concurrently with several unique MLI installation and design features. The mission phases to be simulated included ground hold, ascent flight, and orbital storage. Design and test goals included verification of the following:

- A SOFI could provide thermal protection during the ground hold phase and simultaneously enable a dry gaseous nitrogen (GN_2) surface purge on the MLI, in lieu of a helium (He) purge under the MLI.
- A roll-wrap MLI installation technique, previously used in commercial applications, could be implemented to reduce both man-hours and heat leak on a tank size representative of a cryogenic upper stage.
- A variable-density MLI with larger, more widely spaced vent holes would substantially improve thermal performance.
- A 45-day orbit hold period can be accommodated by a representative upper stage LH_2 tank with a passive thermal control subsystem.

2. TEST ARTICLE ELEMENTS

The major test article elements consist of the test tank with supporting equipment (including an environmental shroud), cryogenic insulation subsystem, and test article instrumentation. Technical descriptions of each of these elements are presented in sections 2.1 through 2.4.

2.1 Test Tank and Supporting Equipment

The MHTB 5083 aluminum tank is cylindrical in shape with a height of 3.05 m (10 ft), a diameter of 3.05 m (10 ft), and 2:1 elliptical domes as shown in figure 1. It has an internal volume of 18.09 m^3 (639 ft^3) and a surface area of 35.74 m^2 (379 ft^2), with a resultant surface area-to-volume ratio of 1.92 1/m (0.58 1/ft) that is reasonably representative of a full-scale vehicle LH_2 tank. The tank is ASME pressure vessel coded (section VIII, division 1) for a maximum operational pressure of 344 kPa (50 psid) and unlimited cycle life. The average wall thickness is 1.27 cm (0.5 in.), resulting in an overall weight of 1,270 kg (2,800 lbm). The tank was designed to accommodate various CFM technology and advanced concepts as updated versions become available. Major accommodations include a 60.9-cm- (24-in.-) diameter manhole; 2.54-cm- (1-in.-) diameter pressurization and 5.08-cm- (2-in.-) diameter vent port; 2.54-cm- (1-in.-) fill/drain line (through tank top); 15.24- and 7.5-cm (6- and 3-in.) general purpose penetrations with flanges on top; the zero gravity (zero-g) pressure control subsystem (thermodynamic vent subsystem (TVS)) penetration provisions on the tank bottom (one 5.08-, one 3.81-, and one 1.27-cm tube) and an enclosure external to the tank; a 7.62-cm- (3-in.-) diameter drain at the tank bottom for future growth; a continuous liquid level capacitance probe; two vertical temperature rakes; wall temperature measurements at selected locations; ullage pressure sensors; pressure control/relief safety provisions; internal mounting brackets for future equipment and structural "hard points" for temporary scaffolding and ladder; and low heat leak composite structural supports. Each of the penetrations is equipped with an LH_2 heat guard to intercept heat leak, thereby enabling more accurate measurement of the tank insulation performance. The heat guards consist of two independent cooling loops, one for all the stainless steel penetrations on top of the tank and the other for the composite support legs at the tank bottom. Although the TVS interface provisions are shown in figure 1, those elements were the subject of activities subsequent to the insulation testing described in this Technical Memorandum.

All tank fluid penetrations employ aluminum to stainless steel transition joints to ease the burden of integrating the test article with the facility. Fluid connections are welded wherever possible and all mechanical seals are the knife-edge/copper gasket (Conflat®) design. The exception is the primary manhole cover design (fig. 2), which incorporates a soft crushable indium wire as a seal material and Invar® expansion collars on the stainless steel bolts to offset thermal expansion effects. The secondary manhole cover is equipped with a pump-out port so that any primary seal leakage can be intercepted and routed to a facility vacuum pump. Appendix A contains an MHTB tanking table with information regarding fill height, percent liquid/ullage volume, and LH_2 mass.

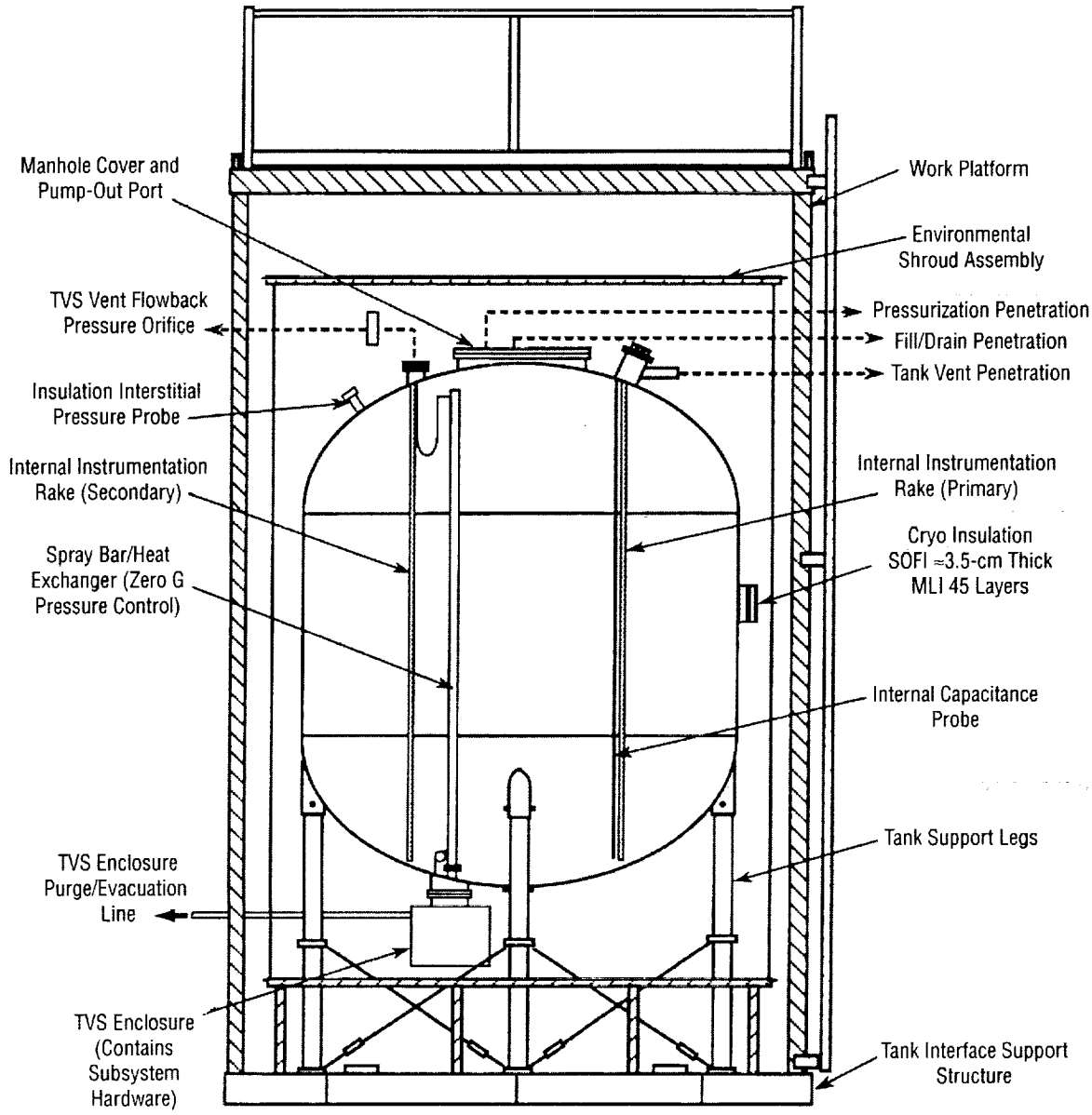

Figure 1. MHTB test tank and supporting hardware schematic.

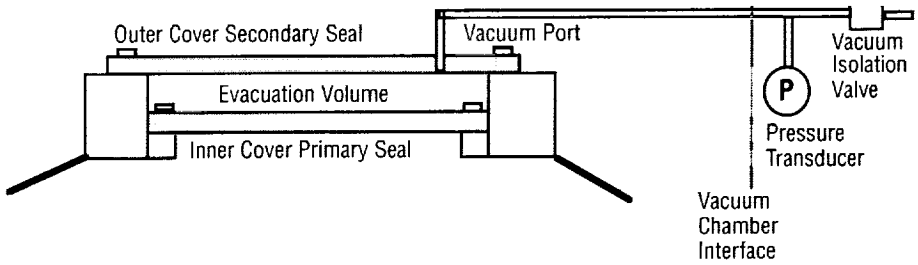

Figure 2. Manhole cover sealing arrangement.

2.2 Environmental Shroud

To both contain the ground hold GN_2 conditioning purge—similar to that in a payload bay—and impose a range of uniform temperatures on the MLI external surfaces, an environmental shroud that totally encloses the test article was used. The shroud (fig. 3) is fabricated from a 1-mm- (0.04-in.-) thick aluminum sheet, is 4.57 m (15 ft) high by 3.56 m (12 ft) in diameter, and contains a purge ring for distributing dry N_2. The shroud heater strips/cooling loops can impose either constant or time-dependent boundary temperatures ranging from 80 K (144 °R) to 320 K (576 °R).

2.3 Cryogenic Insulation Subsystem

The MHTB insulation concept consists of a foam/multilayer combination. The foam element enables the use of a payload bay-type GN_2 purge as opposed to the complex He purge bag subsystem normally required with MLI on cryogenic tankage during ground hold periods. That is, the foam ensures surface temperatures adjacent to the MLI inner layer at or above 117 K to preclude GN_2 liquefaction. Additionally, the foam reduces the heat leak during the ground hold and ascent flight periods. SOFI (Isofoam SS–1171) was applied directly to the tank surface with a robotic process at a thickness of 3.18 ± 0.63 cm (1.25 ± 0.5 in.) which was the minimum that could be applied with available equipment and procedures. An average thickness of 3.53 cm (1.4 in.) was calculated based on measurements with a Kaman eddy current device. In an actual application, only 1.4 cm (0.56 in.) of foam would be required to avoid N_2 liquefaction.

A 45-layer MLI blanket, placed over the SOFI, provides thermal protection while at vacuum or orbital conditions. The blanket is composed of ½-mil double-aluminized Mylar® (DAM) radiation shielding and separated by a combination of B4A Dacron® netting and B2A bumper strips (although ¼-mil Mylar would be used in an actual application, it could not be obtained for this test without incurring a substantial cost increase for the MLI material). Unique, innovative features of the MLI concept include utilization of a variable density (layers-per-unit thickness) concept for the radiation shields to provide a more weight-efficient insulation system and the use of fewer but larger perforations for venting during ascent to orbit. As illustrated in figure 4, the variable density was accomplished using bumper strips of variable thickness to provide more layers in warmer regions (16 layers/cm on outside segment) and fewer layers in the colder region where radiation blockage is less important (8 layers/cm). The layup resulted in an estimated average layer density of 12 layers/cm (30 layers/in.). The variable density provides a maximum theoretical heat leak reduction of 50 percent compared with uniform density MLI. The vent hole perforation pattern, which provides a 2-percent open area, is unusual in that the perforation size is large, 1.27-cm- (0.5-in.-) diameter, and the holes are more widely spaced (7.6 cm (3 in.). Standard perforations are 0.16- to 0.08-cm diameter with ≈0.95-cm (0.375-in.) spacing and 2–4 percent open area. The larger holes reduce the radiation view factor—hence, the radiation exchange—between layers, thereby enabling a maximum theoretical heat leak reduction of 35 percent. Additionally, the virtually seamless insulation enabled by the MLI roll-wrap installation technique further reduces heat leak. However, the lack of seams, together with the vent hole arrangement, can decrease the vent-down rate during ascent flight and orbital injection.

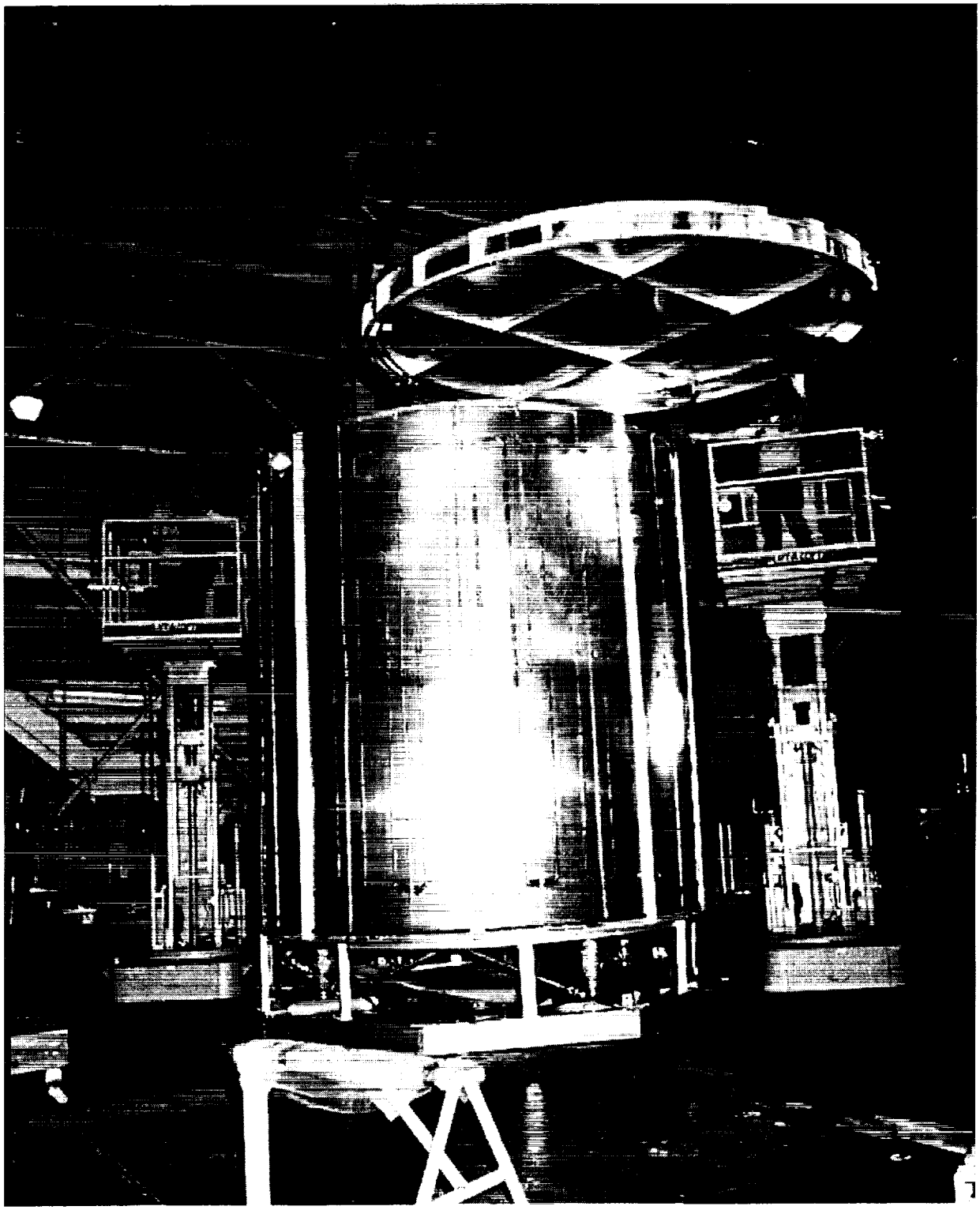

Figure 3. Environmental shroud assembly.

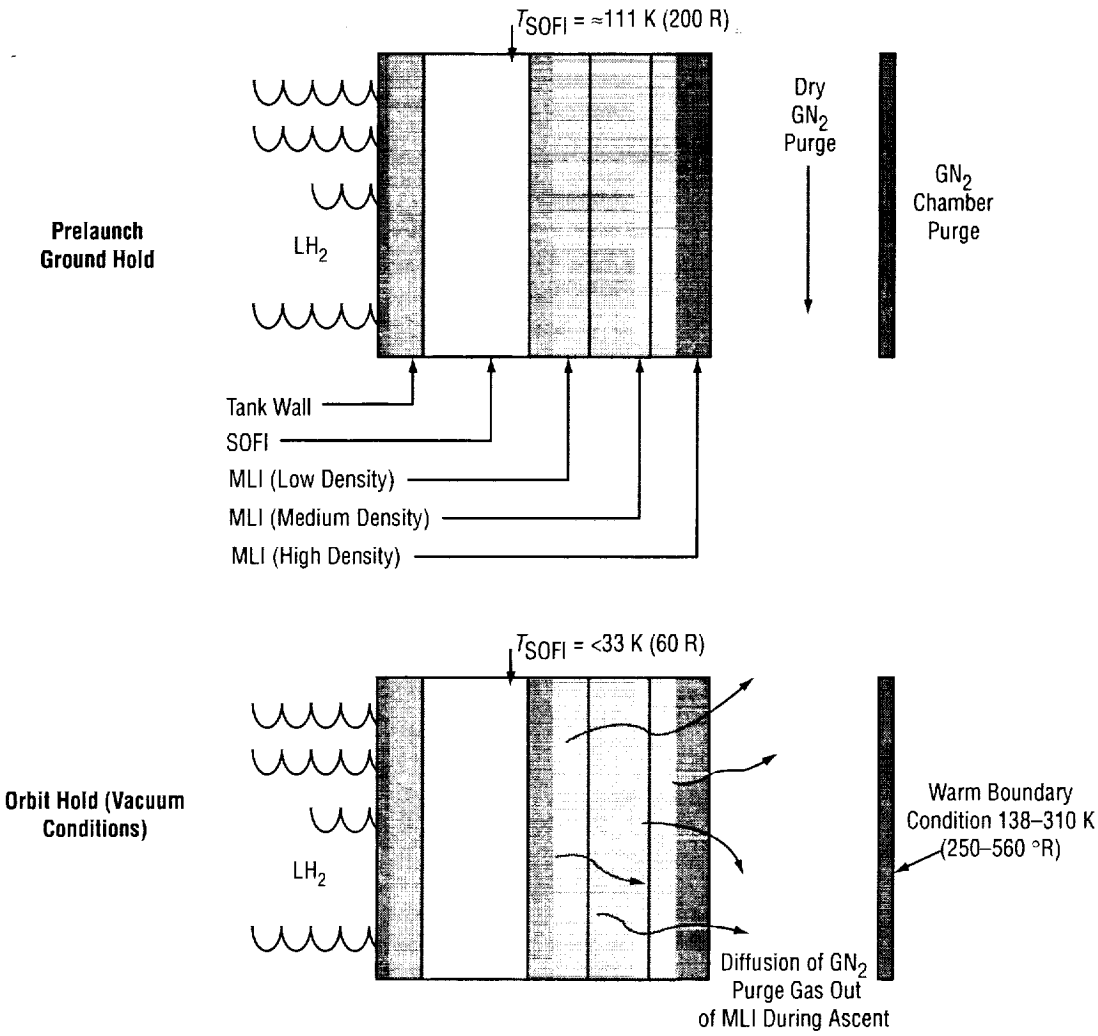

SOFI	Isofoam SS–1171, 3.53-cm Average Thickness		
MLI	45 Layers		
	Low-Density Layers 1–10	6 Bumper Strips	(≈8 Layers/cm)
	Medium-Density Layers 11–25	4 Bumper Strips	(≈12 Layers/cm)
	High-Density Layers 26–45	2 Bumper Strips	(≈16 Layers/cm)

Figure 4. MHTB variable density insulation concept.

The insulation material weight properties and applied insulation weights are presented in tables 2 and 3, respectively. The foam and MLI element weights totaled 45 and 32 kg (100 and 72 lb), respectively. However, as presented in table 3, the insulation weights in an actual application would be less with the ¼-mil aluminized Mylar and the foam thickness reduced to 1.4 cm (0.56 in.). The applied foam and MLI weights in a flight application with the same geometry as the MHTB tank would be 24.5 kg (54 lb) and 18 kg (40 lb), respectively, for a total of 42 kg (94 lb).

Table 2. MHTB insulation material weight properties.

Material Weight Properties	
• Aluminized Mylar (1/2 mil)	0.0088 kg/m^2 (0.0018 lb/ft^2)
• Aluminized Mylar (1/4 mil)	0.0044 kg/m^2 (0.009 lb/ft)
• Dacron netting	0.00635 kg/m^2 (0.0013 lb/ft^2)
• Aluminized tape	0.00223 kg/m (0.0015 lb/ft)
• Isofoam SOFI	3.68 kg/m^3 (2.3 lb/ft^3)
• Dacron bumpers	
–2 ply	0.000327 kg/m (0.00022 lb/ft)
–4 ply	0.000655 kg/m (0.00044 lb/ft)
–6 ply	0.000982 kg/m (0.00066 lb/ft)

Table 3. Applied insulation weight breakdown—MHTB and flight application.

MHTB APPLICATION	FLIGHT APPLICATION—SAME TANK
• Insulation Geometry	**• Insulation Geometry**
– SOFI applied at average thickness of 3.56 cm (1.4 in.)	– SOFI average thickness of 1.4 cm (0.56 in.)
– 45 layers of aluminized Mylar	– 45 layers of 1/4 mil aluminized Mylar
– 45 layers of Dacron netting	– Other MLI components same as MHTB
– 1,219 m (4,000 ft) of aluminized tape	
– Bumpers	
– 533 m (1,750 ft) of 6 ply, layers 1–10	
– 721 m (2,365 ft) of 4 ply, layers 11–25	
– 1,073 m (3,520 ft) of 2 ply, layers 26–45	
Applied Insulation Weight	**Applied Insulation Weight**
• MLI System Weight = 32.68 kg (72 lb)	**• MLI System Weight = 24.4 kg (53.8 lb)**
– 1.36 kg (3.0 lb Dacron bumpers)	– 8.4 kg (18.3 lb) aluminized Mylar
– 2.72 kg (6.0 lb) aluminized tape	– Other components same as MHTB
– 12 kg (26.5 lb) Dacron netting	
– 16.6 kg (36.5 lb) aluminized Mylar	
• SOFI System Weight = 45.36 kg (100 lb)	**• SOFI System Weight = 18.14 kg (40 lb)**

2.4 Insulation Installation

The foam was robotically applied beginning at the midpoint of the barrel section and covering one-half of the tank; the operation was then repeated on the other half of the tank (figs. 5 and 6). All penetrations were masked during the robotic operation and later covered with hand-sprayed insulation (fig. 7). The hand-sprayed foam around the penetrations was then hand-carved to appropriate dimensions (fig. 8).

Figure 5. SOFI robotic application.

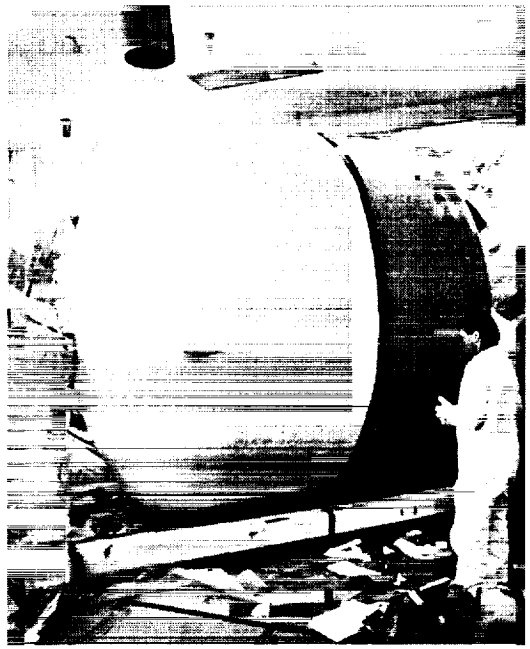

Figure 6. SOFI robotic application half complete.

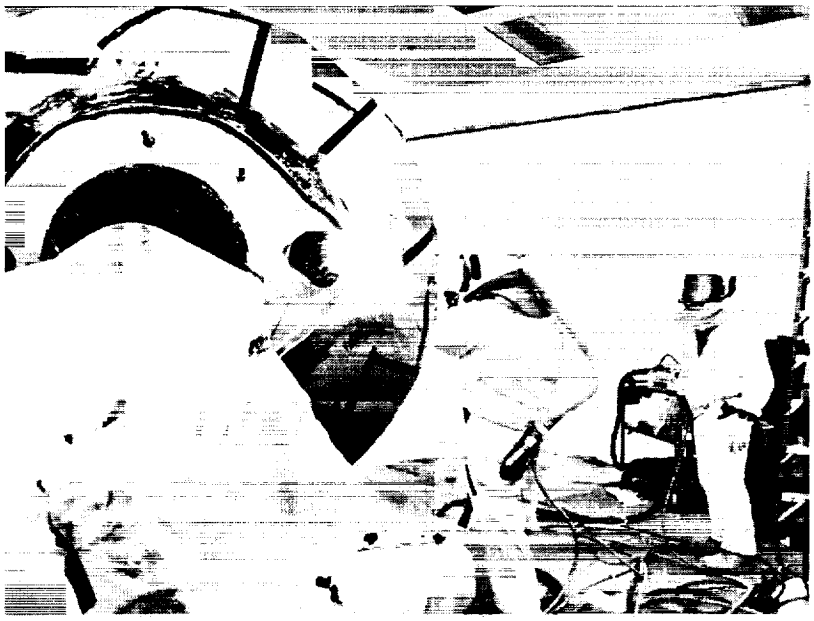

Figure 7. SOFI manual application on penetrations.

Figure 8. Trimmed foam insulation near leg penetration.

The MLI installation technique was unique relative to the usual aerospace approach. The B2A Dacron net was folded, pressed, and tagged to create 7.62-cm- (3-in.-) wide bumper strips. These bumper strips were layed up in three thicknesses: the two-layer strips were formed with a single fold, the four-layer strips with three folds, and the six-layer strip with five folds. Then a commercial roll-wrapping technique was used for the barrel section application wherein the Mylar, B4A Dacron net spacer, and B2A Dacron bumper materials were rolled on simultaneously (figs. 9 and 10). The dome insulation was prefabricated on a flat table (fig. 11). Then, as shown in figure 12, approximately six layers were temporarily attached to a holding fixture fabricated from lightweight PVC piping material. The holding fixture was then positioned against the dome while two people installed the MLI layer by layer using Mylar tape and interleaving each dome layer with the corresponding barrel blanket layer (figs. 13 and 14). The dome/barrel section layers were overlapped by ≈25 cm (10 in.) and the completed upper dome blanket installation is shown in figure 15. Each tank penetration was closed out with both foam and MLI. The MLI performance around the penetrations was enhanced using a temperature matching technique wherein the MLI layers along the penetration's longitudinal axis were attached at penetration locations predicted to have the same temperature as that particular MLI layer. This approach minimized temperature gradients and therefore heat transfer parallel to the insulation layers. Using the preceding MLI installation techniques on a 3-m-diameter tank set (hydrogen and oxygen) would result in an estimated savings of 2,400 man-hours.

It is important to note that although MLI is typically described in terms of layer density and total blanket thickness, the actual layed-up density and thickness varies on the top, bottom, and sidewall due to gravity effects. Once in orbit, the MLI tends to expand or "fluff" somewhat due to the absence of gravity. Hence, the thickness assumed in calculating an effective thermal conductivity or the traditional density-conductivity product for the MLI performance comparisons becomes somewhat arbitrary. A more accurate parameter for performance comparisons is the heat leak per unit area (q_{insul}) multiplied by the insulation mass (M_{insul}) per unit surface area, or $q\,M_{insul}$, with the units kg-W/m^4 (Btu-lb/sec ft^4). Thus, the smaller the $q\,M_{insul}$ product, the better the insulation performance.

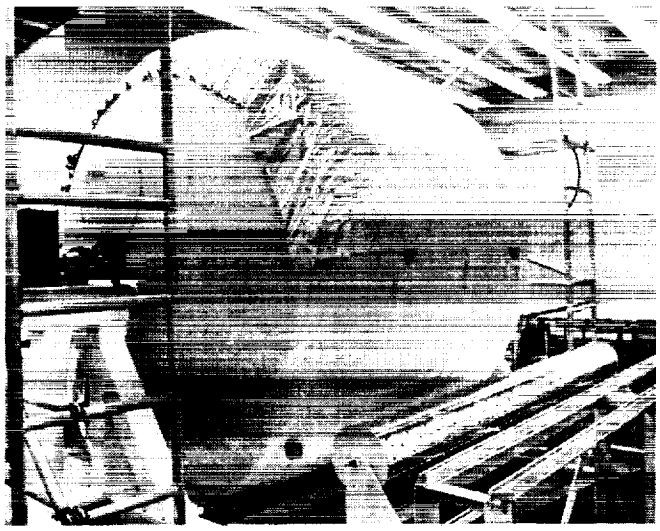

Figure 9. Roll-wrapping application of MLI and Dacron net spacing material—beginning.

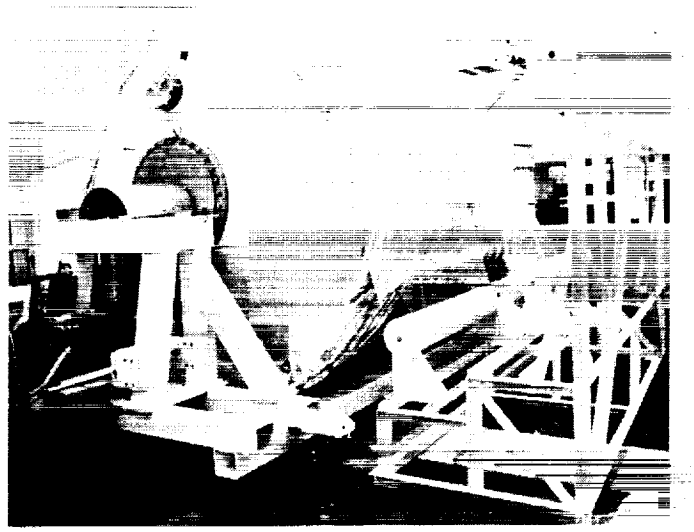

Figure 10. Roll-wrapping application of MLI and Dacron net spacing material—partially complete.

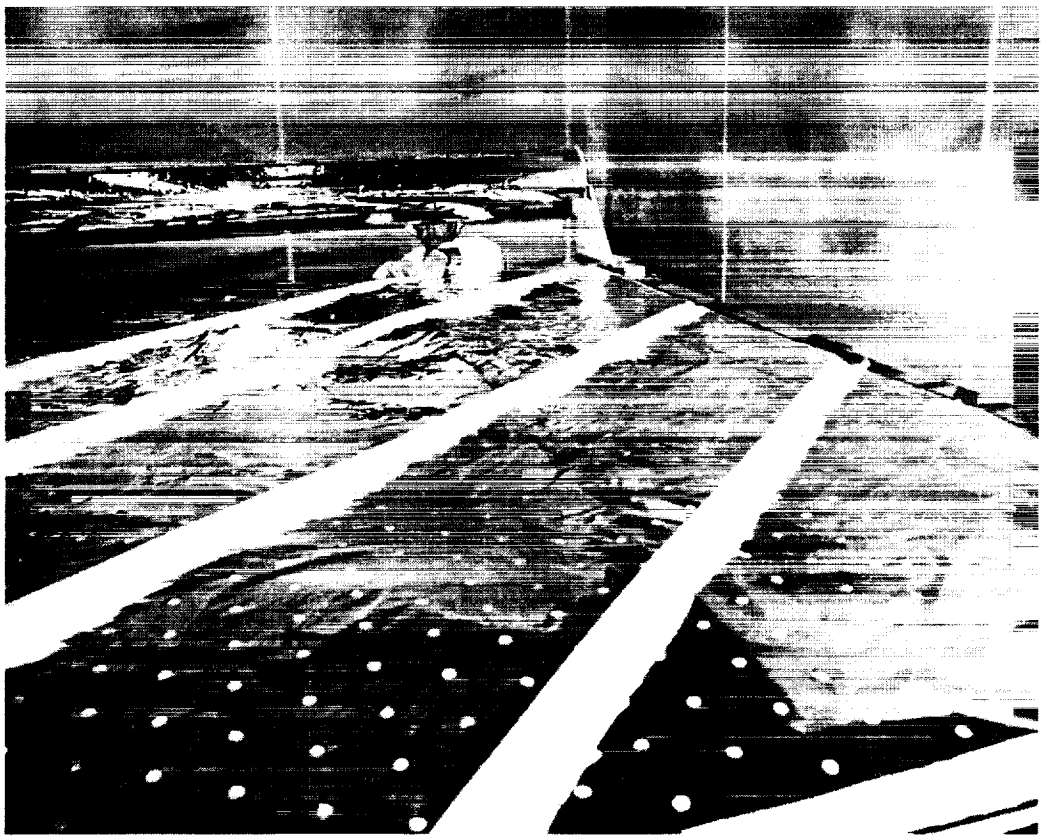

Figure 11. Dome MLI blanket assembly.

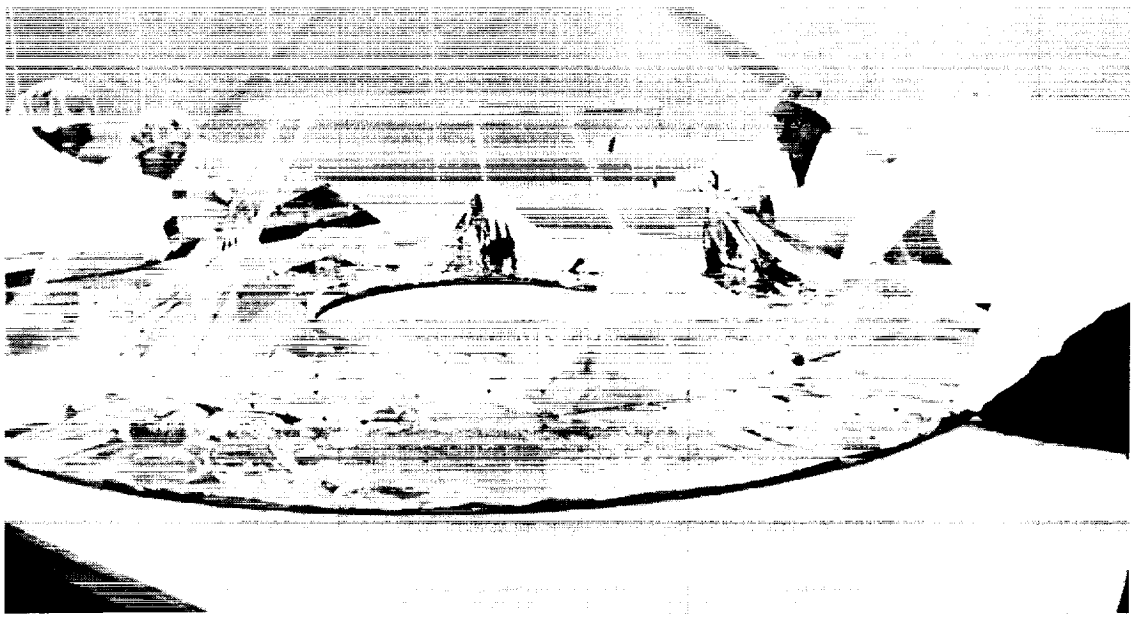

Figure 12. Dome MLI blanket attachment to holding fixture.

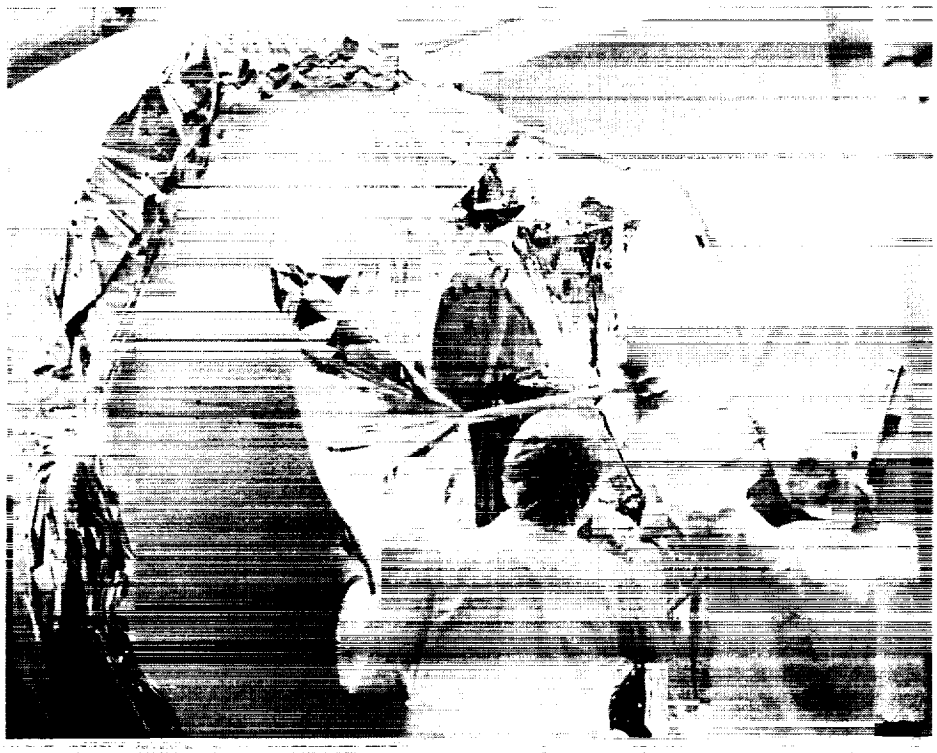

Figure 13. Top dome MLI blanket installation—beginning.

Figure 14. Top dome MLI blanket installation—partially complete.

Figure 15. Top dome MLI blanket installation—complete.

2.5 Instrumentation

The test article and environmental shroud instrumentation details are presented in appendix B; however, the instrumentation arrangement for each primary segment is summarized in this section. The test article instrumentation consists primarily of thermocouple and silicon diodes to measure insulation, fluid, and tank wall temperatures. The general instrumentation layout is illustrated in figures 16–18, which represent the top, front, and bottom views of the test tank without insulation for clarification. Typically, silicon diodes (Lakeshore type DT–470–11A) temperature transducers are positioned in areas of lowest temperatures because of higher accuracy as compared with thermocouples. As illustrated in figure 17, MLI temperature profiles or gradients are measured at seven positions with one silicon diode and four thermocouples (fig. 19) placed at each of the seven measurement positions. The MLI interstitial pressure is measured at the foam/MLI interface with two pressure sensors mounted on top of a 5.08-cm-(2-in.-) diameter, thin-walled probe 22.86 cm (9 in.) in length. The probe is also equipped with a sampling port for both dew point level and gas species sampling. The pressure transducers, a Gran Philips 275 and a cold cathode, encompass a pressure range of 760 to 10^{-7} torr. The dew point instrument is an Endress Hauser® model 2200 hydrometer.

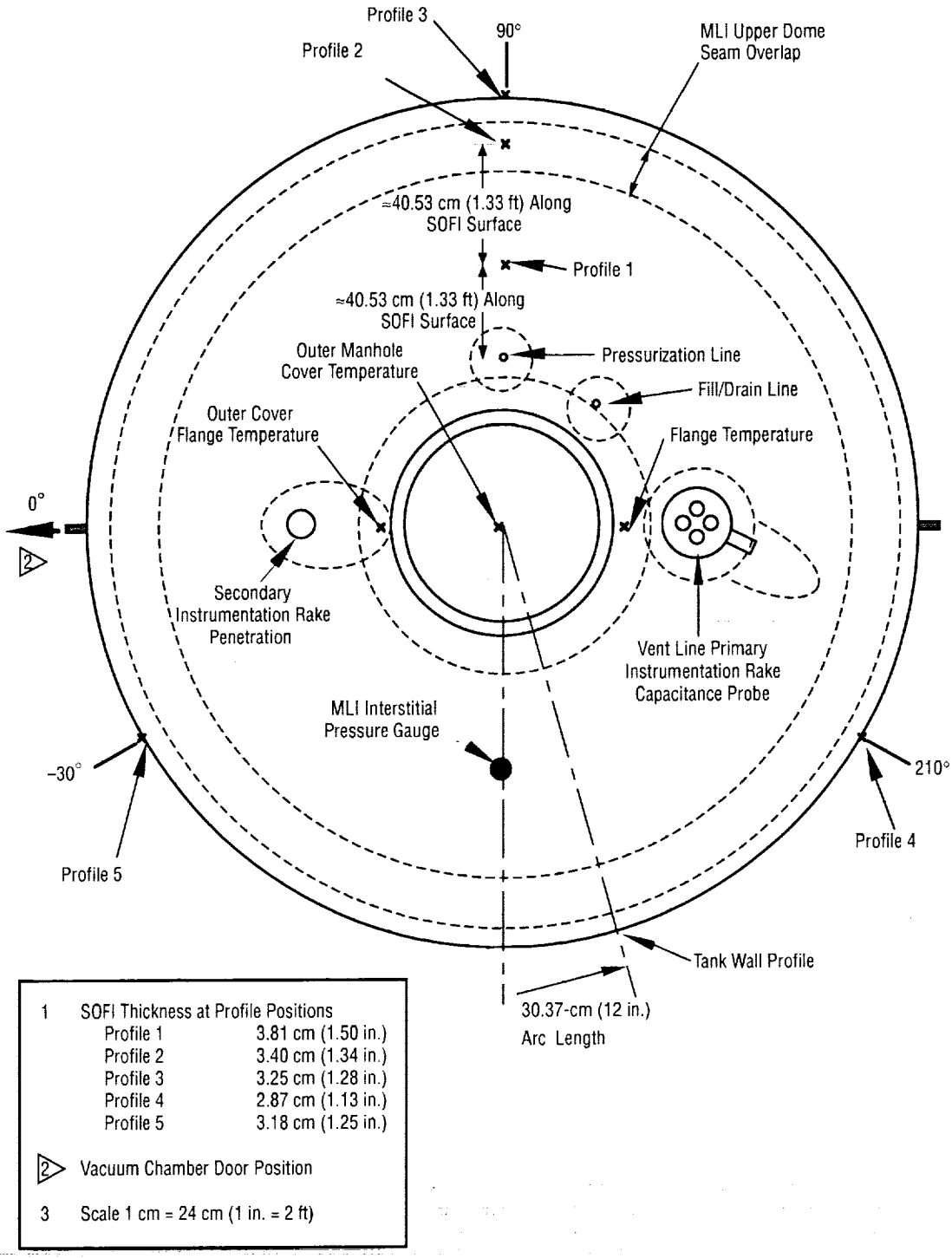

Figure 16. MHTB temperature measurement positions—top view.

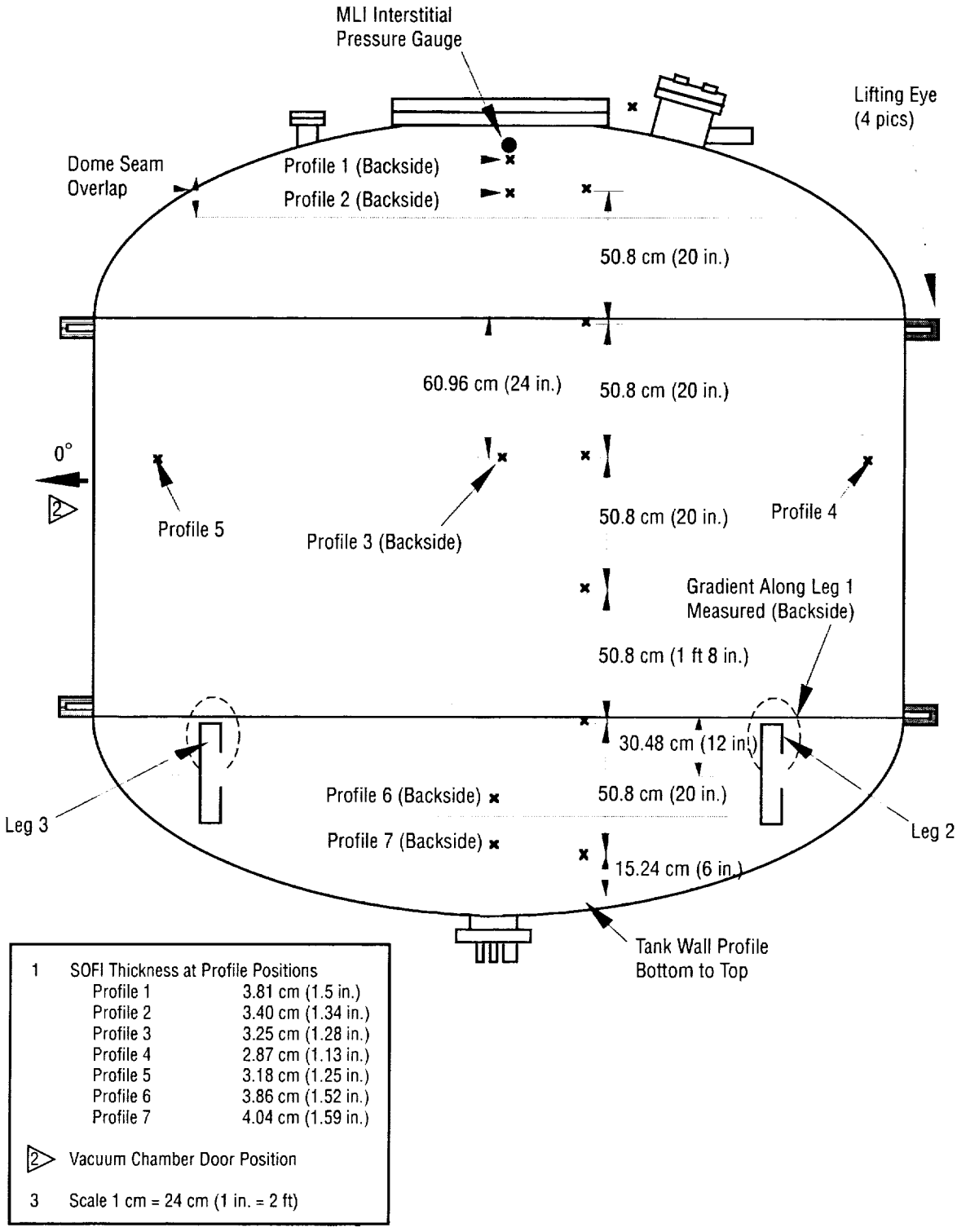

Figure 17. MHTB instrumentation—side view.

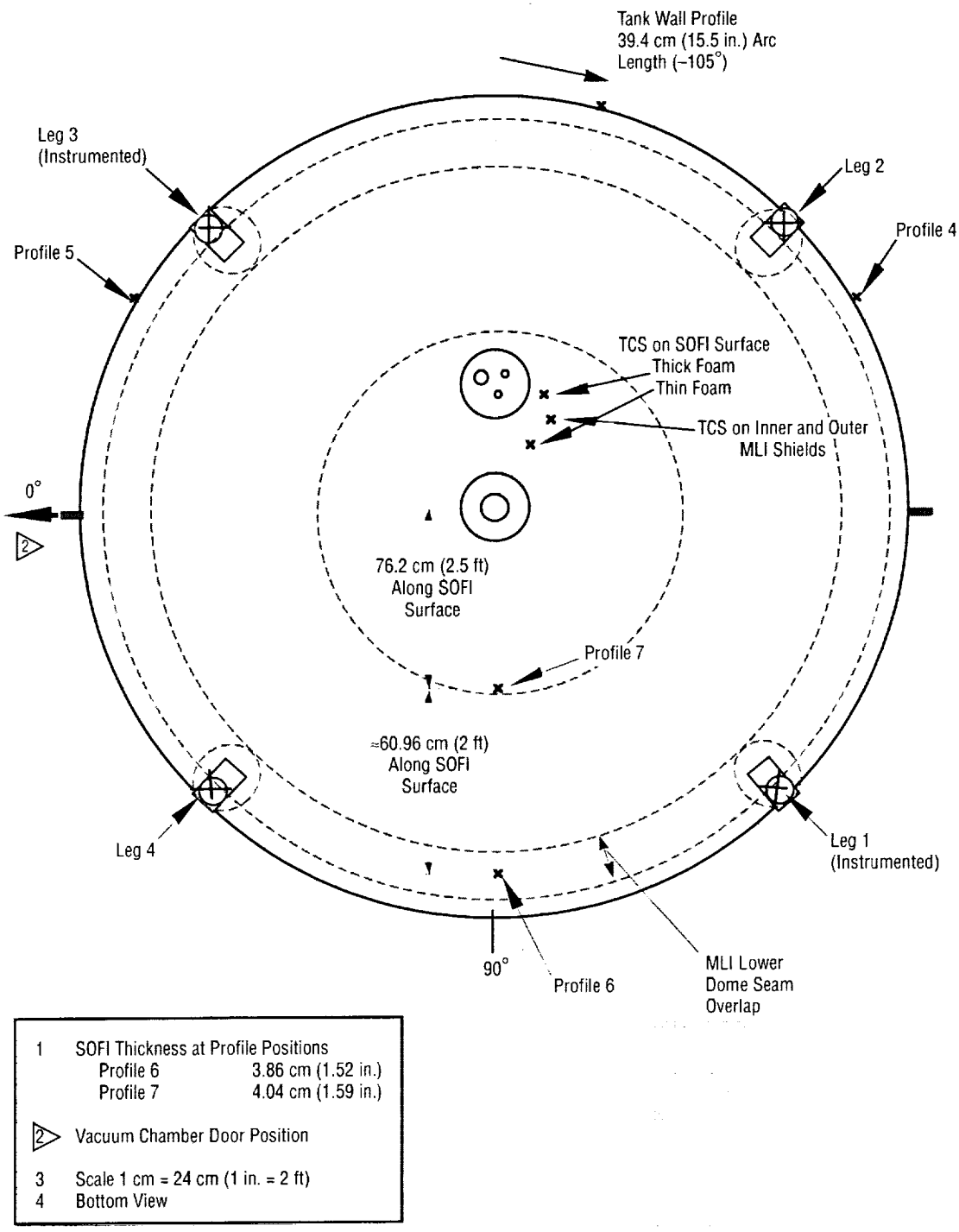

Figure 18. MHTB temperature measurement positions—bottom view.

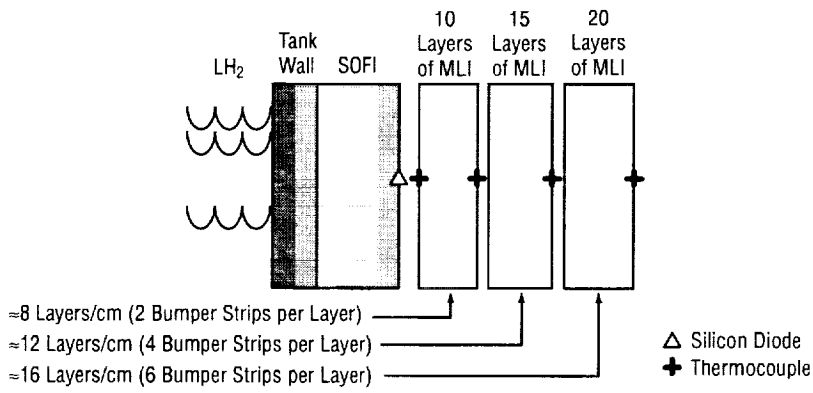

Figure 19. Representative MLI instrumentation profile on MHTB.

Two of the four composite legs are instrumented with a combination of diodes and thermocouples to measure heat guard boundary temperature and insulation profiles and to determine heat input along the legs and structural supports (fig. 20). Similarly, the vent, fill/drain, pressurization, MLI sampling probe, and manhole pump-out port penetrations are all instrumented to determine heat leak.

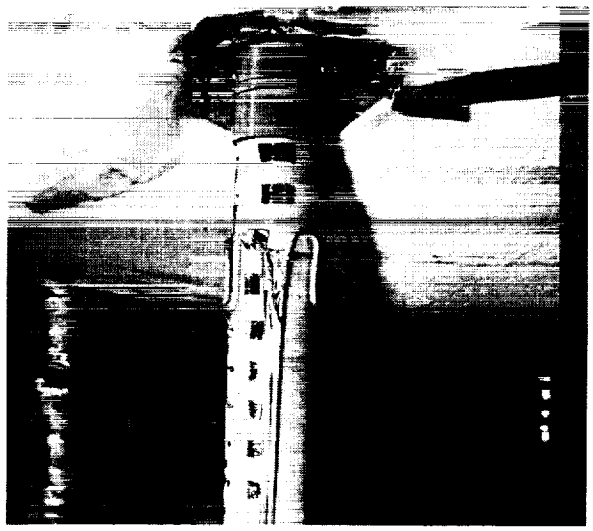

Figure 20. MHTB composite leg instrumentation.

The tank is internally equipped with two instrumentation rakes and a capacitance liquid level probe, all supported from the top of the tank (fig. 21). The rakes, constructed from a fiberglass epoxy channel section, are equipped with silicon diodes attached at 22.9-cm (9 in.-) intervals using nylon rod offsets and cryogenic epoxy. The instrumentation rakes provide temperature-gradient measurements within both ullage and liquid, in addition to providing a backup to the continuous liquid level capacitance probe.

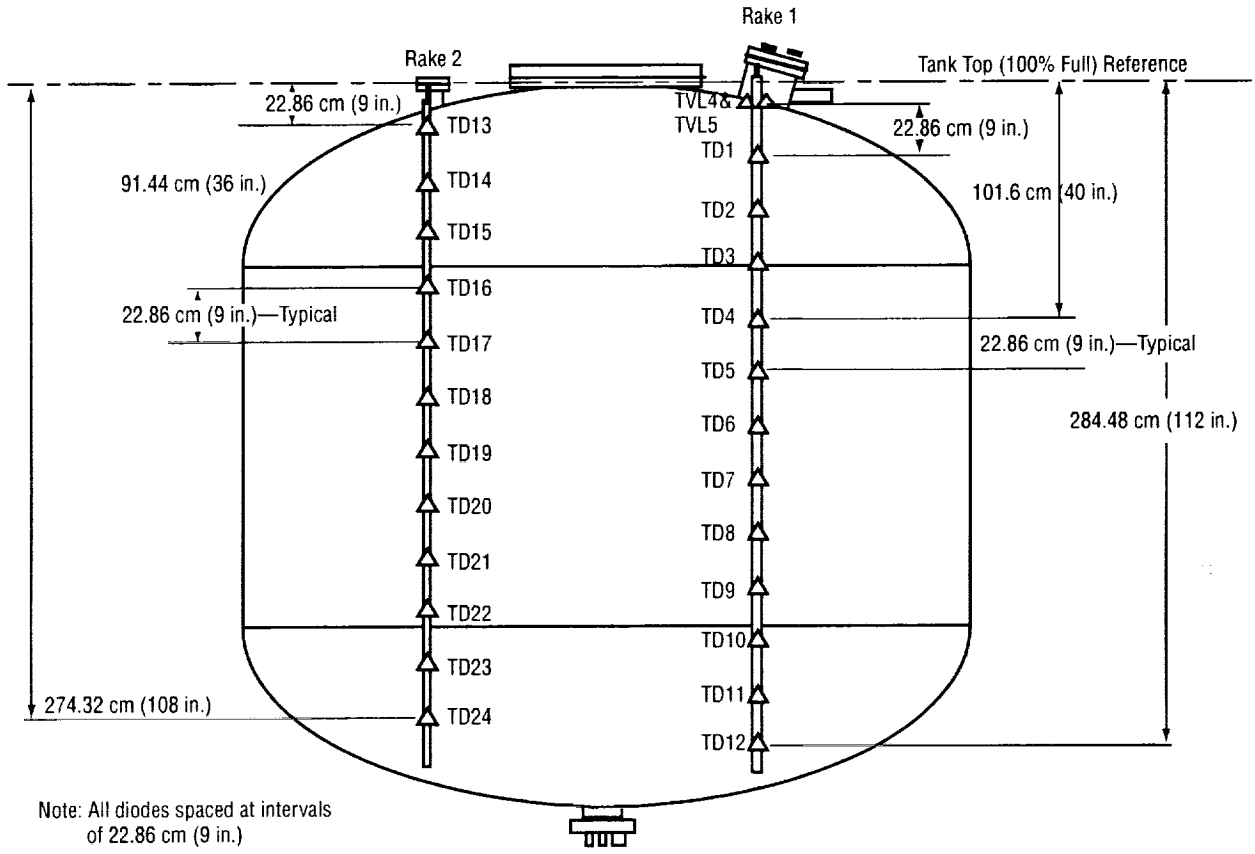

Figure 21. MHTB internal instrumentation rake.

The environmental shroud is composed of 17 individual panels, each equipped with a minimum of two thermocouples attached to the inner surfaces and placed beneath the electrical heating strips. These thermocouples are used with a closed-loop control system to regulate each shroud panel temperature. Five thermocouples are also placed at a position within the vertical annular region created between the shroud and tank insulation to measure purge gas temperatures. Vacuum chamber free air space temperatures are measured with facility-provided thermocouples, mounted external to the test article shroud. These thermocouples are placed at 1.525-m (5-ft) intervals above the chamber floor. Purge gas dew point within the environmental shroud is measured with a facility-supplied Endress Hauser model 2200 hydrometer.

3. TEST FACILITY AND PROCEDURES

3.1 Facility Description

Testing was performed at the MSFC east test area thermal vacuum facility, test stand 300 (fig. 22). The test article and facility flow schematic is presented in figure 23. The vacuum chamber is cylindrical in shape and has usable internal dimensions of 5.5 m (18 ft) in diameter and 7.9 m (26 ft) in height. Personnel access is through a small side-entry door, but the chamber lid is removable for installation of large test articles (figs. 24 and 25). The chamber pumping train consists of a single-stage GN_2 ejector, three mechanical roughing pumps (rated at 140 L/sec (300 ft^3/min each)) with blowers (rated at 610 L/sec (1,300 ft^3/min each)), and two 1.2-m- (48-in.-) oil diffusion pumps (rated at 95,000 L/sec (200,000 ft^3/min N_2 each). Liquid nitrogen (LN_2) cold walls provide cryopumping and thermal conditioning capability and are comprised of five parallel zones, which totally surround the usable chamber volume with a surface emissivity of ≈0.95. The facility systems in combination with the test article shroud enabled simulation of orbit environmental conditions by providing vacuum levels of 10^{-8} torr and a temperature range of 80–320 K (140–576 °R). The GN_2 ejector system enables a rapid pumpdown capability (ambient pressure to 30 torr in 120 sec) to simulate the ascent flight portion of a mission. Two solid-state video cameras were mounted inside the chamber to view the test article dome and sidewall during the ground hold and ascent flight test phases.

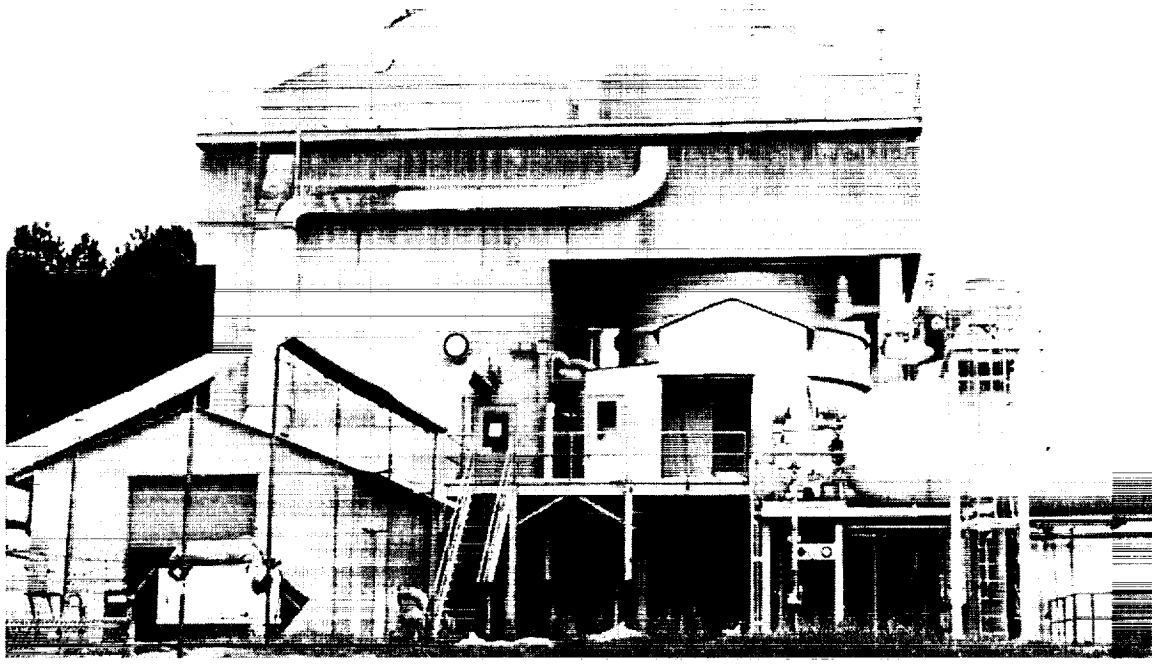

Figure 22. MSFC east test area thermal vacuum facility, test stand 300.

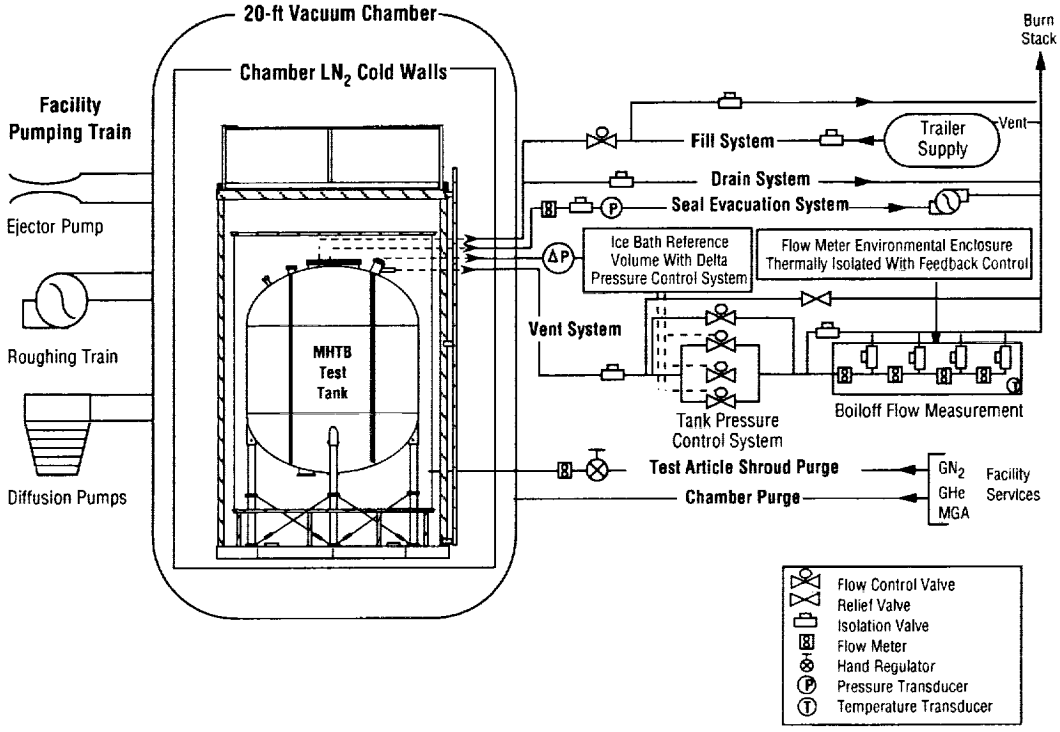

Figure 23. MHTB and test stand 300 facility simplified flow schematic.

Figure 24. MHTB installation in test stand 300 vacuum chamber—beginning.

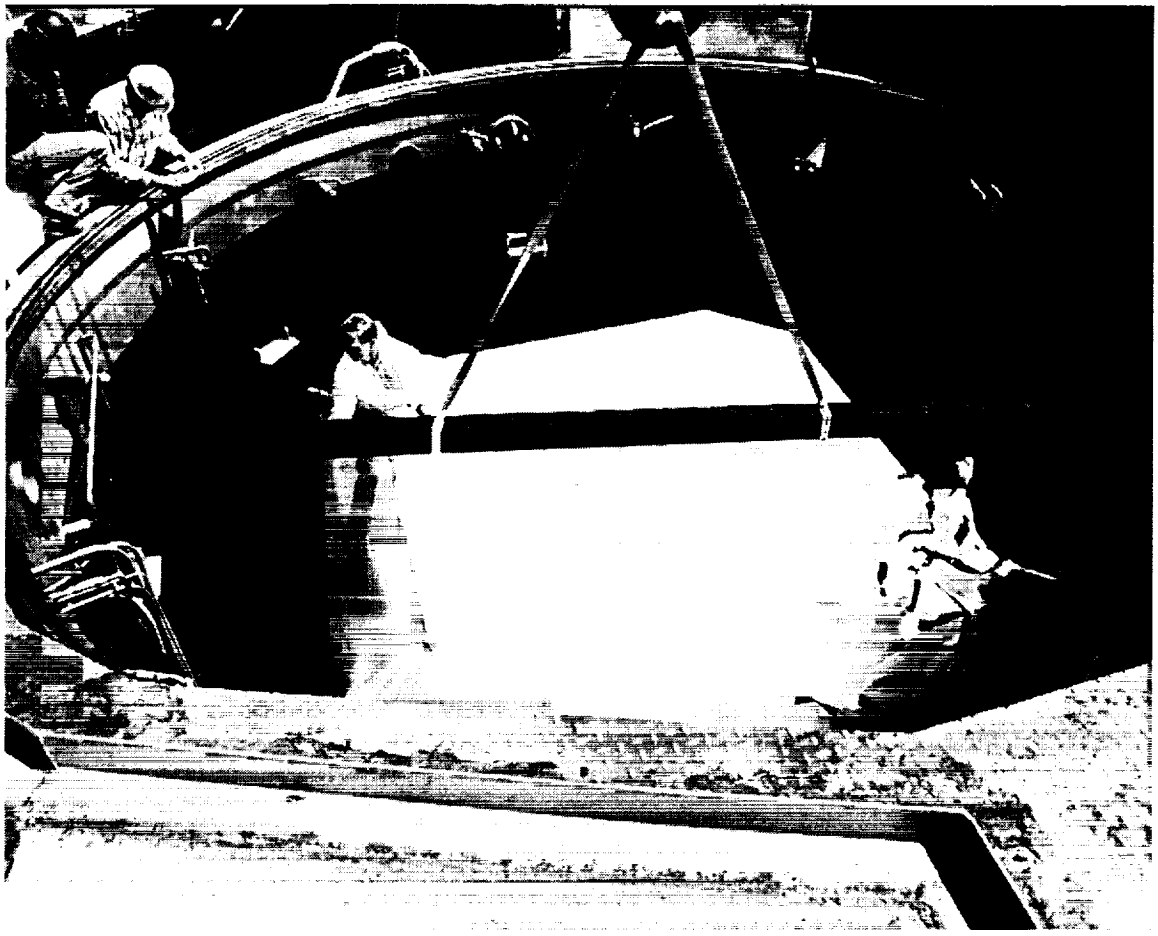

Figure 25. MHTB installation in test stand 300 vacuum chamber—in chamber.

In addition to the chamber, conditions within the MHTB were controlled within the MHTB utilizing the facility subsystems described below:

- A vacuum-jacketed fill and drain system provided cryogenic fluid servicing to and from the test article. All facility lines had welded construction.

- A tank pressure control subsystem was used to maintain the MHTB ullage pressure at the required steady-state conditions. The system was composed of several flow control valves (located in the vent line), each of which was regulated through a closed-loop control system. This control loop manipulated the valve positions based on a comparison of the measured tank ullage pressure and the desired set point. An MKS Instrument Inc. Baratron 0–133 kPa (0–19 psia) absolute pressure transducer (accuracy of ±0.02 percent) and an MKS delta pressure transducer (1 torr or 133 Pa head with an accuracy of ±0.04 percent) located outside the vacuum chamber were used to measure ullage pressure. The system successfully maintained set points ranging from 110–124 kPa (16–18 psia) with tolerances of ±0.0689 kPa (±0.01 psi) and ±0.00689 kPa (±0.001 psi) for ground hold and orbital simulation conditions, respectively.

- Hydrogen boiloff flow instrumentation was located in the vent downstream of the flow control valves. During orbit hold simulations, one of three mass flow meters (MKS model 258C, Hastings model 200, and Hastings model H–3MS) was used. These meters spanned flow ranges of 0–280 standard liters per minute (SLPM), 0–50 SLPM, and 0–1 SLPM with accuracies of ±0.8, ±1.0, and ±1.0 percent of full scale, respectively. To prevent ambient temperature effects on measurement accuracy, the flow meter system was placed within a containment box and equipped with a temperature-controlled purge, which maintained the box interior at constant temperature, typically 306 K (550 °R).

- A seal evacuation system—MKS model 258 with a range of 0–61 standard cubic inches per minute (SCIM)—captured and measured any boiloff gases leaked past the 61-cm (24-in.) primary tank seal. This setup was required to prevent degradation of vacuum levels during orbit simulation and ensure boiloff measurement accuracy. This system, illustrated in figure 2, was connected to the volume formed between the tank's primary and secondary seals. This system was used as required to maintain a seal volume pressure of 133 Pa (1 torr).

3.2 Test Procedures

The procedures utilized for test preparations, the simulation of ground hold, ascent flight, and orbital hold conditions are summarized in sections 3.2.1 through 3.2.4.

3.2.1 Pretest Operations

Prior to testing, the vacuum chamber and environmental shroud were purged at a trickle rate with dry GN_2 for ≈5 days while the chamber and MLI dew point was maintained. Prior to tanking, the environmental shroud purge ring was operated at a GN_2 flow rate of 5 kg/min (11.2 lb/min) with a dew point not to exceed –54 °C (–65 °F). Also, the seal evacuation system was activated and held steady at a level of 2×10^{-2} torr or less. About 2 hr prior to tanking, dry GN_2 (followed by gaseous hydrogen (GH_2)) with a dew point of –54 °C (–65 °F) was used for the internal purge/conditioning operations of the test tank, fill/drain line, and vent line. This purge and conditioning process was accomplished using charge-vent cycles during which the tank was pressurized to ≈103 kPa (15 psig) with GH_2, held for ≈1 min, and then vented back down to near atmospheric pressure. This sequence was typically repeated 15–20 times prior to loading LH_2 into the MHTB. The test tank is designed to withstand an internal vacuum against external atmospheric pressure enabling vacuum cycling with GH_2 pressurization, a much more efficient method of conditioning. However, the vacuum cycling approach was not implemented during this test program.

The test article was then filled with LH_2 to the 85-percent level while maintaining the ullage pressure ≈103.4 torr (2 psi) above the required set point pressure. Completion of fill to the 95-percent level was then accomplished with the automated pressure control subsystem activated to control the ullage ≈25.8 torr (0.5 psi) above the set point. Once filling was completed, the transition to the test set point pressure occurred over a period of 10–20 min. Several hours were required to saturate and equilibrate the tanked LH_2 at the set point pressure.

3.2.2 Ground Hold Simulation

The ground hold purge simulated a payload bay environment by providing an inert GN_2 purge with the following conditions:

- Dew point of –54 °C (–65 °F) or less
- Flow rate of 5 kg/min ± 0.907 kg/min (11 lb/min ± 2 lb/min)
- Temperature range of 6 to 17 °C ± 5.5 °C (–60 to –40 °F ±10 °F)
- Dew point and gas purity verified by instrumentation within shroud.

The vacuum chamber internal volume gas temperature was measured periodically prior to and continuously during each test using thermocouples located at 1.52, 3.05, and 4.57 m (5, 10, and 15 ft), respectively, above the chamber floor and ≈0.61 m (2 ft) from the chamber coldwall at a 90° clockwise position with respect to the chamber door, as illustrated in figure 26.

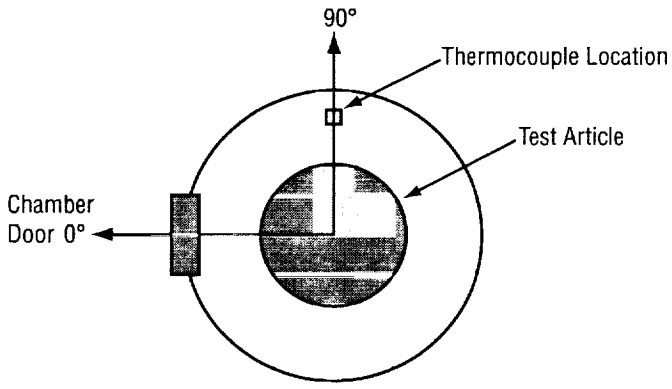

Figure 26. Vacuum chamber gas temperature locations—top view.

The tank ullage pressure was maintained at a set point selected in a range of 110.316–124.106 Kpa (16–18 psia) with a tolerance of ±0.0689 Kpa (±0.01 psi). The pressure rise rate within the tolerance band was held to within 0.689 Kpa/hr (0.1 psi/hr) to control venting oscillations. The ground hold test duration, after tanking and ullage pressure control was established, was typically 1–2 hr. Ground hold data included vent flowrate along with all other pertinent thermal parameters such as shroud and insulation surface temperatures.

3.2.3 Ascent Flight Simulation

The vacuum chamber GN_2 ejector system enables a rapid pumpdown that was used to simulate, insofar as possible, the ascent flight portion of a heavy lift launch—National Launch System (NLS) vehicle or Space Shuttle (Space Transportation System (STS))—mission as defined in table 4. Although the present pumping train cannot closely simulate the ascent profile beyond the first 100 sec of flight, every effort was made at pumping the chamber into the 10^{-6} torr range as rapidly as possible.

Table 4. MHTB flight ascent simulation pressure decay requirements.

Time (sec)	STS Pressure (torr)	NLS Pressure (torr)
0	760.0	760.0
40	411.0	692.0
60	178.0	375.0
100	8.9	57.8
120	5.4	11.1
140	1.13	3.76
160	0.247	1.13
180	2.8E-2	0.247
200	3.1E-3	2.8E-2
220	9.5E-4	3.1E-3
240	8.5E-5	9.5E-4
260	1.6E-5	8.5E-5
290	6.3E-6	1.6E-5
350	4.5E-6	6.3E-6
380	3.5E-6	4.5E-6
420	1.0E-6	3.5E-6

Other conditions pertaining to the ascent simulation include the following:

- Termination of all vacuum chamber and test article purges several minutes prior to initiating the pumpdown
- Vacuum chamber LN_2 cold wall activation once a vacuum level sufficient to prevent gross condensation of contaminates was attained ($\approx 10^{-3}$ torr)
- Environmental shroud activation during the ascent phase to begin establishment of specified on-orbit temperature conditions
- Residual gas analyzer (RGA) system recorded vacuum chamber gas composition throughout the pumpdown once the chamber pressure reached a level of ≈ 1 torr
- Activation of the two video cameras for the first 3 min of pumpdown to observe any billowing of the MLI.

3.2.4 On-Orbit Simulation

Upon completion of the ascent flight simulation, establishment of steady-state vacuum and thermal conditions—within both the chamber and MLI—was achieved before the on-orbit test phase. The four criteria, which had to occur simultaneously, for steady-state orbital simulation conditions were as follows:

1. Interstitial MLI pressures had to be 10^{-5} torr or less to preclude a transient convective heat transfer effect as the insulation pressure continues to drop. A vacuum chamber pressure of 10^{-6} torr or less was required to ensure an adequate vacuum within the insulation.

2. Insulation temperatures (MLI and SOFI) had to be in a steady-state condition with the MLI surface temperature at the prescribed set point imposed by the environmental shroud. Insulation equilibrium was assumed to exist once temperature transients of no more than 0.55 K in 6 hr is measured in any section of the insulation system.

3. Thermal equilibrium of the LH_2 had to be maintained through precise ullage pressure control during the low heat leak, orbital simulation. Ullage pressure, was maintained at a set point in the range of 110.316–124.106 Kpa (16–18 psia) with a tolerance of ±0.00689 Kpa (0.001 psi).

4. The vented ullage gas temperature had to increase with time (positive slope), indicating that the tank dome was in thermal equilibrium; i.e., the dome was no longer cooling and contributing to the vented gas enthalpy.

When performing low heat leak cryogenic storage testing, either a loss of ullage pressure control or the chamber vacuum can result in significant increases in unproductive test time. Each 6.89 Kpa (1 psi) of LH_2 subcooling, due to a sudden reduction in ullage pressure, requires 30 hr for recovery to saturation (due to the low heat leak conditions). Similarly, a sudden increase in vacuum chamber pressure (10^{-4} torr or above) can dramatically alter the MLI temperatures, necessitating several days to recover the steady-state temperature profile. Therefore, great care was taken to ensure tight control of the tank ullage and vacuum chamber pressures during the on-orbit or deep space simulations. The MSFC vacuum facility and associated controls performed well, meeting required vacuum levels and ullage pressure control limits. The vacuum chamber LN_2 cold walls were maintained with all zones in the LN_2 temperature range with a maximum difference between zones of 23 °C (40 °F). This was required to minimize temperature influences on the test article environmental shroud system.

An RGA system was used to record vacuum chamber and MLI interstitial gas composition periodically during steady-state orbit hold periods. RGA sampling intervals varied depending on the vacuum chamber pressure stability and assisted in determining the source of any chamber pressure variations; e.g., test article or chamber leakage, or outgassing. Species possibilities included H_2O, N_2, O_2, CO_2, and the foam-blowing agent CFC–11 (CCL_3F molecular weight of 137.4).

3.3 Post-Test Operations

Return-to-Earth operations and effects on insulation were not addressed in this program. Therefore, chamber repressurization conditions after the on-orbit simulation were selected primarily to protect the test article and facility. Also, following a test, the MHTB was not held under vacuum conditions for needlessly long periods. The chamber and test article were warmed and repressurized within 8–12 hr after testing was concluded. Chamber repressurization occurred slowly (≈30 min) with dry GN_2 (dew point –54 °C (–65 °F)) in the 4–27 °C (40–80 °F) temperature range. To prevent water condensation, repressurization was initiated only after the vacuum chamber cold walls and all test article insulation (SOFI/MLI) had reached ≈15.5 °C (60 °F). Warming of the cold walls and test tank internal volume could be performed with heated 37 °C (100 °F) GHe/GH_2 (or GN_2 for quick turnaround (4–6 hr of heating)).

Dry GN_2 with a dew point of –54 °C (–65 °F) was used to accomplish purge and inerting operations for the test article volume and all service lines. These operations were designed so that the test article was not subjected to a positive differential pressure in excess of 344 kPa (50 psid). Typically, the GN_2 shield purge remained on for 24 hr after completion of testing.

4. TEST RESULTS

The insulation system performance was recorded during three tests in which a total of four vacuum and tank fill/drain cycles were performed over a 10-mo period, resulting in 1,429 hr at vacuum conditions and 1,335 hr at LH_2 temperatures. Table 5 details the MHTB thermal/vacuum test environment history. Subsequent testing increased the vacuum exposure and LH_2 storage times to 2,030 and 1,732 hr, respectively, with no further degradation. The data evaluation approach and the ground hold, ascent flight, and orbit hold test results are described in sections 4.1 and 4.2.

4.1 Data Reduction and Evaluation Approach

4.1.1 Data Reduction

Digital data were recorded at sample rates ranging from 1–0.017 Hz. These raw data were then time averaged over the steady-state period of interest to obtain measurement values required to calculate thermal performance. The heat input was expressed as an energy balance across the tank boundary by equating the total measured boiloff with the sum of heat flow through the insulation, the penetrations, and the rate of energy storage, if any:

$$\dot{Q}_{\text{boiloff}} = \dot{Q}_{\text{insul}} + \dot{Q}_{\text{conduction}} + \frac{\Delta U_{\text{system}}}{\Delta t} \quad . \tag{1}$$

The terms $\dot{Q}_{\text{boiloff}}$ and $\dot{Q}_{\text{conduction}}$ were defined using the measured test data. The thermal storage term, $\frac{\Delta U_{\text{system}}}{\Delta t}$, (energy stored in the test tank wall, insulation, and fluid mass) is driven by the fluid saturation temperature, which varies as ullage pressure fluctuates. The storage term was eliminated since the ullage pressure was maintained within a tight control band about the set point. The insulation performance term $\dot{Q}_{\text{insul}}$ could then be determined from the other measured quantities.

The $\dot{Q}_{\text{boiloff}}$ term represents the total energy vented as boiloff and includes both the evaporated fluid latent heat and the sensible heat absorbed while the vented gas passes through the ullage space (also known as ullage superheat):

$$\dot{Q}_{\text{boiloff}} = \dot{m} h_{fg} \left(\frac{\rho_{\text{satliq}}}{\rho_{\text{satliq}} - \rho_{\text{satvap}}} \right) + \dot{m} \left(h_{\text{vent}} - h_{\text{satvap}} \right) \quad . \tag{2}$$

The latent heat term of equation (2) contains a density ratio that accounts for the increased volume of gas and hence the remaining energy resulting from the decrease in liquid volume due to boiloff losses.

The solid conduction term $\dot{Q}_{conduction}$ represents the heat flow through the tank support legs, vent assembly, and other fluid lines. Solid conduction was evaluated by using the Fourier heat transfer equation[2] with known structural geometry, material properties, and a measured temperature difference as follows:

$$\dot{Q}_{conduction} = \left(\frac{A}{L}\right) \int_{T_{cold}}^{T_{hot}} K(T)dT \quad . \tag{3}$$

The heat input through the insulation, Qinsul, was then assessed using experimental data, fluid properties, and the assumption that no energy is stored in the tank material, insulation, and fluid; that is:

$$\dot{Q}_{insul} = \dot{Q}_{boiloff} - \dot{Q}_{conduction} \quad . \tag{4}$$

4.1.2 Ground Hold Simulation

Tank heat leak during the ground hold phase was estimated using the Systems Improved Numerical Differencing Analyzer and Fluid Integrator (SINDA'85/FLUINT) program.[3] The primary heat leak path was the insulation acreage that was modeled assuming (1) solid conduction through the SOFI and (2) gaseous conduction through the stagnant GN_2 filling the MLI. The boundary condition on the outer MLI was imposed as convective heat transfer to the surroundings.

4.1.3 Orbit Hold Simulation

As described in section 4.1.1, the heat leak performance of the MHTB insulation system was computed from the measured boiloff rate, fluid properties, and solid conduction based on measured penetration temperatures. For comparison with the MHTB variable density MLI, the MLI blanket performance of a standard constant density MLI blanket was calculated assuming both ¼-mil DAM and equal blanket weights per unit area. The standard blanket performance was based on the following assumptions: (1) The blanket consists of one Dacron B4A layer for every DAM layer, resulting in an approximate packing density of 27 layers/cm, and (2) the DAM is perforated with standard, small, closely spaced holes, 0.15875-cm (1/16-in.) diameter with 2-percent open area. After adjusting the number of layers in the standard blanket to match the variable density blanket weight, a standard MLI with 55 layers and an approximate weight of 0.7 kg/m^2 (0.144 lb/ft^2) resulted. Similarly, the boiloff can be held constant and the relative blanket weights compared.

A one-dimensional model was then set up to evaluate the standard MLI blanket heat leak when subjected to the same boundary conditions as those measured in the variable density MLI testing; that is, with a cold boundary condition at the SOFI surface and a warm boundary at the environmental shroud. The standard MLI was modeled with the semiempirical equation, commonly referred to as the Lockheed equation,[4] while the heat transfer from the MLI to its surroundings (SOFI and shroud) was treated as pure radiation. The Lockheed equation, which was developed from flat plate calorimeter test data

(and hence provides ideal performance), contains three terms representing the modes of heat transfer through a blanket—radiation, solid conduction, and gaseous conduction:

$$\dot{Q}_{\mathrm{MLI}} = \frac{7.07\times10^{-10}\varepsilon_{\mathrm{TH}}\left(T_{\mathrm{hot}}^{4.67} - T_{\mathrm{cold}}^{4.67}\right)}{N_{\mathrm{shield}} - 1} + \frac{7.30\times10^{-8}\overline{N}_{\mathrm{layers}}^{2.63}\left(T_{\mathrm{hot}} - T_{\mathrm{cold}}\right)\left(T_{\mathrm{hot}} + T_{\mathrm{cold}}\right)}{2\left(N_{\mathrm{shield}} - 1\right)} + \frac{1.46\times10^{4} P\left(T_{\mathrm{hot}}^{0.52} - T_{\mathrm{cold}}^{0.527}\right)}{N_{\mathrm{shield}} - 1} \quad (5)$$

Using a Microsoft® Excel spreadsheet and MLI surface temperature, the model iterated until the solution reached convergence for the heat leak. The output of this model will be discussed, along with the experimental results, in section 4.4.

Table 5. MHTB thermal/vacuum test environment history.

Test	Type of Test	Chamber/MLI Purge[a]				Average Vacuum Levels			LH_2 Loaded
		Type	Dew Point Chamber	Dew Point MLI	Duration (hr)	Chamber[b] Press (torr)	MLI Press[b] (torr)	Total Time (hr)	Total Time (hr)
P9502	Thermal/vacuum gnd/asc/orbit	GN_2	−80 °C	−50 °C	151	3×10^{-8}	–[c]	414	370
[d] P9601	Thermal/vacuum gnd/asc/orbit	GN_2	−80 °C	−68 °C	28	5×10^{-8}	4×10^{-6}	560	530
[e] P9602A	Thermal ground hold only	GN_2	−80 °C	−75 °C	81	NA	NA	NA	35
P9602B	Thermal/vacuum orbit hold only	Evacuated 5×10^{-5} torr			6	5×10^{-8}	2×10^{-6}	455	400
						Cummulative Exposure Times		[f] 1,429	[f] 1,335

a Purge duration prior to LH_2 loading (purges continued through ground hold tests)
b Vacuum chamber/MLI pressure fluctuated on all tests between levels as low as 10^{-8} torr with occassional bumps into the 10^{-4} torr range
c MLI pressure transducer nonoperational during test P9501
d Test preceded by a 96-hr chamber/test article vacuum checkout of test article heat guards. Average vacuum level 0.05 torr, chamber repressurized with GN_2
e Ground hold test failed to reach steady state boiloff. Test terminated, tank drained, and vacuum chamber evacuated in preparation for steady-state orbit test. No ascent profile performed
f Subsequent testing increased the vacuum exposure time to 2,030 hr and the LH_2 storage time to 1,732 hr with no further degradation.

4.2 Ground Hold Simulation Results

Table 6 defines the test environmental conditions and MHTB insulation thermal performance for the simulated ground hold phase. Three tests were performed with warm MLI boundary temperatures of 305, 235, and 164 K producing average insulation heat leak rates ($\dot{Q}_{\mathrm{insul}}$) ranging from 2,111 to 2,225 W (60.7–64 W/m^2). Penetration heat leak contributed a very small fraction (<0.2 percent) of the total. The environmental shroud GN_2 purge was maintained at a flow rate of ≈5 kg/min at nearly

constant temperature during each test (ranged from 270 to 279 K). The average heat leak was numerically predicted to be 2,172 W (62.5 W/m^2), which corresponds favorably with that measured. The temperature distribution through the insulation was averaged based on measured profile data in test P9601 and is presented in figure 27. The SOFI surface temperatures were maintained at or above –123 °C (150 K) and therefore successfully prevented purge gas liquefaction (except for a small localized area near an odd-shaped penetration peculiar to the MHTB on the lower dome). Post-test inspection of the foam insulation indicated no degradation except for minor surface cracking along the "knit lines" where the hand-sprayed or poured foam intersected with that robotically applied.

Table 6. TCS steady-state measured ground hold performance.

	Test Conditions							Measured TCS Performance (W)							Insul. Heat Flux W/m^2
	Chamber		MLI Purge			Chamber Press (torr)	Ullage Range (%)	$\dot{Q}_{boiloff}$	$\dot{Q}_{vent}$	$\dot{Q}_{fill\ line}$	$\dot{Q}_{press\ line}$	$\dot{Q}_{legs}$	$\dot{Q}_{others}$[a]	$\dot{Q}_{insul}$[b]	$\dot{Q}_{insul}$ / A_{tank}[c]
Test No.	Gas	Temp (K)	Gas	Rate (kg/min)	Temp. (K)										
P9502	GN_2	290	GN_2	5.7	279	753	4–10[d]	2,116	0.23	1.33	1.99	0.80	0.60	2,111	60.7
P9601	GN_2	279	GN_2	4.9	290	743	4–12[d]	2,213	0.12	1.04	2.23	0.75	0.50	2,208	63.5
P9602A[e]	GN_2	279	GN_2	4.7	270	752	1–23	2,227	0.12	0.95	0.31	0.62	0.47	2,224	64.0
Numerical Prediction	GN_2	300	GN_2	5.0	300	760	2	2,177[f]	–	2.57	2.00	0.81	–	2,172	62.5

a Includes the sum of solid conduction from interstitial pressure probe, manway pumpout line and ullage pressure line

b $\dot{Q}_{insul}$ calculated as $\dot{Q}_{boiloff}$ – the sum of $\dot{Q}_{penetrations}$

c Tank surface area taken as 34.75 m^2

d Liquid level estimated based on silicon diode temperature rake (continous liquid level sensor not operational)

e Insulation damage prior to test

f Predicted $\dot{Q}_{boiloff}$ calculated as predicted $\dot{Q}_{insul}$ + the sum of predicted $\dot{Q}_{penetrations}$

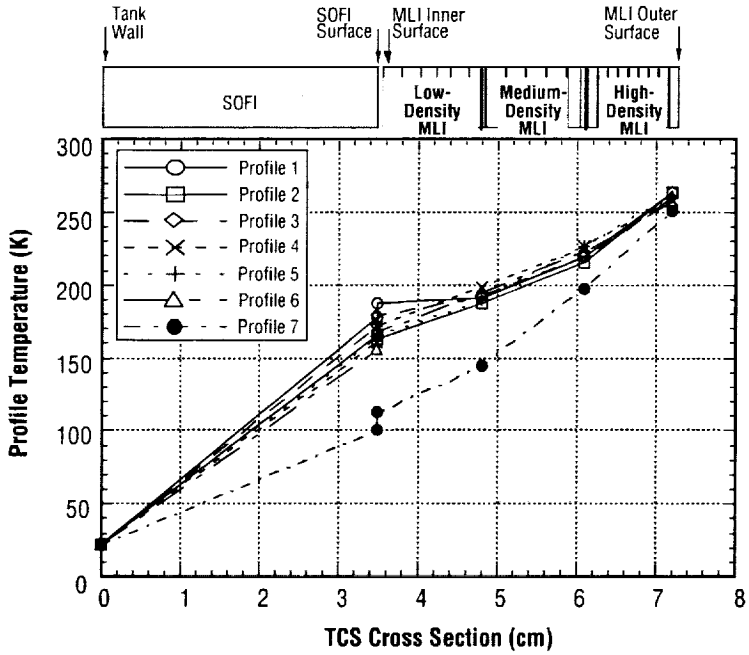

Figure 27. Test P9601—ground hold TCS temperature profiles.

An additional benefit of the foam insulation is that it minimizes the influence of heat flux on loaded propellant density. As described in reference 5, a representative ground hold heat leak for a He-purged MLI only (without foam) is 867 W/m^2 (275 Btu/hr-ft^2) as measured on a 2.67-m- (105-in.-) diameter tank tested. Reference 6 indicates that loaded hydrogen propellant density degradation with increasing ground hold heat flux can range from 5 to 13 percent for corresponding heat fluxes of 300–850 W/m^2. In comparison, the MHTB GN_2 purged foam/MLI arrangement yielded a hydrogen density degradation of 3 percent.

4.3 Ascent Simulation Results

Key items of interest observed during the ascent simulation included both insulation structural integrity under broadside venting loads and the time required to achieve insulation thermal equilibrium. The two video cameras positioned within the environmental shroud provided views of the entire lower dome and a portion of the tank sidewall enabled MLI observation during ascent. During the rapid evacuation (transition from 760 to 35 torr in ≈120 sec) the roll-wrapped MLI was observed to expand only slightly, which is attributed to its seamless robust construction.

The transient heat leak and chamber pressure experienced during ascent is illustrated in figures 28 and 29 for tests P9502 and P9601, respectively. The ground heat leak at the beginning of the ascent (at ≈1,000 min) is in the 2,000-W range in both tests. The heat leak decreased much faster during the second test (P9601) and reached the 10-W range, ≈1,000 min sooner than in the first test (P9502), supporting the idea that increased vacuum exposure is beneficial for reducing outgassing activity. The large pressure and heat leak excursions at ≈4,500 min on the first test (P9502) is attributed to outgassing with subsequent smaller heat leak spikes attributed to minor outgassing. Such outgassing effects were not experienced during the second test (P9601). Another observation is that the heat leak temporarily decreased due to MLI cooling below steady-state values during evacuation. This is clearly visible in figure 29 at 3,000 min where the heat leak is ≈30 percent below the steady-state value. An additional 5,000 min past this point were required to obtain steady-state boiloff.

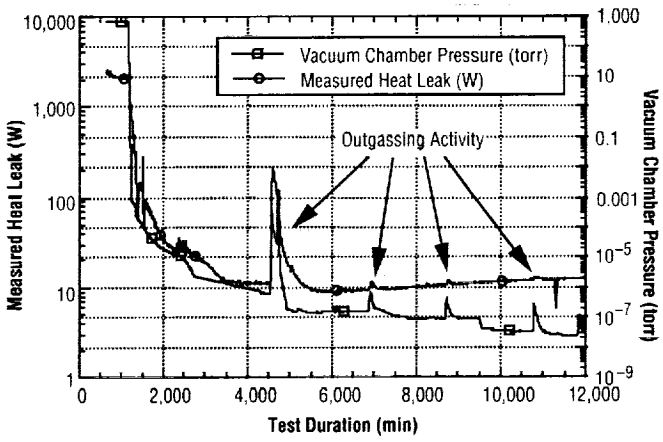

Figure 28. First test series (test P9502) ascent flight simulation thermal response.

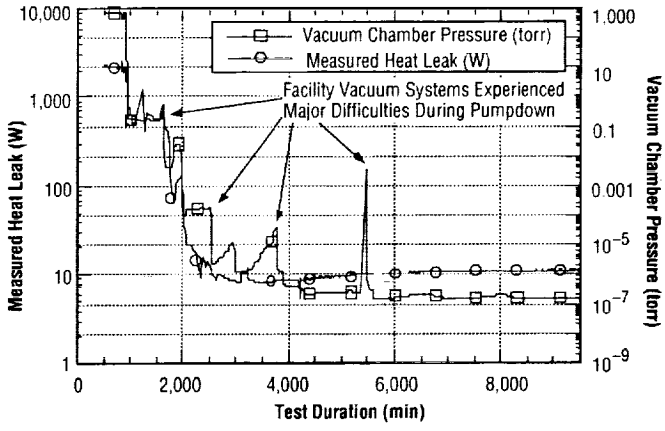

Figure 29. Second test series (test P9601) ascent flight simulation thermal response.

4.4 Orbit Hold Simulation Results

4.4.1 Measured Multilayer Insulation Performance

Results of the three orbit hold simulations are tabulated in table 7 and graphically presented in figure 30. The insulation heat leak ($\dot{Q}_{insul}$) ranged from 10.93 to 2.98 W (0.31 to 0.085 W/m^2) for warm boundaries ranging from 305 to 164 K, with and without penetration heat guards, and include some off-nominal conditions. The first test (P9502), conducted without heat guards, yielded heat leaks of 10.71 and 4.38 W with boundaries of 305 and 164 K, respectively. The second test (P9601) yielded lower heat leaks than in the first test; that is, 8.66 and 8.51 W without the heat guards and with the 305 K boundary. The lower heat leak observed in the second test is attributed to reduced outgassing, probably from the foam insulation. With the penetration heat guards activated, an even lower heat leak of 7.6 W (0.22 W/m^2) occurred with the 305 K boundary. The insulation heat leak of 7.64 W with the heat guards on is believed to most closely represent the true insulation performance at the 305 K boundary condition.

Table 7. TCS steady-state measured orbit hold performance.

	Test Conditions						Measured TCS Performance (W)							Insul. Heat Flux W/m^2
Test No.	Initial Conditions	Chamber Press (torr)	Interstitial[a] Press (torr)	Heat Guards	Heater Shroud Temp (K)	Ullage[b] Range (%)	$\dot{Q}_{boiloff}$	$\dot{Q}_{vent}$	$\dot{Q}_{fill\ line}$	$\dot{Q}_{press\ line}$	$\dot{Q}_{legs}$	$\dot{Q}_{others}$[c]	$\dot{Q}_{insul}$[d]	$\dot{Q}_{insul}$[e] / A_{tank}
P9502	Vacuum chamber rapid evacuation to orbit conditions after completion of ground hold test	6×10^{-8}	–	Off	305	12–17	13.10	0.05	0.07	0.71	1.45	0.10	10.71	0.31
		9×10^{-8}	–	Off	164	17–21	5.34	0.04	0.03	0.36	0.49	0.03	4.38	0.13
P9601	Vacuum chamber rapid evacuation to orbit conditions after completion of ground hold test	2×10^{-7}	–	Off	305	25–30	11.07	0.05	0.13	0.70	1.40	0.11	8.66	0.25
		6×10^{-8}	–	On	305	25–30	7.89	0.00	0.03	0.00	0.13	0.10	7.64	0.22
		2×10^{-7}	–	Off	305	25–30	10.90	0.05	0.16	0.67	1.40	0.11	8.51	0.24
		9×10^{-8}	–	Off	164	30–35	3.90	0.05	0.07	0.29	0.48	0.02	2.98	0.086
P9602A[f]	Vacuum chamber evacuated to 10^{-5} torr and test article vacuum conditioned prior to tanking of LH_2	5×10^{-8}	8×10^{-6}	Off	235	5–8	8.41	0.05	0.09	0.52	0.89	0.05	6.82	0.20
		4×10^{-8}	4×10^{-6}	On Legs Only	235	5–8	7.28	0.05	0.09	0.50	0.08	0.05	6.52	0.19
		4×10^{-8}	1×10^{-7}	Off	305	8–12	12.87	0.06	0.12	0.78	1.37	0.11	10.47	0.30
		4×10^{-8}	1×10^{-7}	On Legs Only	305	8–12	12.11	0.05	0.12	0.81	0.13	0.09	10.93	0.31

a On tests P9502 and P9601 the MLI interstitial pressure measurement system failed to operate

b Liquid level estimated based on silicon diode temperature rake (continous liquid level sensor not operational)

c Includes the sum of solid conduction from interstitial pressure probe, manway pumpout line, and ullage pressure line

d $\dot{Q}_{insul}$ calculated as ($\dot{Q}_{boiloff}$) – (the sum of $\dot{Q}_{penetrations}$)

e Tank surface area taken as 34.75 m^2.

f Insul damage prior to test.

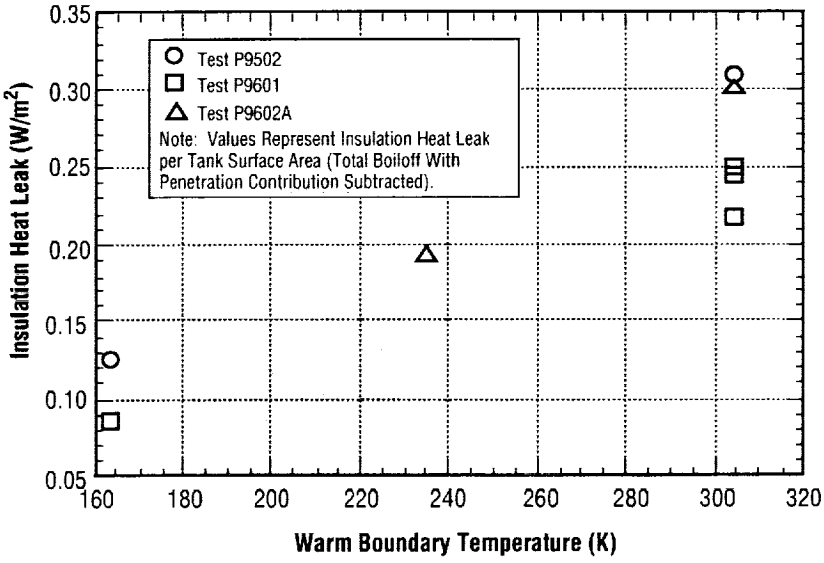

Figure 30. MHTB TCS steady-state orbit hold measured performance.

The heat leaks ascribed to penetrations for the various test conditions are also presented in table 7. The individual penetration heat leak magnitudes were calculated based on the temperatures measured on the various penetrations. The measured and computed penetration heat leak totals can be directly compared using the P9601 test data since testing was conducted both with and without the heat guards. With the warm boundary condition (305 K) in test P9601, the calculated penetration heat leak total was 2.39–2.41 W for the two test conditions without the heat guards and total measured heat leak of 10.9–11.07 W resulted. With the heat guards activated, the total heat leak measured was 7.89 W and the insulation heat leak was estimated to be 7.64 W (0.26 W was calculated to have occurred through the penetrations, primarily the composite tank legs). Thus, the actual penetration heat leak for the "without heat guards" condition was 3.3–3.4 W, that is, was higher than that calculated (2.4 W). With an average penetration heat leak of 3.35 W, the insulation heat leak for all the testing at the 305 K boundary condition ranged from 7.55 to 9.75 W. Further details regarding insulation temperature profiles on the insulation are presented in appendix C.

Results from the third test (P9602B) were compromised by significant MLI damage that occurred at the conclusion of the second test (test P9601). During a pressurized liquid expulsion test, the tank seal developed a leak, which overpressured and tore the manhole cover MLI ($\approx$1.5 m^2). The outer DAM layer was also torn loose, exposing $\approx$11 m^2 of Dacron (resulting in 44 DAM shields on a third of the tank surface area). The two video cameras located within the environmental shroud failed to reveal the damage; however, the incident accidentally demonstrated TCS robustness. Even with the damaged insulation, the measured boiloff rates of 10.47–10.93 W (with the 305 K boundary) clearly demonstrate TCS robustness. Additionally, a 235 K boundary was imposed in the third test and produced heat leaks of 6.52–6.82 W.

4.4.2 Multilayer Insulation Performance Comparisons

Historical MLI performance, expressed in terms of percent boiloff per day versus tank volume, is compared with the MHTB MLI data in figure 31. With the MHTB 45-layer blanket and the warm boundary condition (305 K), boiloff losses of 0.117 and 0.16 percent per day were measured with and without heat guards, respectively. McDonnell Douglas set the standard for demonstrated MLI performance in 1973.[5] A boiloff rate of 0.2 percent per day was achieved on a 2.67-m- (105-in.-) diameter tank with 70 layers of DAM and no penetration heat leak. Therefore, the variable density MLI decreased boiloff relative to that with the standard MLI by 41 percent with 25 fewer layers. Additionally, as illustrated in figure 32, when compared with calculated performance of a constant density MLI using the industry standard Lockheed equation and holding the blanket weight constant, variable density MLI heat leak was "half" that of the standard blanket for the highest boundary temperature. Similarly, with equal boiloff the standard blanket weighed 18 kg (40 lb) more (or 74 percent more) than the variable density MLI. System performances, however, tend to converge at the lowest boundary temperature of 160 K due to the decreased significance of radiation exchange between layers.

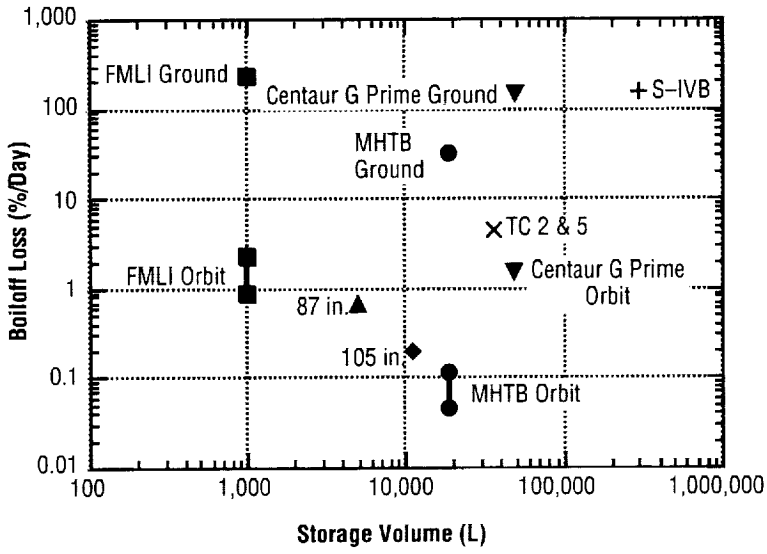

Symbols and Notes

+ AS-203 S-IVB Flight (Surf. Area/Vol = 1.21 (L/m), Hot Boundary =155 K, Internal Foam)

× Titan Centaur-2 and 5 Flight (Surf. Area/Vol=1.94 (L/m), Hot Boundary =144 to 311 K), (One Layer Mylar and Two Layers of Aluminized Mylar)

▼ Centaur G Prime LeRC Ground Tests (Surf. Area/Vol =1.64 (L/m), Hot Boundary = 222 K, 2×19 mm Foam Panels With Three Layers of DAM MLI)

▲ General Dynamics Corp. 87-in. Tank MSFC Ground Tests (Surf. Area/Vol = 2.82 (L/m), Hot Boundary = 277 K, 44 Layers of Goldized Kapton MLI)

◆ MDC 105-in. Tank MSFC Ground Tests (Surf. Area/Vol = 2.07 (L/m), Hot Boundary = 294 K, 70 Layers of DAM MLI), Ref. 5

■ FMLI Tank MSFC Ground Tests (Surf. Area/Vol = 5.25 (L/m), Hot Boundary =166 to 255 K, 10.2 mm SOFI, 16 Layers of DAM MLI)

● MHTB MSFC Ground Tests (Surf. Area/Vol = 1.92 (L/m), Hot Boundary =164 to 305 K, 31.75 mm SOFI, 45 Layers Variable Spaced DAM MLI)

Figure 31. Historical comparison of cryogenic insulation flight and test data.

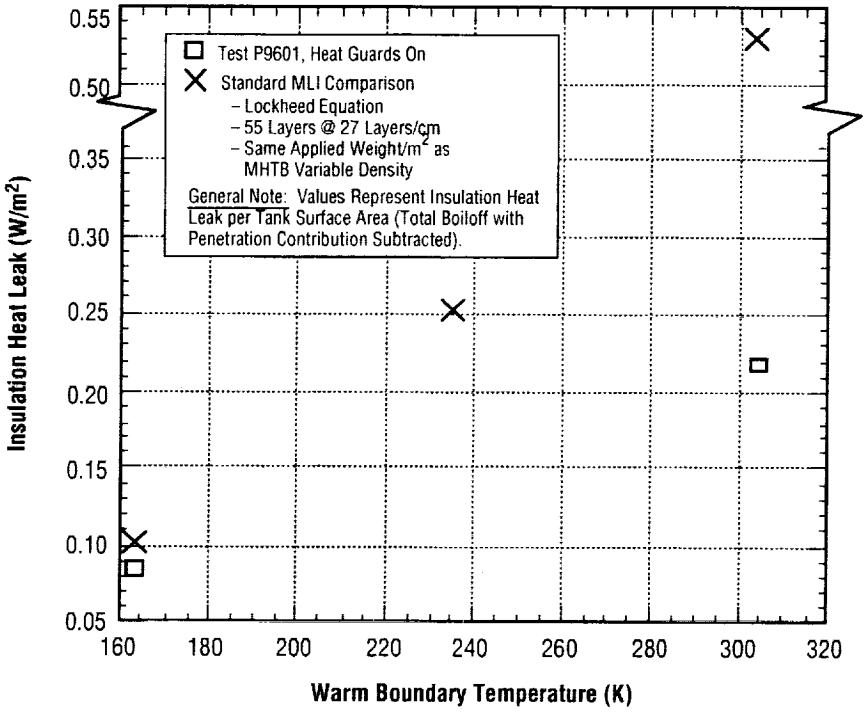

Figure 32. MHTB TCS steady-state orbit hold performance comparison with industry standard MLI computations.

MLI application examples for an upper stage (Centaur G Prime) with 0.25-mil DAM are tabulated in table 8. With an upper stage LH_2 tank surface area of 81.6 m^2 (878 ft^2), the blanket weight difference between the standard and variable density MLI would be 43 kg (95 lb). The weight difference is greater with 1/2-mil DAM (standard MLI is 65 kg heavier). However, thermally the 1/4- and 1/2-mil DAM radiation shielding performance is about equal for the warm boundary condition. The Centaur application weights for the 70-layer, 0.15-mil DAM blanket tested in 1973[5] are also listed in table 8 for comparison purposes. The 70 layer applied MLI weight, with facesheets, would be 96 kg (212 lb) with a 45-day boiloff loss of 8.4 percent (294 kg (648 lb) as compared with 4.5 percent (159 kg (350 lb) with the variable density. MLI facesheets in reference 6 were used to provide structural integrity; however, even without facesheets and with the lighter 0.15-mil DAM, the MHTB insulation is 10.7 kg (24 lb) lighter.

A second MLI application example that was explored was the effect of insulation performance on the manned Mars missions. Based on standard insulation performance, the boiloff was 0.73 percent per month with an injected mass into low-Earth orbit (IMLEO) of 177.5 metric tons. If the insulation mass is held constant and the boiloff is reduced by one half, then the IMLEO is reduced by 8.1 metric tons. The IMLEO reduction does not account for the smaller tank sizes and insulation weight decrease enabled by the boiloff reduction.

Table 8. MLI flight application comparison.

Upper Stage LH_2 Tank MLI Application Examples			
MLI System	Applied MLI Weight (kg)	45-Day Boiloff (kg)	45-Day Boiloff (%)
Variable density (1/4 mil)	57	159	4.5
Standard Lockheed equation (1/4 mil)	56 100	382 159	11.0 4.6
70-layer DAM, 1973 (Ref. 6)	96* 67.7**	294	8.4

Assumptions:
- Centaur G Prime Stage LH_2 Tank
- LH_2 Tank Surface Area 81.57 m^2
- LH_2 Propellant Weight 3,499 kg

* With Face Sheets
** Without Face Sheets

In comparing the MHTB data with historical data, it was noted that the density × effective conductivity, or the $\rho\ \kappa$ product, was a term frequently used to compare applied MLI weights in past programs. However, an insulation thickness must be assumed to compute both the density and effective conductivity. Although MLI layer density is usually described in terms of layers per unit thickness, the reality is that the applied thickness cannot be accurately ascertained. The layer density varies with position on the tank, especially in normal gravity; i.e., the layers are compressed on top of the tank, expanded (sag) on the bottom, and somewhere in between on the sides. Further, in a zero-g environment, the MLI is likely to be more fluffed relative to the normal gravity geometry. A more appropriate comparison basis would be provided by the product of heat leak × MLI mass per unit tank surface area. The $q\ M_{insul}$ product for the variable density MLI without penetration heat leak was 0.15 W-kg/m^4 with the 305 K boundary condition, whereas it is 0.36 W-kg/m^4 with standard MLI (Lockheed equation). The $q\ M_{insul}$ product for the reference 5 blanket is 0.48 and 0.34 W-kg/m^4 with and without facesheets, respectively. Therefore, compared with historic standards, the MHTB MLI performance improvement is substantial and ranges from 42–69 percent based on the product "heat leak × MLI mass" or $q\ M_{insul}$ performance measurement parameter.

4.4.3 Spray-On Foam Performance

As expected, the SOFI layer provides essentially no thermal protection at vacuum conditions. Averaged temperatures measured at various MLI layer locations and on the SOFI are presented in figure 33 for both ground hold and orbital conditions. The ground hold data indicate that most of the temperature gradient, or energy stored, occurs in the SOFI. However, during orbital conditions, the SOFI surface temperature is only slightly warmer than the LH_2 and most of the gradient occurs across the MLI, which for the 305 K boundary set point, is radiation dominated as illustrated by the 4th-order temperature profile shape. The MLI temperature profile is nearly linear with a 164 K boundary since solid conduction is the dominate mode. The excess thermal energy stored in the SOFI during ground hold, which is rejected into the LH_2 during the transition into the orbit hold environment, resulted in about 5 kg or 0.4 percent of additional boiloff. Thus, the heat soakback effect of the foam is almost negligible, and the primary consideration becomes that of the on-orbit foam weight as compared with that of the purge bag/He purge subsystem weight.

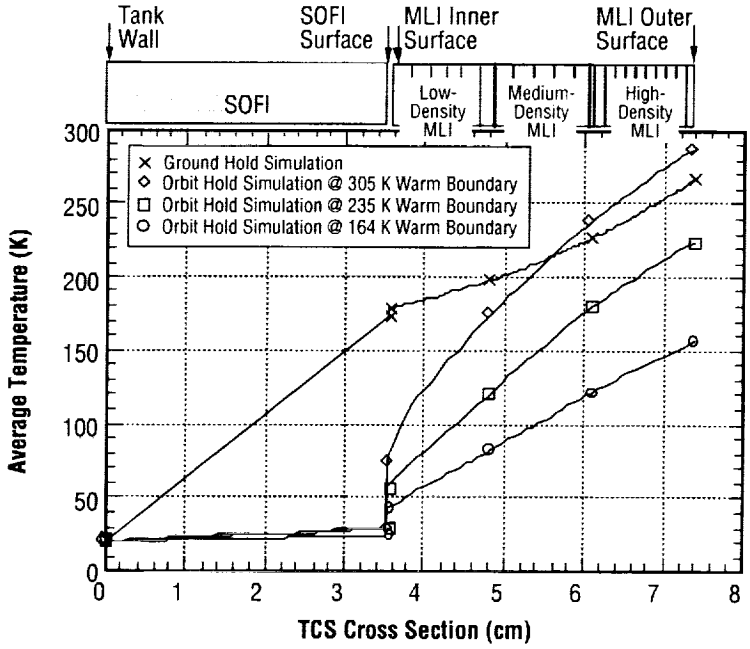

Figure 33. Test program average TCS temperature profiles.

4.5 Test Facility and Hardware Performance

Overall, the test facility performed very well, especially during the critical orbital simulations. For the ground hold phase, the vacuum chamber was maintained at ambient pressure with a dry GN_2 purge (dew point of –54 °C) to provide MLI protection. Rapid ascent vacuum chamber operations were somewhat erratic due to chamber control problems and, in the first test, outgassing problems. For all orbital tests the vacuum chamber pressure was maintained in the low 10^{-6} torr range (with LN_2 cold walls engaged), with the exception of transients due to test article leakage and outgassing. During orbit hold simulations, the desired warm or cold boundary temperatures on the MLI surfaces were successfully controlled by the environmental shroud. The facility back-pressure control system was especially effective in maintaining the tight ullage pressure control requirements during the orbit hold testing and controlled ullage pressures to within ±0.00689 kPa (0.001 psi) of the set point.

The MHTB continuous liquid level capacitance probe did not operate properly during the testing, necessitating that the ullage volume for each test be estimated based on the discreet level sensing provided by the silicon diode sensors on the instrumentation rake. It was subsequently realized that mounting the capacitance probe oscillator on a cold frame structure had compromised the probe operation; i.e., the oscillator should have been mounted on a warmer surface. (In subsequent tests, the probe performed satisfactorily.) Additionally, the MLI interstitial pressure sensor failed to operate until the third test. The interstitial pressure probe results were questionable, but typically indicated a pressure level in the mid-10^{-6} torr range or less.

5. CONCLUSIONS AND RECOMMENDATIONS

The MHTB, an 18-m^3 hydrogen test article, was successfully utilized to experimentally evaluate the performance of a FMLI thermal control concept in the MSFC vacuum facility at test stand 300. The Isofoam SS–1171 SOFI was designed to protect against ground hold/ascent flight environments and enabled the use of a dry N_2 purge as opposed to the more complex/heavy He-purge subsystem normally required. The 45-layer MLI, designed for an on-orbit storage period of 45 days, included several unique features including a variable density MLI layup, larger but fewer DAM perforations for ascent venting, and roll-wrap installation of the MLI with a commercially established process. The MLI roll-wrap installation process resulted in a very robust, virtually seamless insulation and would enable an estimated man-hour savings of 2,400 hr per LH_2 and O_2 tank set (3-m diameter). Further, the installation concept enables a more repeatable, consistent product as compared with individually constructed MLI blankets.

The MSFC vacuum facility and associated controls performed very well, producing over 2,000 hr of testing. During orbital simulations, the vacuum was successfully maintained at 10^{-6} torr or less and the ullage pressure control system maintained LH_2 tank pressure within ±0.00689 kPa (±0.001 psi) of the prescribed set point.

Ground hold testing produced the expected average heat leak of 63 W/m^2 at a foam surface temperature of 170 K. The SOFI successfully prevented LN_2 purge gas liquefaction except for a small localized area near an odd-shaped penetration peculiar to the MHTB. It is concluded that SOFI-type insulation is a feasible means for eliminating the need for He purge-bag subsystems. Furthermore, the foam insulation reduced the influence of heat flux on effective propellant density; i.e., a hydrogen density degradation of <3 percent occurred as compared with 13 percent with "MLI only" and a He purge. The simulated ascent test successfully demonstrated MLI venting with the large (1.27-cm-diameter), widely spaced (7.6 cm apart) perforations. The heat leak decreased to the orbital steady-state value much faster in the second test series due to reduced outgassing associated with the foam insulation. Including testing subsequent to the TCS performance testing, the thermal cycling effects of five fill/drain cycles, 1,730 hr of hydrogen storage, and 2,030 hr of vacuum time on the SOFI were minor. No performance degradation was measured and no surface cracking occurred except in two areas along knit lines where thick hand-sprayed foam intersected with the robotically sprayed foam. The excess thermal energy stored in the SOFI and released after orbit insertion (or heat soakback) was almost negligible (≈0.4 percent added boiloff).

The simulated orbit hold periods produced MLI heat leaks ranging from 0.083 to 0.21 W/m^2 at warm boundary temperatures of 164 and 305 K, respectively. This performance translates into a 3-percent boiloff loss in a 30-day orbital hold period with the 305 K boundary temperature. When compared to the best previously measured performance of a traditional MLI system, a 41-percent heat leak reduction with 25 fewer layers at the 300 K boundary condition was achieved. When compared with the calculated performance of a constant density MLI using the industry standard Lockheed equation, the MHTB insulation

heat leak was half that with the standard blanket. On a Centaur upper stage hydrogen tank, the insulation weight reduction would be 43 kg (95 lb) or the boiloff can be reduced by 223 kg (490 lb) compared with a standard blanket. This substantial performance improvement is attributed to the variable density layup, the vent perforation pattern, and the almost seamless MLI roll-wrap installation.

Historically, the product of density and effective conductivity $\rho\,\kappa$ has been used to compare MLI "in orbit" performance. However, such a comparison necessitates an assumed MLI thickness that cannot be accurately verified. A more appropriate comparison basis is the product of the heat leak per unit area and the MLI mass per unit area or $q\,M_{insul}$ with the units of W-kg/m^4. Assuming equal heat leak, the MHTB and standard MLI $q\,M_{insul}$ products are 0.15 and 0.26 W-kg/m^4, respectively.

Overall, the MHTB insulation demonstrated excellent performance for all mission phases representative of a cryogenic upper stage. The development of analytical modeling techniques is planned to enable the application of the MHTB MLI (variable density and large vent holes) to other design/mission requirements.

APPENDIX A—MULTIPURPOSE HYDROGEN TEST BED TANKING TABLE

A tanking table has been calculated based on the design geometry of the multipurpose hydrogen test bed (MHTB) test tank. This table provides volume, ullage, and mass estimates based on the fluid level as referenced to the tank bottom. Tank fluid level is measured with a capacitance probe mounted such that its active length begins 10 cm above the tank bottom and continues for 2.878 m (113.3125 in.) or to a height 2.978 m (117.25 in.) above the tank bottom. Therefore, all capacitance probe height data must be corrected by adding 10 cm (3.9375 in.) to the recorded height value to obtain the actual liquid height inside the tank.

Multipurpose Hydrogen Test Bed Tanking Table

Total Tank Volume = 639.34 ft^3 18.10 m^3
LH_2 Density = 4.419 lbm/ft^3 70.786 kg/m^3
Note: Height is measured from the bottom of the tank.

Height (in.)	Height (cm)	Volume (ft^3)	Volume (m^3)	Ullage (%)	Liquid (%)	Liquid Mass (lbm)	Liquid Mass (kg)
0.00	0.00	0.00	0.0000	100.00	0.00	0.00	0.0000
0.50	1.27	0.05	0.0015	99.99	0.01	0.24	0.1087
1.00	2.54	0.22	0.0061	99.97	0.03	0.95	0.4324
1.50	3.81	0.48	0.0137	99.92	0.08	2.13	0.9673
2.00	5.08	0.85	0.0242	99.87	0.13	3.77	1.7098
2.50	6.35	1.33	0.0375	99.79	0.21	5.86	2.6560
3.00	7.62	1.90	0.0537	99.70	0.30	8.38	3.8025
3.50	8.89	2.57	0.0727	99.60	0.40	11.34	5.1453
4.00	10.16	3.33	0.0944	99.48	0.52	14.73	6.6809
4.50	11.43	4.19	0.1187	99.34	0.66	18.53	8.4055
5.00	12.70	5.15	0.1457	99.20	0.80	22.74	10.3154
5.50	13.97	6.19	0.1753	99.03	0.97	27.35	12.4068
6.00	15.24	7.32	0.2073	98.85	1.15	32.36	14.6762
6.50	16.51	8.54	0.2419	98.66	1.34	37.74	17.1198
7.00	17.78	9.85	0.2788	98.46	1.54	43.51	19.7338
7.50	19.05	11.23	0.3181	98.24	1.76	49.64	22.5146
8.00	20.32	12.70	0.3597	98.01	1.99	56.13	25.4585
8.50	21.59	14.25	0.4035	97.77	2.23	62.97	28.5618
9.00	22.86	15.88	0.4495	97.52	2.48	70.15	31.8207
9.50	24.13	17.58	0.4977	97.25	2.75	77.67	35.2316
10.00	25.40	19.35	0.5480	96.97	3.03	85.52	38.7907
10.50	26.67	21.20	0.6003	96.68	3.32	93.68	42.4943
11.00	27.94	23.12	0.6546	96.38	3.62	102.16	46.3388
11.50	29.21	25.10	0.7109	96.07	3.93	110.94	50.3204
12.00	30.48	27.16	0.7690	95.75	4.25	120.01	54.4354
12.50	31.75	29.28	0.8290	95.42	4.58	129.37	58.6801
13.00	33.02	31.46	0.8907	95.08	4.92	139.00	63.0509
13.50	34.29	33.70	0.9542	94.73	5.27	148.91	67.5439
14.00	35.56	36.00	1.0193	94.37	5.63	159.08	72.1556
14.50	36.83	38.36	1.0861	94.00	6.00	169.50	76.8821
15.00	38.10	40.77	1.1545	93.62	6.38	180.16	81.7198
15.50	39.37	43.24	1.2243	93.24	6.76	191.06	86.6650

Multipurpose Hydrogen Test Bed Tanking Table (Continued)

Height (in.)	Height (cm)	Volume (ft^3)	Volume (m^3)	Ullage (%)	Liquid (%)	Liquid Mass (lbm)	Liquid Mass (kg)
16.00	40.64	45.76	1.2957	92.84	7.16	202.19	91.7140
16.50	41.91	48.32	1.3684	92.44	7.56	213.55	96.8630
17.00	43.18	50.94	1.4425	92.03	7.97	225.11	102.1084
17.50	44.45	53.60	1.5179	91.62	8.38	236.88	107.4464
18.00	45.72	56.31	1.5946	91.19	8.81	248.84	112.8734
18.50	46.99	59.06	1.6724	90.76	9.24	261.00	118.3856
19.00	48.26	61.85	1.7515	90.33	9.67	273.33	123.9794
19.50	49.53	64.68	1.8316	89.88	10.12	285.83	129.6510
20.00	50.80	67.55	1.9128	89.43	10.57	298.50	135.3967
20.50	52.07	70.45	1.9949	88.98	11.02	311.32	141.2128
21.00	53.34	73.39	2.0780	88.52	11.48	324.29	147.0957
21.50	54.61	76.35	2.1620	88.06	11.94	337.40	153.0415
22.00	55.88	79.35	2.2469	87.59	12.41	350.64	159.0467
22.50	57.15	82.37	2.3325	87.12	12.88	364.00	165.1074
23.00	58.42	85.42	2.4188	86.64	13.36	377.48	171.2200
23.50	59.69	88.49	2.5059	86.16	13.84	391.06	177.3808
24.00	60.96	91.59	2.5935	85.67	14.33	404.74	183.5861
24.50	62.23	94.71	2.6818	85.19	14.81	418.51	189.8321
25.00	63.50	97.84	2.7705	84.70	15.30	432.36	196.1152
25.50	64.77	100.99	2.8598	84.20	15.80	446.29	202.4317
26.00	66.04	104.16	2.9494	83.71	16.29	460.28	208.7778
26.50	67.31	107.34	3.0394	83.21	16.79	474.32	215.1498
27.00	68.58	110.53	3.1298	82.71	17.29	488.42	221.5441
27.50	69.85	113.73	3.2204	82.21	17.79	502.56	227.9569
28.00	71.12	116.93	3.3112	81.71	18.29	516.73	234.3845
28.50	72.39	120.15	3.4021	81.21	18.79	530.92	240.8233
29.00	73.66	123.36	3.4932	80.70	19.30	545.14	247.2695
29.50	74.93	126.58	3.5843	80.20	19.80	559.36	253.7193
30.00	76.20	129.80	3.6755	79.70	20.30	573.58	260.1718
30.50	77.47	133.02	3.7666	79.19	20.81	587.80	266.6225
31.00	78.74	136.23	3.8577	78.69	21.31	602.02	273.0731
31.50	80.01	139.45	3.9489	78.19	21.81	616.24	279.5237
32.00	81.28	142.67	4.0400	77.68	22.32	630.47	285.9743
32.50	82.55	145.89	4.1311	77.18	22.82	644.69	292.4250
33.00	83.82	149.11	4.2222	76.68	23.32	658.91	298.8756
33.50	85.09	152.33	4.3134	76.17	23.83	673.13	305.3262
34.00	86.36	155.54	4.4045	75.67	24.33	687.35	311.7768
34.50	87.63	158.76	4.4956	75.17	24.83	701.57	318.2275
35.00	88.90	161.98	4.5868	74.66	25.34	715.79	324.6781
35.50	90.17	165.20	4.6779	74.16	25.84	730.01	331.1287

Multipurpose Hydrogen Test Bed Tanking Table (Continued)

Height (in.)	Height (cm)	Volume (ft^3)	Volume (m^3)	Ullage (%)	Liquid (%)	Liquid Mass (lbm)	Liquid Mass (kg)
36.00	91.44	168.42	4.7690	73.66	26.34	744.24	337.5793
36.50	92.71	171.63	4.8601	73.15	26.85	758.46	344.0300
37.00	93.98	174.85	4.9513	72.65	27.35	772.68	350.4806
37.50	95.25	178.07	5.0424	72.15	27.85	786.90	356.9312
38.00	96.52	181.29	5.1335	71.64	28.36	801.12	363.3818
38.50	97.79	184.51	5.2247	71.14	28.86	815.34	369.8325
39.00	99.06	187.73	5.3158	70.64	29.36	829.56	376.2831
39.50	100.33	190.94	5.4069	70.13	29.87	843.78	382.7337
40.00	101.60	194.16	5.4980	69.63	30.37	858.00	389.1843
40.50	102.87	197.38	5.5892	69.13	30.87	872.23	395.6350
41.00	104.14	200.60	5.6803	68.62	31.38	886.45	402.0856
41.50	105.41	203.82	5.7714	68.12	31.88	900.67	408.5362
42.00	106.68	207.03	5.8626	67.62	32.38	914.89	414.9868
42.50	107.95	210.25	5.9537	67.11	32.89	929.11	421.4375
43.00	109.22	213.47	6.0448	66.61	33.39	943.33	427.8881
43.50	110.49	216.69	6.1359	66.11	33.89	957.55	434.3387
44.00	111.76	219.91	6.2271	65.60	34.40	971.77	440.7893
44.50	113.03	223.13	6.3182	65.10	34.90	986.00	447.2400
45.00	114.30	226.34	6.4093	64.60	35.40	1000.22	453.6906
45.50	115.57	229.56	6.5005	64.09	35.91	1014.44	460.1412
46.00	116.84	232.78	6.5916	63.59	36.41	1028.66	466.5918
46.50	118.11	236.00	6.6827	63.09	36.91	1042.88	473.0425
47.00	119.38	239.22	6.7738	62.58	37.42	1057.10	479.4931
47.50	120.65	242.43	6.8650	62.08	37.92	1071.32	485.9437
48.00	121.92	245.65	6.9561	61.58	38.42	1085.54	492.3943
48.50	123.19	248.87	7.0472	61.07	38.93	1099.76	498.8450
49.00	124.46	252.09	7.1384	60.57	39.43	1113.99	505.2956
49.50	125.73	255.31	7.2295	60.07	39.93	1128.21	511.7462
50.00	127.00	258.53	7.3206	59.56	40.44	1142.43	518.1968
50.50	128.27	261.74	7.4117	59.06	40.94	1156.65	524.6475
51.00	129.54	264.96	7.5029	58.56	41.44	1170.87	531.0981
51.50	130.81	268.18	7.5940	58.05	41.95	1185.09	537.5487
52.00	132.08	271.40	7.6851	57.55	42.45	1199.31	543.9993
52.50	133.35	274.62	7.7763	57.05	42.95	1213.53	550.4500
53.00	134.62	277.83	7.8674	56.54	43.46	1227.76	556.9006
53.50	135.89	281.05	7.9585	56.04	43.96	1241.98	563.3512
54.00	137.16	284.27	8.0496	55.54	44.46	1256.20	569.8018
54.50	138.43	287.49	8.1408	55.03	44.97	1270.42	576.2525
55.00	139.70	290.71	8.2319	54.53	45.47	1284.64	582.7031
55.50	140.97	293.93	8.3230	54.03	45.97	1298.86	589.1537

Multipurpose Hydrogen Test Bed Tanking Table (Continued)

Height (in.)	Height (cm)	Volume (ft^3)	Volume (m^3)	Ullage (%)	Liquid (%)	Liquid Mass (lbm)	Liquid Mass (kg)
56.00	142.24	297.14	8.4142	53.52	46.48	1313.08	595.6043
56.50	143.51	300.36	8.5053	53.02	46.98	1327.30	602.0550
57.00	144.78	303.58	8.5964	52.52	47.48	1341.53	608.5056
57.50	146.05	306.80	8.6875	52.01	47.99	1355.75	614.9562
58.00	147.32	310.02	8.7787	51.51	48.49	1369.97	621.4068
58.50	148.59	313.23	8.8698	51.01	48.99	1384.19	627.8575
59.00	149.86	316.45	8.9609	50.50	49.50	1398.41	634.3081
59.50	151.13	319.67	9.0521	50.00	50.00	1412.63	640.7587
60.00	152.40	322.89	9.1432	49.50	50.50	1426.85	647.2093
60.50	153.67	326.11	9.2343	48.99	51.01	1441.07	653.6600
61.00	154.94	329.33	9.3254	48.49	51.51	1455.29	660.1106
61.50	156.21	332.54	9.4166	47.99	52.01	1469.52	666.5612
62.00	157.48	335.76	9.5077	47.48	52.52	1483.74	673.0118
62.50	158.75	338.98	9.5988	46.98	53.02	1497.96	679.4625
63.00	160.02	342.20	9.6900	46.48	53.52	1512.18	685.9131
63.50	161.29	345.42	9.7811	45.97	54.03	1526.40	692.3637
64.00	162.56	348.63	9.8722	45.47	54.53	1540.62	698.8143
64.50	163.83	351.85	9.9633	44.97	55.03	1554.84	705.2650
65.00	165.10	355.07	10.0545	44.46	55.54	1569.06	711.7156
65.50	166.37	358.29	10.1456	43.96	56.04	1583.29	718.1662
66.00	167.64	361.51	10.2367	43.46	56.54	1597.51	724.6168
66.50	168.91	364.73	10.3278	42.95	57.05	1611.73	731.0675
67.00	170.18	367.94	10.4190	42.45	57.55	1625.95	737.5181
67.50	171.45	371.16	10.5101	41.95	58.05	1640.17	743.9687
68.00	172.72	374.38	10.6012	41.44	58.56	1654.39	750.4193
68.50	173.99	377.60	10.6924	40.94	59.06	1668.61	756.8700
69.00	175.26	380.82	10.7835	40.44	59.56	1682.83	763.3206
69.50	176.53	384.03	10.8746	39.93	60.07	1697.06	769.7712
70.00	177.80	387.25	10.9657	39.43	60.57	1711.28	776.2218
70.50	179.07	390.47	11.0569	38.93	61.07	1725.50	782.6725
71.00	180.34	393.69	11.1480	38.42	61.58	1739.72	789.1231
71.50	181.61	396.91	11.2391	37.92	62.08	1753.94	795.5737
72.00	182.88	400.13	11.3303	37.42	62.58	1768.16	802.0243
72.50	184.15	403.34	11.4214	36.91	63.09	1782.38	808.4750
73.00	185.42	406.56	11.5125	36.41	63.59	1796.60	814.9256
73.50	186.69	409.78	11.6036	35.91	64.09	1810.82	821.3762
74.00	187.96	413.00	11.6948	35.40	64.60	1825.05	827.8268
74.50	189.23	416.22	11.7859	34.90	65.10	1839.27	834.2775
75.00	190.50	419.43	11.8770	34.40	65.60	1853.49	840.7281
75.50	191.77	422.65	11.9682	33.89	66.11	1867.71	847.1787

Multipurpose Hydrogen Test Bed Tanking Table (Continued)

Height (in.)	Height (cm)	Volume (ft^3)	Volume (m^3)	Ullage (%)	Liquid (%)	Liquid Mass (lbm)	Liquid Mass (kg)
76.00	193.04	425.87	12.0593	33.39	66.61	1881.93	853.6293
76.50	194.31	429.09	12.1504	32.89	67.11	1896.15	860.0800
77.00	195.58	432.31	12.2415	32.38	67.62	1910.37	866.5306
77.50	196.85	435.53	12.3327	31.88	68.12	1924.59	872.9812
78.00	198.12	438.74	12.4238	31.38	68.62	1938.82	879.4318
78.50	199.39	441.96	12.5149	30.87	69.13	1953.04	885.8824
79.00	200.66	445.18	12.6061	30.37	69.63	1967.26	892.3331
79.50	201.93	448.40	12.6972	29.87	70.13	1981.48	898.7837
80.00	203.20	451.62	12.7883	29.36	70.64	1995.70	905.2343
80.50	204.47	454.83	12.8794	28.86	71.14	2009.92	911.6849
81.00	205.74	458.05	12.9706	28.36	71.64	2024.14	918.1356
81.50	207.01	461.27	13.0617	27.85	72.15	2038.36	924.5862
82.00	208.28	464.49	13.1528	27.35	72.65	2052.58	931.0368
82.50	209.55	467.71	13.2440	26.85	73.15	2066.81	937.4874
83.00	210.82	470.93	13.3351	26.34	73.66	2081.03	943.9381
83.50	212.09	474.14	13.4262	25.84	74.16	2095.25	950.3887
84.00	213.36	477.36	13.5173	25.34	74.66	2109.47	956.8393
84.50	214.63	480.58	13.6085	24.83	75.17	2123.69	963.2899
85.00	215.90	483.80	13.6996	24.33	75.67	2137.91	969.7406
85.50	217.17	487.02	13.7907	23.83	76.17	2152.13	976.1912
86.00	218.44	490.23	13.8819	23.32	76.68	2166.35	982.6418
86.50	219.71	493.45	13.9730	22.82	77.18	2180.58	989.0924
87.00	220.98	496.67	14.0641	22.32	77.68	2194.80	995.5431
87.50	222.25	499.89	14.1552	21.81	78.19	2209.02	1001.9937
88.00	223.52	503.11	14.2464	21.31	78.69	2223.24	1008.4443
88.50	224.79	506.33	14.3375	20.80	79.20	2237.46	1014.8949
89.00	226.06	509.54	14.4286	20.30	79.70	2251.68	1021.3456
89.50	227.33	512.76	14.5198	19.80	80.20	2265.90	1027.7962
90.00	228.60	515.98	14.6108	19.30	80.70	2280.12	1034.2433
90.50	229.87	519.19	14.7019	18.79	81.21	2294.33	1040.6895
91.00	231.14	522.41	14.7929	18.29	81.71	2308.52	1047.1282
91.50	232.41	525.61	14.8837	17.79	82.21	2322.69	1053.5559
92.00	233.68	528.81	14.9743	17.29	82.71	2336.83	1059.9687
92.50	234.95	532.00	15.0646	16.79	83.21	2350.93	1066.3630
93.00	236.22	535.18	15.1546	16.29	83.71	2364.98	1072.7350
93.50	237.49	538.35	15.2443	15.80	84.20	2378.97	1079.0811
94.00	238.76	541.50	15.3335	15.30	84.70	2392.89	1085.3976
94.50	240.03	544.63	15.4223	14.81	85.19	2406.74	1091.6807
95.00	241.30	547.75	15.5105	14.33	85.67	2420.51	1097.9267
95.50	242.57	550.84	15.5982	13.84	86.16	2434.19	1104.1320

Multipurpose Hydrogen Test Bed Tanking Table (Continued)

Height (in.)	Height (cm)	Volume (ft^3)	Volume (m^3)	Ullage (%)	Liquid (%)	Liquid Mass (lbm)	Liquid Mass (kg)
96.00	243.84	553.92	15.6852	13.36	86.64	2447.78	1110.2928
96.50	245.11	556.97	15.7716	12.88	87.12	2461.25	1116.4054
97.00	246.38	559.99	15.8572	12.41	87.59	2474.61	1122.4661
97.50	247.65	562.99	15.9420	11.94	88.06	2487.85	1128.4713
98.00	248.92	565.95	16.0260	11.48	88.52	2500.96	1134.4171
98.50	250.19	568.89	16.1091	11.02	88.98	2513.93	1140.3000
99.00	251.46	571.79	16.1913	10.57	89.43	2526.75	1146.1161
99.50	252.73	574.66	16.2724	10.12	89.88	2539.42	1151.8618
100.00	254.00	577.49	16.3526	9.67	90.33	2551.92	1157.5334
100.50	255.27	580.28	16.4316	9.24	90.76	2564.26	1163.1272
101.00	256.54	583.03	16.5095	8.81	91.19	2576.41	1168.6394
101.50	257.81	585.73	16.5861	8.38	91.62	2588.37	1174.0664
102.00	259.08	588.40	16.6615	7.97	92.03	2600.14	1179.4044
102.50	260.35	591.01	16.7356	7.56	92.44	2611.71	1184.6498
103.00	261.62	593.58	16.8084	7.16	92.84	2623.06	1189.7988
103.50	262.89	596.10	16.8797	6.76	93.24	2634.19	1194.8478
104.00	264.16	598.57	16.9496	6.38	93.62	2645.09	1199.7930
104.50	265.43	600.98	17.0179	6.00	94.00	2655.76	1204.6307
105.00	266.70	603.34	17.0847	5.63	94.37	2666.18	1209.3572
105.50	267.97	605.64	17.1498	5.27	94.73	2676.34	1213.9689
106.00	269.24	607.88	17.2133	4.92	95.08	2686.25	1218.4619
106.50	270.51	610.06	17.2751	4.58	95.42	2695.88	1222.8327
107.00	271.78	612.18	17.3350	4.25	95.75	2705.24	1227.0774
107.50	273.05	614.23	17.3932	3.93	96.07	2714.31	1231.1924
108.00	274.32	616.22	17.4494	3.62	96.38	2723.09	1235.1740
108.50	275.59	618.14	17.5037	3.32	96.68	2731.57	1239.0185
109.00	276.86	619.99	17.5560	3.03	96.97	2739.73	1242.7221
109.50	278.13	621.76	17.6063	2.75	97.25	2747.58	1246.2812
110.00	279.40	623.46	17.6545	2.48	97.52	2755.10	1249.6921
110.50	280.67	625.09	17.7005	2.23	97.77	2762.28	1252.9510
111.00	281.94	626.64	17.7444	1.99	98.01	2769.13	1256.0543
111.50	283.21	628.11	17.7860	1.76	98.24	2775.62	1258.9981
112.00	284.48	629.49	17.8253	1.54	98.46	2781.75	1261.7790
112.50	285.75	630.80	17.8622	1.34	98.66	2787.51	1264.3930
113.00	287.02	632.02	17.8967	1.15	98.85	2792.90	1266.8366
113.50	288.29	633.15	17.9288	0.97	99.03	2797.90	1269.1060
114.00	289.56	634.19	17.9583	0.80	99.20	2802.51	1271.1974
114.50	290.83	635.15	17.9853	0.66	99.34	2806.72	1273.1073
115.00	292.10	636.01	18.0097	0.52	99.48	2810.52	1274.8319
115.50	293.37	636.77	18.0313	0.40	99.60	2813.91	1276.3675

Multipurpose Hydrogen Test Bed Tanking Table (Continued)

Height (in.)	Height (cm)	Volume (ft^3)	Volume (m^3)	Ullage (%)	Liquid (%)	Liquid Mass (lbm)	Liquid Mass (kg)
116.00	294.64	637.44	18.0503	0.30	99.70	2816.87	1277.7103
116.50	295.91	638.01	18.0665	0.21	99.79	2819.40	1278.8567
117.00	297.18	638.49	18.0799	0.13	99.87	2821.48	1279.8030
117.50	298.45	638.86	18.0904	0.08	99.92	2823.12	1280.5455
118.00	299.72	639.12	18.0979	0.03	99.97	2824.30	1281.0804
118.50	300.99	639.28	18.1025	0.01	99.99	2825.01	1281.4041
119.00	302.26	639.34	18.1040	0.00	100.00	2825.25	1281.5128

APPENDIX B—TEST ARTICLE INSTRUMENTATION

This appendix contains the instrumentation database document that describes the MHTB instrumentation used in the insulation performance testing. Some of the information repeats that presented in the main body of this Technical Memorandum and some is applicable only to testing subsequently performed with a zero-g pressure control system. However, in the interest of completeness the entire document is presented.

Multipurpose Hydrogen Test Bed Instrumentation Database Document

James Martin/EP25

This document details the instrumentation used on the multipurpose hydrogen test bed (MHTB) hardware. This includes instrumentation used on the tank interior/exterior, tank insulation/penetrations, tank support system and environmental shroud. This document is dedicated primarily to instrumentation that was installed during fabrication and assembly of test hardware; however, some facility instrumentation is noted if it is mounted in close proximity to the test hardware.

The breakdown of test article instrumentation used on the MHTB is outlined by the following categories:

1. Program Overview and Hardware Description
2. General Tank Instrumentation Layout
3. Thermal Control System Instrumentation
4. Tank Support Leg Penetration Instrumentation
5. Vent Penetration Instrumentation
6. Fill/Drain Penetration Instrumentation
7. Pressurization Penetration Instrumentation
8. Multilayer Insulation Interstitial Pressure Probe Instrumentation
9. Manhole Cover and Pump-Out Penetration Instrumentation
10. Internal Rake and Fluid Instrumentation
11. Environmental Shroud Instrumentation
12. Zero-g Thermodynamic Vent System Instrumentation.

Other related documents are as follows :

- MHTB Test Requirements Document (EP25 (93–25))
- MHTB Thermal Control Subsystem (TCS) Test Plan (EP25 (94–04))
- MHTB Preinstallation Operations Document (EP25 (94–13))
- MHTB Thermodynamic Vent System (TVS) Test Plan (EP25 (94–12))
- MHTB Thermodynamic Vent System Installation Procedure.

1. Program Overview and Hardware Description

Marshall Space Flight Center (MSFC) has established a technology/advanced development program to address the area of cryogenic fluid management (CFM) for orbital applications, an area common to practically all future space programs. As part of this activity, the MHTB was devised such that a variety of CFM subsystems could be integrated and evaluated in a ground-based test environment.

To minimize the reliance on scaling analyses in extrapolating overall performance data, the test bed is representative in both size and shape to that of a full-scale space transfer vehicle liquid hydrogen tank. Current plans include baseline testing of two key technology needs in representative spacecraft thermal and vacuum environments. The first involves evaluation of a foam multilayer insulation (FMLI) thermal control concept. This concept incorporates a spray-on foam insulation (SOFI) attached to the surface of the test bed tank and is in turn covered with a 45-layer variable density multilayer insulation (MLI) blanket. This blanket is constructed of double-aluminized Mylar (DAM) sheets separated by Dacron netting. The second, an active tank pressure control system, is referred to as a zero-g thermodynamic vent system (TVS). This hardware will be installed after completion of the thermal control subsytem (TCS) test phase and consists of a tank internal spray bar/heat exchanger and tank external recirculation pump, Joule Thompson valve, and back pressure orifice. More information regarding exact details of each test program can be found in the respective subsystem test plans.

The MHTB tank is constructed of aluminum 5083 and has a cylindrical shape with both a height and diameter of 3.05 m (10 ft) and elliptical domes as shown in figure 1.1. The tank has an internal volume of 18.09 m^3 (639 ft^3) with a surface area-to-volume ratio of 1.92 L/m (0.58 L/ft). The tank was designed and constructed per the ASME code (section VIII, division 1) for a working differential pressure of 344 kPa (50 psid). The tank's total weight is 1,270 kg (2,800 lbm). The tank is equipped with a variety of penetrations, supporting hardware, and technology subsystems illustrated in figure 1.1.

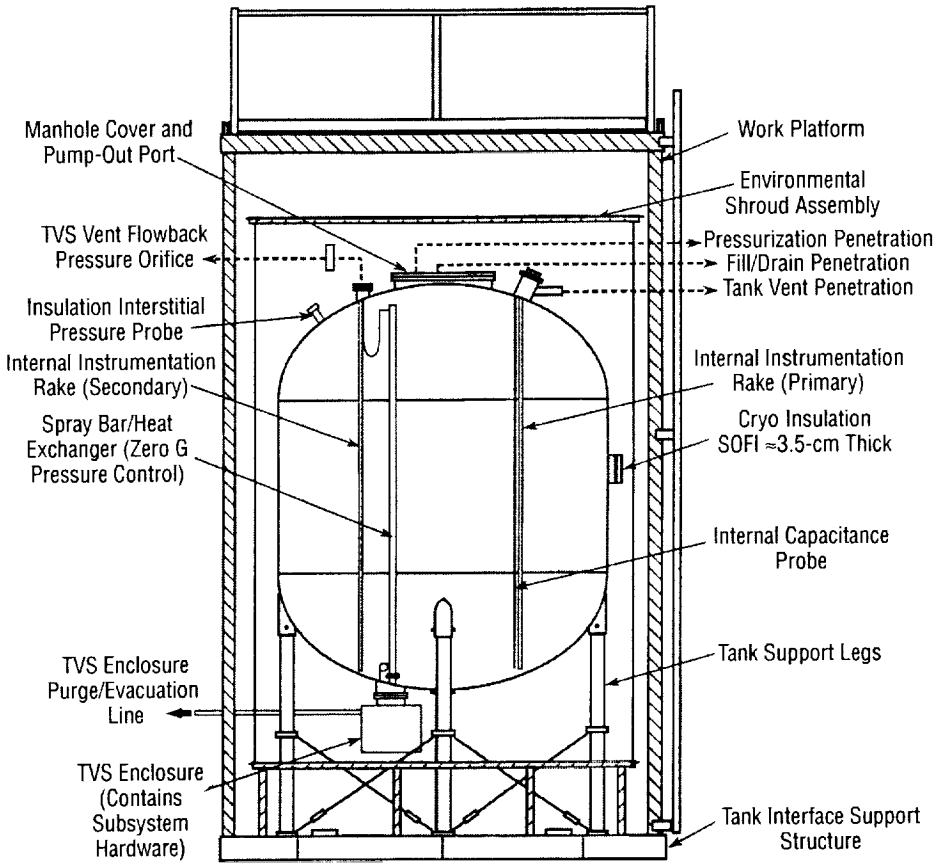

Figure 1.1 General MHTB tank schematic.

2. General Tank Instrumentation Layout

The general layout of instrumentation on the test bed is illustrated in figures 2.1 through 2.3. These figures represent the top, front, and bottom views of the test tank without insulation to avoid confusion. However, the seams between major MLI blanket assemblies are indicated by dotted lines. A detailed description of instrumentation numbers and profiles shown in these figures is discussed in later document sections. Most of the instrumentation is composed of silicon diodes and thermocouples for measurement of thermal gradients (several pressure transducers also are present). Typically, silicon diodes (Lakeshore type DT–470–11A) temperature transducers are placed in areas of lowest temperatures because of higher accuracy at low temperatures when compared to thermocouples. Typical low-temperature areas include the tank aluminum shell and SOFI material covering the tank. Thermocouples (type E) are used in regions of higher temperature, such as within the MLI or on surfaces somewhat distant from the test tank contact point, where accuracy becomes somewhat improved. The bulk of the instrumentation leads for components residing on the upper bulkhead and barrel section were routed toward the tank vent flange, while those on the lower bulkhead were routed out leg 1. There were some exceptions to this rule. Some of the penetration instrumentation was easier to route out along the respective penetration rather than snaking it to the vent or leg 1 area.

The tank orientation with respect to the vacuum chamber is such that the 0° reference is directed from the test tank center through the secondary instrumentation rake penetration toward the chamber door. Positive angle measurement from this reference is taken in a clockwise location from a vacuum chamber perspective looking down on top of the test article.

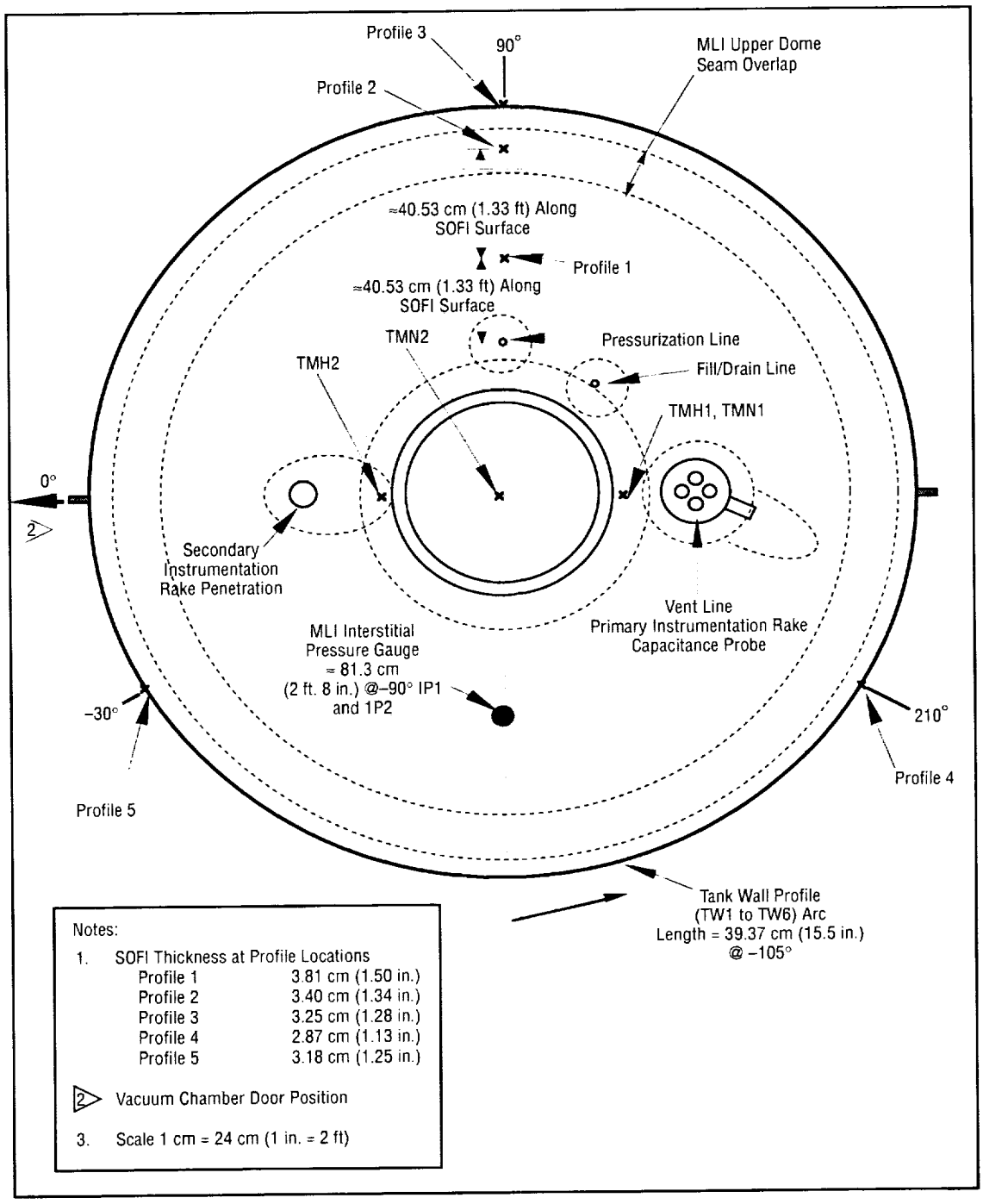

Figure 2.1 MHTB tank instrumentation—top view.

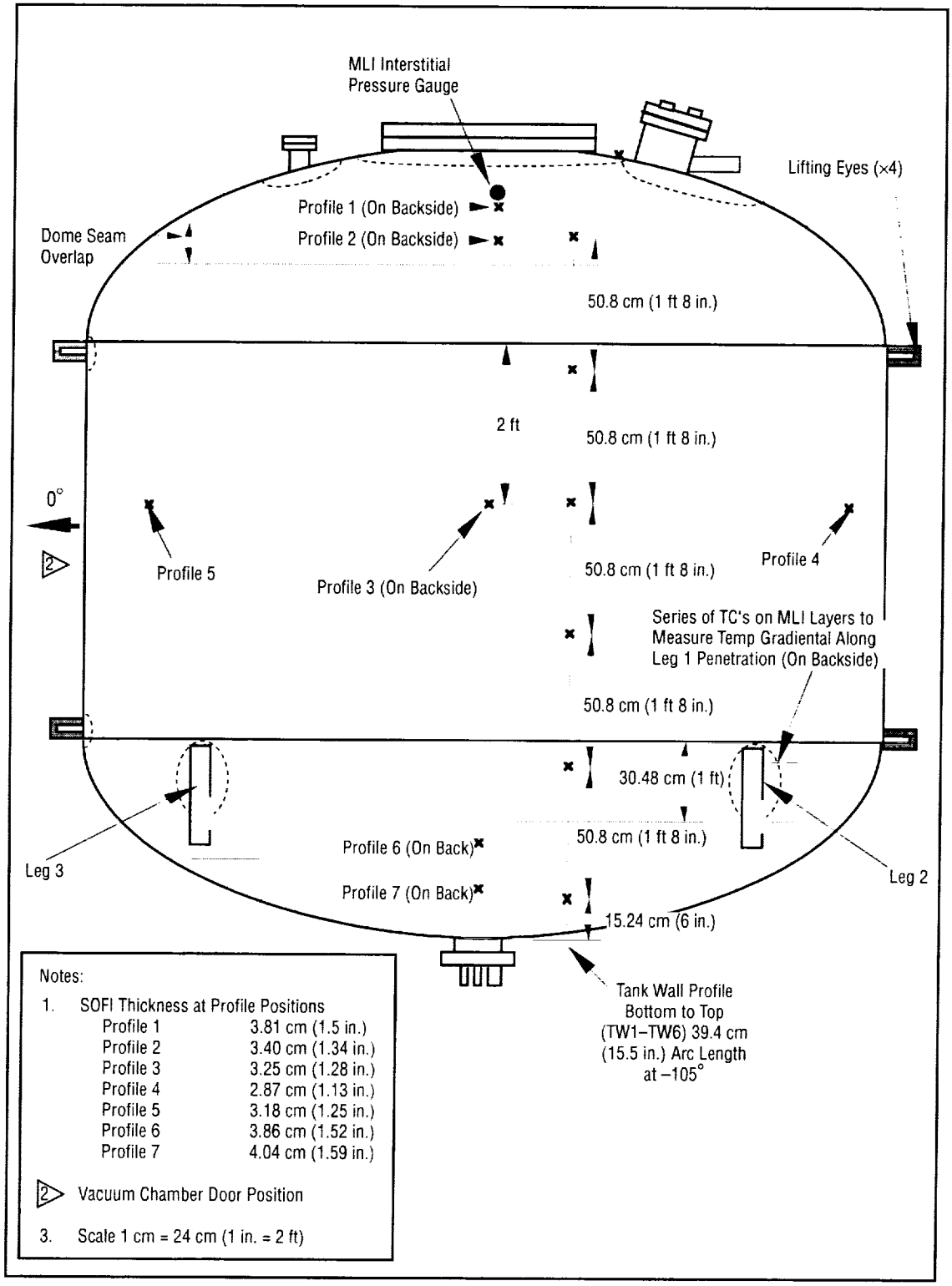

Figure 2.2 MHTB tank instrumentation—side view.

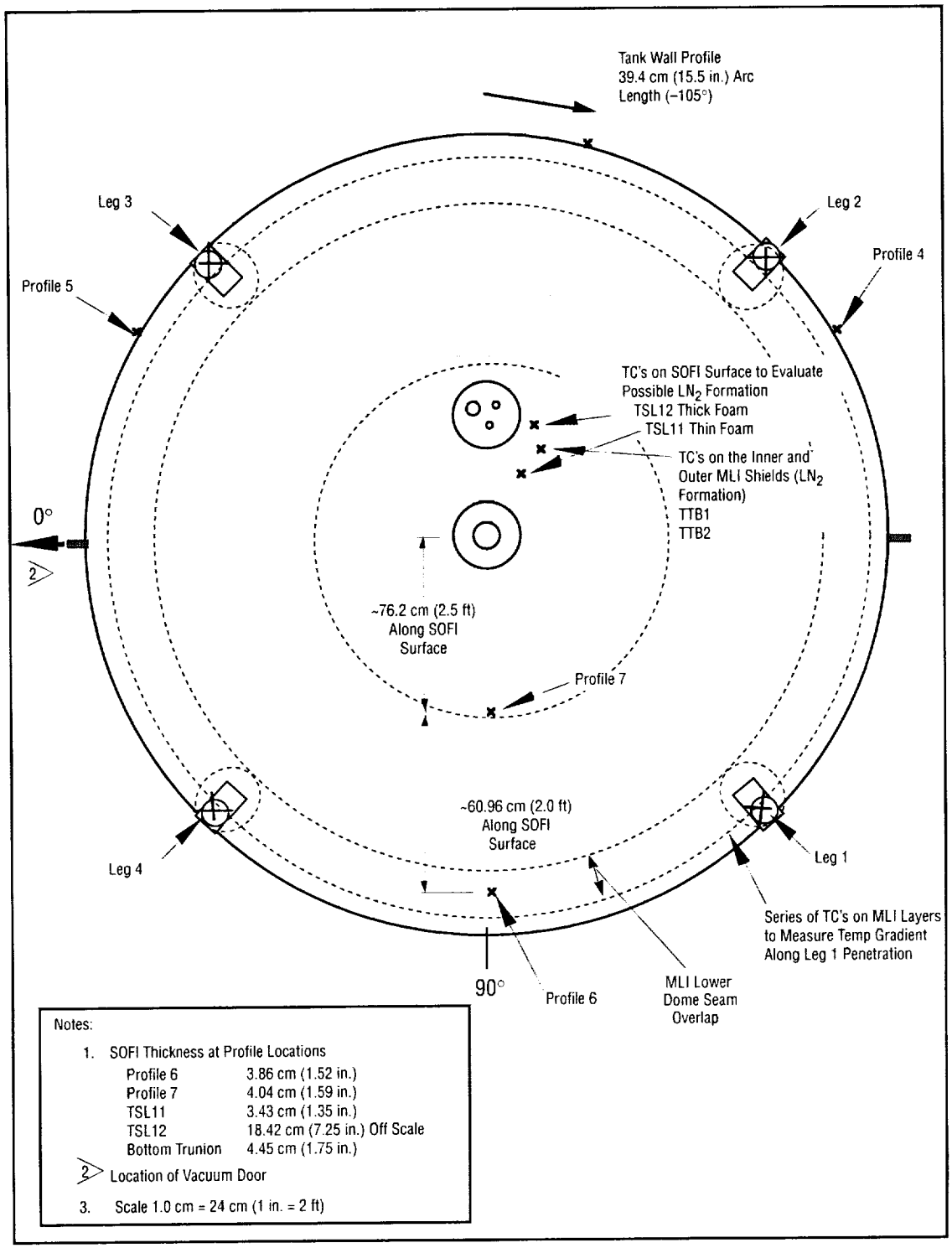

Figure 2.3 MHTB tank instrumentation—bottom view.

3. Thermal Control System Instrumentation

Seven instrumentation profiles are incorporated into the test tank FMLI insulation with each profile composed of one silicon diode and four thermocouples. Figure 3.1 illustrates the typical location of each sensor within the insulation layers. The diode TSF# was attached to the foam surface using a cryogenic epoxy (Lakeshore Stycast) while the thermocouples TM#, TMI#, TMM#, and TMO# were attached to the MLI shields by using a piece of aluminized tape. In an effort to limit heat leak along the thermocouple leads toward the bead attachment point, ≈5.08 cm (2 in.) of lead wire was spiraled around the bead and placed under the tape. Additionally, each thermocouple lead was routed out, toward the exit point, along the same MLI shield to which it was attached. The thermocouples TM# were attached to the outer surface of the innermost MLI shield. The thermocouples TMI# were attached to the outer surface of the 10 MLI shield (interface between low- and medium-density MLI spacing). The thermocouples TMM# were attached to the outer surface of the 25 MLI shield (interface between medium- and high-density MLI spacing). The thermocouples TMO# were attached to the outer surface of the outermost MLI shield (shield 45 of the high-density MLI spacing). The aluminized tape used to attach the thermocouples was manufactured by Lamart Corporation and was type 326L. This tape is electrically conductive on the exterior surface and has the same approximate surface emissivity as the DAM. The tape was purchased from

Can-Do Incorporated
P.O. Box 4366
Nashville, TN 37204
(615) 383–1775.

At each instrumentation profile position, the SOFI thickness was measured using a Kaman eddy current device. Figures 2.1 through 2.3 indicate the SOFI thickness measured at each profile location. These thicknesses were used in determining the thermal performance of the foam insulation.

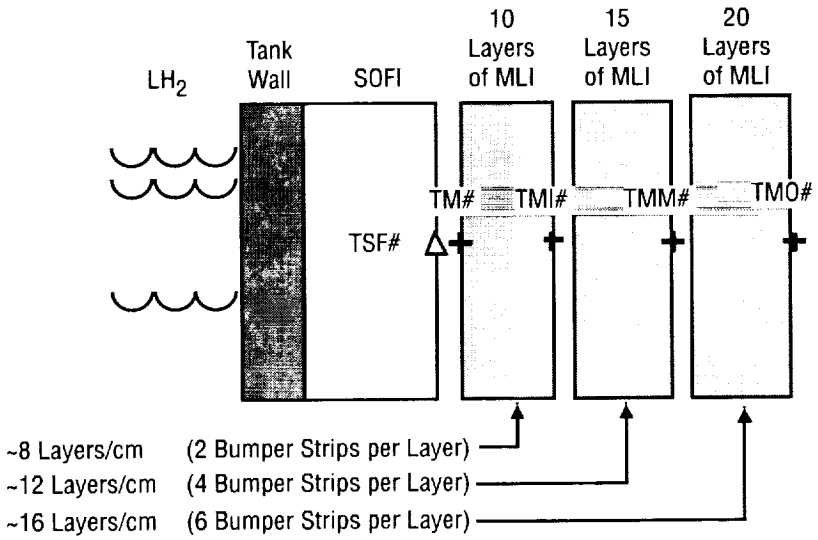

Profile 1	Positioned on tank upper bulkhead at 90° Location, 40.53 cm (1.33 ft) along tank surface away from the pressurization line (see fig. 2.1).	°Location 40.53 cm (1.33 ft) along tank
Profile 2	Positioned on tank upper bulkhead at 90° location, 81.1 cm (2.66 ft) along tank surface away from the pressurization line, located within the upper bulkhead seam (see fig. 2.1).	°Location 81.1 cm (2.66 ft) along tank
Profile 3	Positioned on tank barrel section at 90° location, 60.9 cm (2 ft) below the upper tangency line (see figs. 2.1 and 2.2).	°Location 60.9 cm (2 ft) below the tank
Profile 4	Positioned on tank barrel section at 210° location, 60.9 cm (2 ft) below the upper tangency line (see figs. 2.1 and 2.2).	°Location 60.9 cm (2 ft) below the tank
Profile 5	Positioned on tank barrel section at 330° location, 60.9 cm (2 ft) below the upper tangency line (see figs. 2.1 and 2.2).	°Location 60.9 cm (2 ft) below the tank
Profile 6	Positioned on lower bulkhead at 90° location, 137.2 cm (4.5 ft) away from tank center. Located within the lower bulkhead seam (see fig. 2.3).	°Location 137.2 cm (4.5 ft) away from tank
Profile 7	Positioned on lower bulkhead at 90° location, 76.2 cm (2.5 ft) away from tank center (see fig. 2.3).	°Location 76.2 cm (2.5 ft) away from tank

Δ Silicon Diode	SOFI Surface	TSF1 to TSF7
+ Thermocouple	MLI First Sheet	TM1 to TM7
+ Thermocouple	MLI 10th Sheet	TMI1 to TMI7
+ Thermocouple	MLI 25th Sheet	TMM1 to TMM7
+ Thermocouple	MLI 45th Sheet	TM01 to TM07

Figure 3.1 Typical insulation instrumentation profile.

4. Tank Support Leg Penetration Instrumentation

The MHTB is supported by four legs as shown in figures 2.2 and 2.3. Each leg is comprised of two composite sections joined in the center by a stainless steel union. Each leg end is also equipped with stainless steel end caps that mount to the test tank and interface support structure. Two of the four tank legs are instrumented, one of which (leg 1) is heavily instrumented, as shown in figure 4.1. Silicon diodes (TSL1 and TSL2) and thermocouples (TSL5–TSL10) are attached to the composite material (diodes closest to the tank) for determination of heat input along the support. Diodes TSL3 and TSL4 have been placed on leg 3. Each leg is equipped with a heat guard to reduce the amount of heat input. Legs 1 and 3 are instrumented with diodes (HG1 and HG3, respectively) to measure the heat guard boundary temperature. The SOFI surface (TSL17–TSL19) and MLI (TL13–TL19) are also instrumented for determination of the insulation temperature profile. There are also thermocouples (TSL14 on leg 1 and TSL15 on leg 3) attached to the innermost layer of crumpled MLI (against foam) that occupy the hollow interior of the legs. These measurements were used to determine if condensation of the insulation gaseous nitrogen purge gas occurs within the legs. A foam plug ≈10.16-cm (4-in.) thick was poured into the top section of each leg's interior, above the MLI, to prevent condensation. The outer surface of each leg was also closed out with pour foam, starting at the tank SOFI and extending out over the composite to a distance of ≈15.24 cm (6 in.). Average foam-thickness was based on the applied foam circumference measurements and determined to be 3.81 cm (1.5 in.) for legs 1, 3, and 4 and 4.445 cm (1.75 in.) for leg 2. The leg stainless steel center joint and interface support structure attachment point were instrumented with thermocouples for legs 1 (TLB1 and ISS1) and 3 (TLB3 and ISS3).

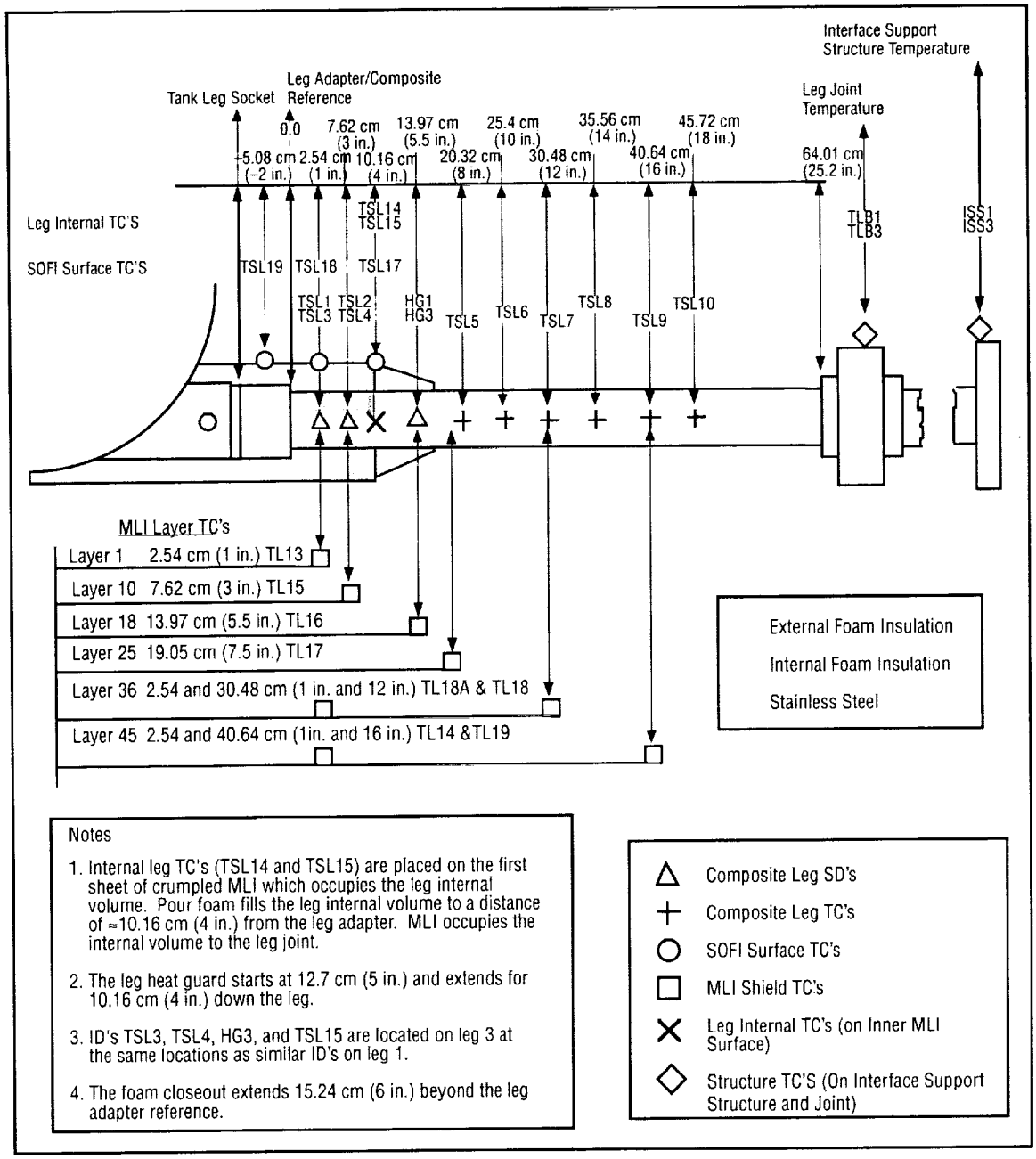

Figure 4.1 Leg 1 instrumentation locations.

5. Vent Penetration Instrumentation

The MHTB tank internal volume is vented through a 5.08-cm- (2-in.-) diameter tube connected to a 20.32-cm (8-in.) tank penetration (Conflat-type flange) as illustrated in figure 5.1. The vent tube transitions to a vacuum-jacketed pipe assembly ≈30.48 cm (12 in.) from the tank penetration. The penetration and tube are closed out with foam extending over the vacuum-jacketed pipe section ≈40.64 cm (16 in.) from the tank penetration. Average thickness of this foam based on the measured circumference is 6.98 cm (2.75 in.). Three silicon diodes are placed along the length of the tube for determination of heat input (TVL1 and TVL2) and evaluation of the heat guard (HG7) operation. The vent tube foam surface is instrumented with two thermocouples (TVL6 and TVL7) to assist in evaluation of heat input through the foam. The vent penetration top flange contains a tank ullage pressure measurement port and 1.27-cm- (0.5-in.-) diameter sampling tube that is equipped with two thermocouples (TUP1 and TUP2). The surface temperature of the top flange is measured by a silicon diode (TVL3). Internal to the tank, the vent flange supports a capacitance probe (CAP1) and an instrumentation rake. Two diodes (TVL4 and TVL5) are supported by the rake at the 99.4-percent tank fill location. These diodes are positioned just below the vent penetration (inside the test tank) and provide a measurement of the outflowing gas temperature. Details regarding the instrumentation rakes will be described in a later section.

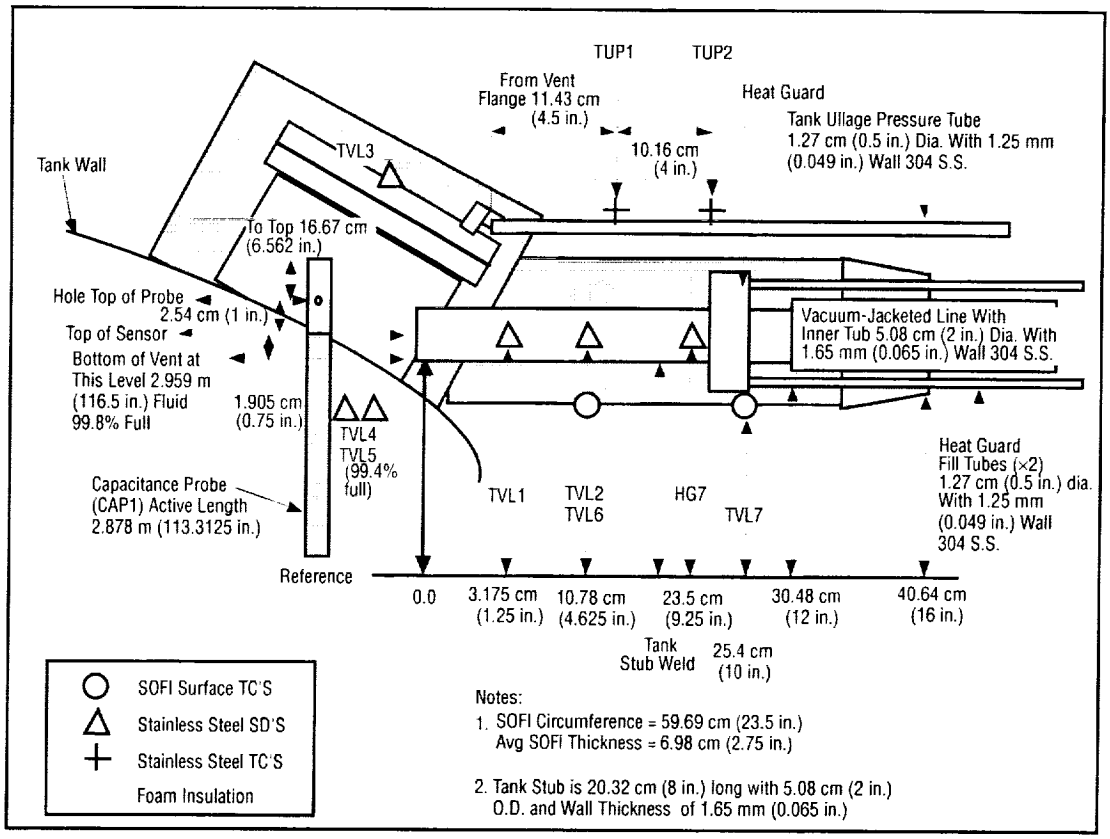

Figure 5.1 MHTB tank vent penetration instrumentation.

6. Fill/Drain Penetration Instrumentation

The MHTB LH_2 fluid service is provided through a 2.54-cm- (1-in.-) diameter fill/drain tube attached to the test tank with an aluminum to stainless steel transition joint as illustrated in figure 6.1. The fill/drain tube transitions to a vacuum-jacketed pipe assembly 16.51 cm (6.5 in.) from the tank penetration. A foam closeout is applied to the line and extends out over the vacuum-jacketed pipe section ≈35.56 cm (14 in.) from the tank penetration. The average foam thickness around the fill/drain line is 6.604 cm (2.6 in.) based on the measured circumference. The tube is instrumented with three silicon diodes placed along its length to determine heat input (TFD1 and TFD2) and operation of the heat guard (HG6). The outer surface of the foam is also instrumented with two thermocouples (TFD3 and TFD4) to assist in evaluation of heat input through the foam.

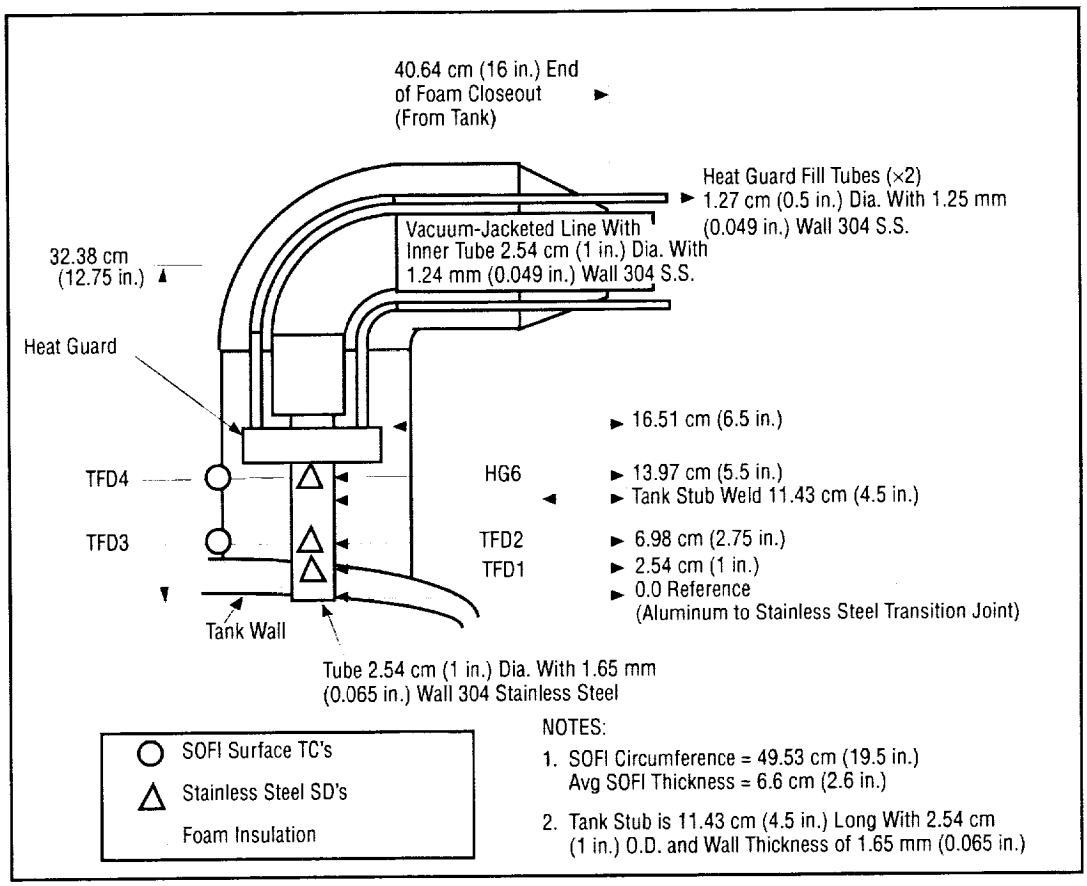

Figure 6.1 MHTB tank fill/drain penetration instrumentation.

7. Pressurization Penetration Instrumentation

The MHTB tank internal volume is pressurized using a 2.54-cm (1-in.) tube attached to the tank with an aluminum to stainless steel transition joint as illustrated in figure 7.1. The pressurization tube transitions to a double-walled jacketed pipe assembly (used for gas conditioning purposes) 32.385 cm (12.75 in.) from the tank wall. A foam closeout extends over the jacketed pipe section ≈40.64 cm (16 in.) from the tank penetration. The average foam thickness around the pressurization line is 3.556 cm (1.4 in.) based on the measured circumference. Three silicon diodes are placed along the length of the tube, between the tank and heat guard, for determination of heat input (TPL1 and TPL2) and evaluation of the heat guard (HG5) operation. The line is also equipped with two thermocouples: TPS1 used to measure the temperature of the pressurant gas flow within the line and TPS2 used to measure the pressurization line outer jacket temperature. The outer surface of the foam closeout is also instrumented with two thermocouples (TPL3 and TPL4) to assist in evaluation of heat input through the foam.

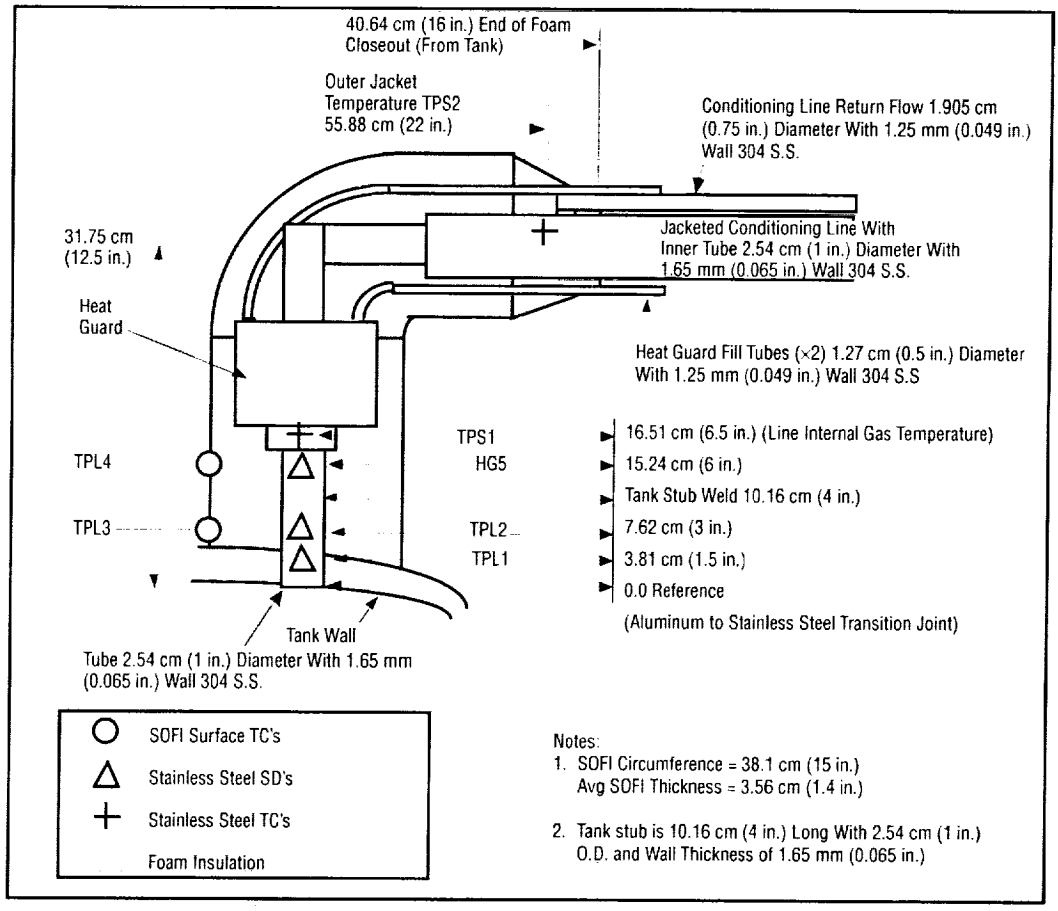

Figure 7.1 MHTB tank pressurization penetration instrumentation.

8. Multilayer Insulation Interstitial Pressure Probe Instrumentation

The gas pressure at the foam/MLI interface is measured with two pressure sensors mounted on top of a 5.08-cm- (2-in.-) diameter, thin wall probe that has a length of 22.86 cm (9 in.) as illustrated in figure 8.1. This probe rests on the tank SOFI surface and is supported by the MLI, which is taped out layer by layer to the surrounding MLI and to the probe body to prevent leakage of trapped MLI gases. The probe is also equipped with a 6.35-mm- (0.25-in.-) diameter sampling port for obtaining both dew point levels (using a hydrometer) and gas species samples (using a residual gas analyzer) from within the MLI. The two pressure transducers, a Gran Philips 275 (IP1) and a cold cathode (IP2), cover a complete pressure range from 760 to 10^{-7} torr. The Gran Philips gauge is remote mounted (for easier access) on top of the heater shroud and connected to the probe body using a flex hose. The probe body tube is equipped with three thermocouples placed along its length (IPP1, IPP2, and IPP3) to determine heat input through the probe. This probe, if necessary, shall be supported off the tank heater shroud structure using stainless steel wire and springs to absorb transportation loads. The dew point measurement within the MLI is taken with a facility-supplied Endress Hauser model 2200 hydrometer (DEW1). The sensing head for this unit is located in the MLI gas sample tube.

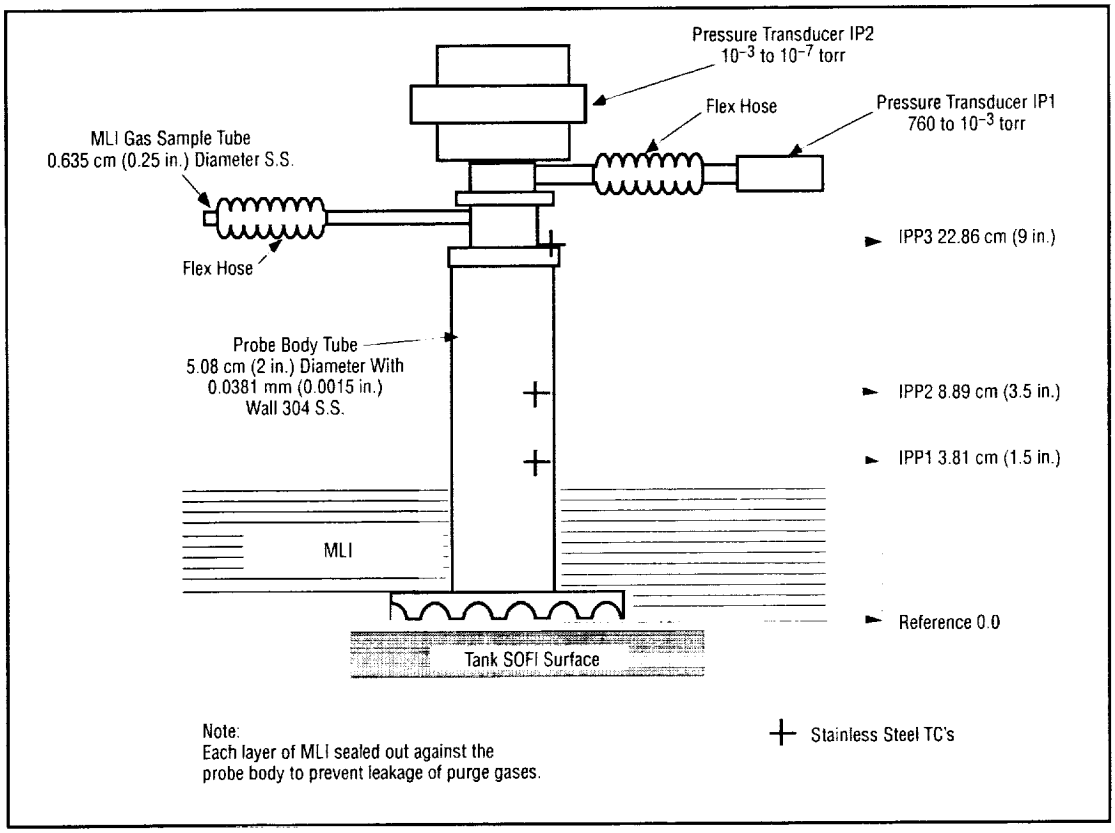

Figure 8.1 MHTB MLI probe instrumentation.

9. Manhole Cover and Pump-Out Penetration Instrumentation

The MHTB tank is equipped with two manhole covers (inner and outer) to control potential leakage which could degrade MLI performance. Figure 9.1 illustrates the manhole cover setup. The inner cover is equipped with two silicon diodes (TMN3 and TMN4) adhesively bonded to its inner surface with cryogenic epoxy (Lakeshore Stycast). The outer manhole cover exterior surface is equipped with a silicon diode (TMN2) bonded to its center with a single diode (TMN1) and two thermocouples (TMH1 and TMH2) bonded to its flange area. These temperature measurements will be used to assess the total thermal capacitance of the massive tank manhole system. The gas volume trapped between the inner and outer manhole covers is connected to a stainless steel evacuation line (flex hose) that is used to intercept potential leakage from the inner cover. This flex line is equipped with two thermocouples (TCP1 and TCP2) to determine heat input. The spatial distance between the thermocouples is 5.08 cm (2 in.); however, the flex hose has a 3 to 1 contraction ratio yielding a material length of 15.24 cm (6 in.). The entire surface of the outer manhole cover is covered with foam insulation at an approximate thickness of 3.175 cm (1.25 in.). The evacuation line is routed along the vent line and as such, is buried beneath the vent line foam insulation.

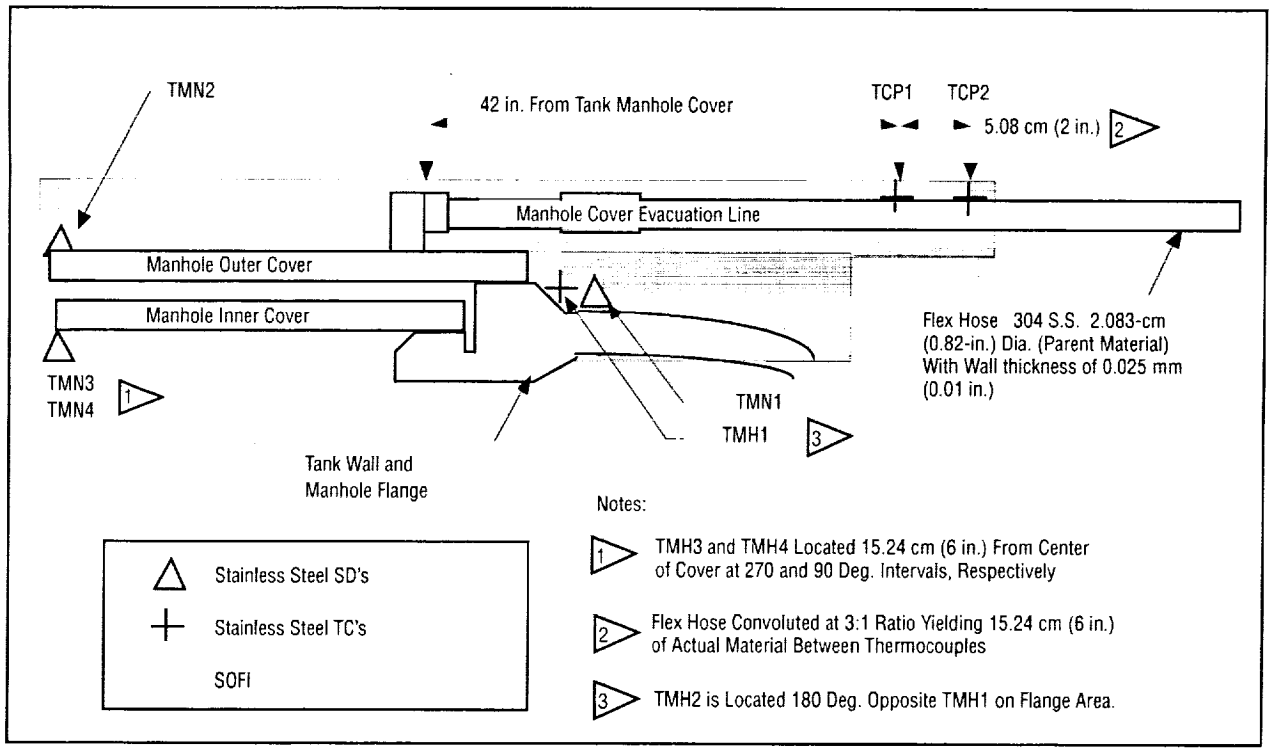

Figure 9.1 MHTB manhole cover and pump-out port instrumentation.

10. Internal Rake and Fluid Instrumentation

The MHTB tank is equipped internally with two instrumentation rakes and a capacitance probe which are supported from the top of the tank and extend downward. The rakes are constructed from a fiberglass epoxy channel section and are equipped with silicon diodes attached at given intervals using nylon rod offsets and cryogenic epoxy as illustrated in figure 10.1. The purpose of the rakes is to provide measurement of the temperature gradient within both the tank ullage and liquid masses in addition to providing a rough check of the liquid level to verify the capacitance probe operation. The primary rake (TD1–TD12) positioned at 180 deg is connected to the vent flange, while the secondary rake (TD13–TD24) is positioned at zero deg as illustrated in figures 2.1 and 10.2. The capacitance probe (CAP1) provides continuous liquid level measurement and is mounted to the vent flange at the 180-deg position beside the primary rake. All tank internal instrumentation is passed through the 20.32-cm (8-in.) vent flange using four 37-pin Deutsche connectors. The exception is the capacitance probe, which is equipped with its own coaxial feedthrough mounted in a 1.27-cm (0.5-in.) Conflat-type connector and attached to the center of the 20.32-cm (8-in.) vent flange. Appendix A contains an MHTB tanking table with information regarding fill height, percent liquid/ullage volume, and LH_2 mass.

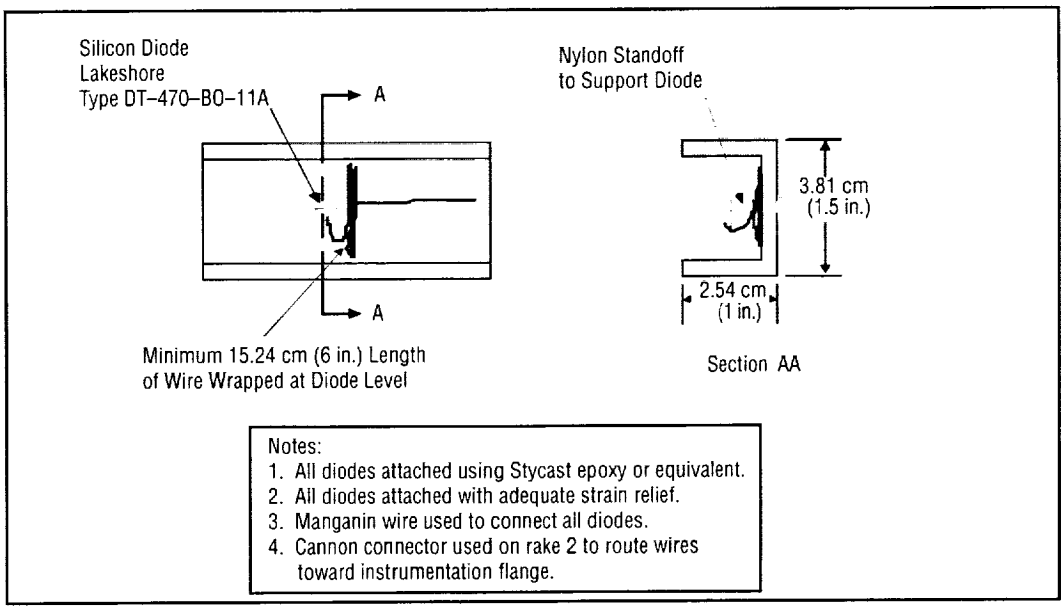

Figure 10.1 MHTB instrumentation rake silicon diode attachment.

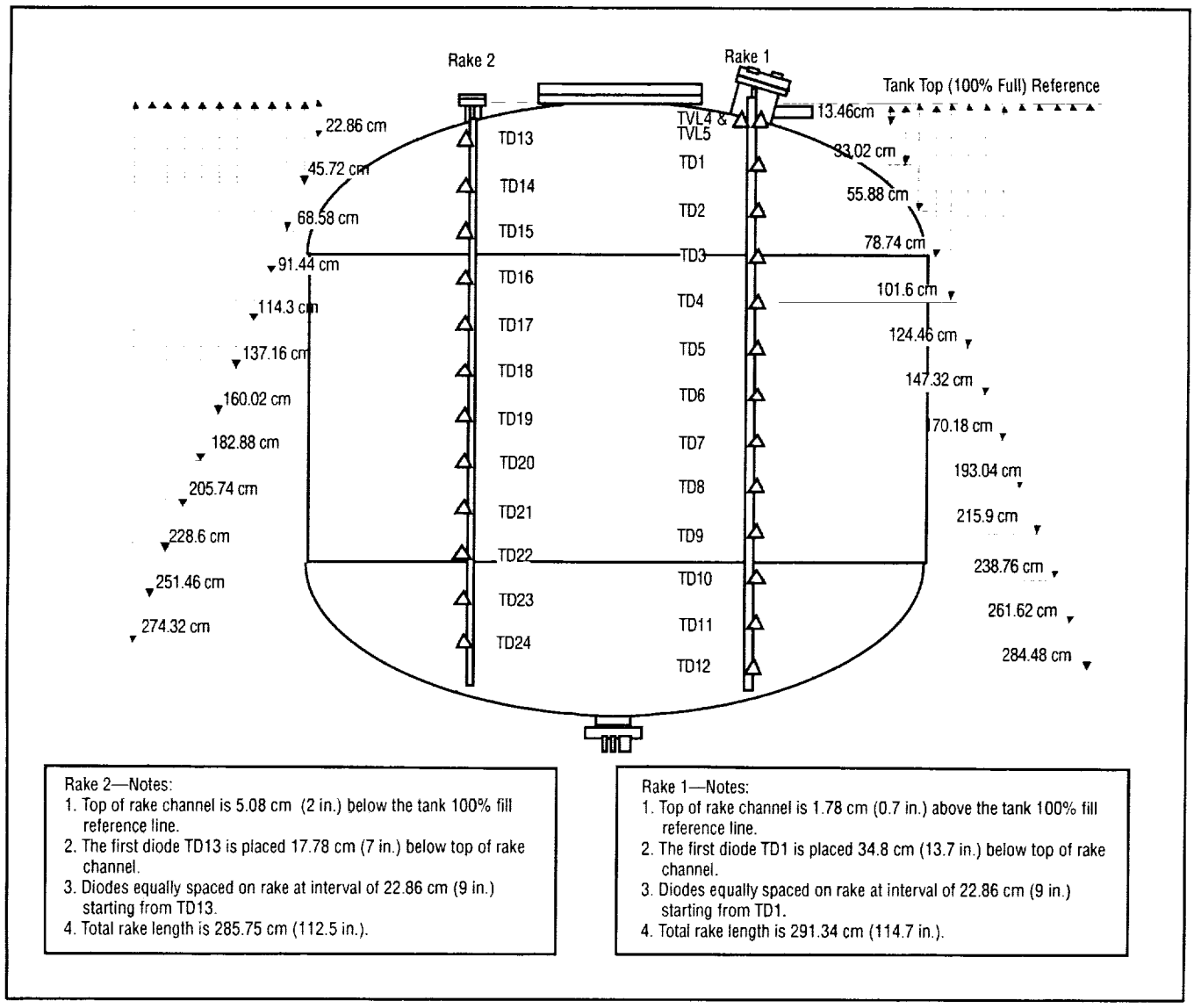

Figure 10.2 MHTB tank rake instrumentation layout.

11. Environmental Shroud Instrumentation

The MHTB tank and insulation systems are completely surrounded by a shroud structure, which provides a warm boundary condition for which performance can be measured during testing. This structure is made completely of aluminum and is supported by the interface support structure as shown in figure 1.1. The shroud is composed of 17 individual panels each equipped with thermocouples attached to the inner surface of the shroud and placed beneath the electrical heating strip. These thermocouples are used with a closed-loop control system to regulate each shroud panel's temperature. A minimum of two thermocouples is applied to each panel providing a primary and a backup in case of failure. Two panels, 5 and 11, are equipped with additional thermocouples to provide data concerning shroud temperature gradients. Panel 11 has six thermocouples while panel 5 is heavily instrumented with 13 thermocouples, since it was used during evaluation of the techniques used to assemble the shroud panels (documented in EP25 (94–03)). The top shroud panels 1–4 are illustrated in figure 11.1. The typical side wall panel (5–12) instrumentation layout is provided in figure 11.2.
The lower shroud panel layout (13–17) is illustrated in figure 11.3.

A series of five thermocouples is also placed within the annular region created between the vertical shroud panel 6 and the test tank insulation at the 90-deg location. These thermocouples (HS18–HS22) are spaced vertically along the panel at an interval of 60.96 cm (24 in.) with the thermocouple bead positioned approximately halfway into the annular region. This instrumentation is used for measuring purge gas temperatures within the annulus. Vacuum chamber, free-air space temperatures are measured with facility-provided thermocouples (CFA1, CFA2, and CFA3) mounted vertically at the 90-deg location and external to the test article shroud. These thermocouples are placed at 1.525-m (5-ft) intervals above the chamber floor. Purge gas dew point within the environmental shroud is measured with a facility-supplied Endress Hauser model 2200 hydrometer (DEW2). The sensing head for this unit is located internal to the shroud and mounted on the lower shroud panel.

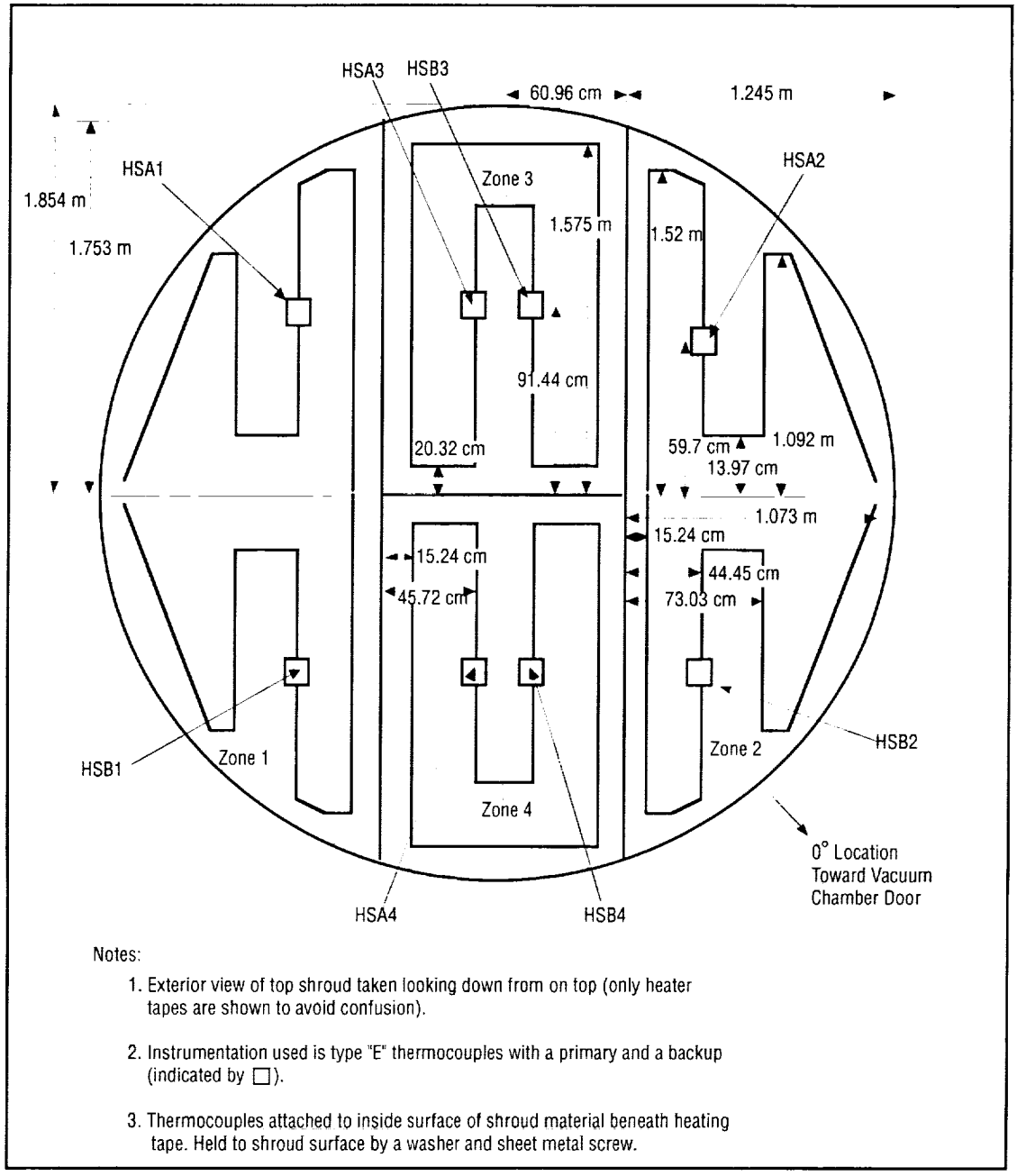

Notes:

1. Exterior view of top shroud taken looking down from on top (only heater tapes are shown to avoid confusion).
2. Instrumentation used is type "E" thermocouples with a primary and a backup (indicated by □).
3. Thermocouples attached to inside surface of shroud material beneath heating tape. Held to shroud surface by a washer and sheet metal screw.

Figure 11.1 MHTB typical top environmental shroud panels.

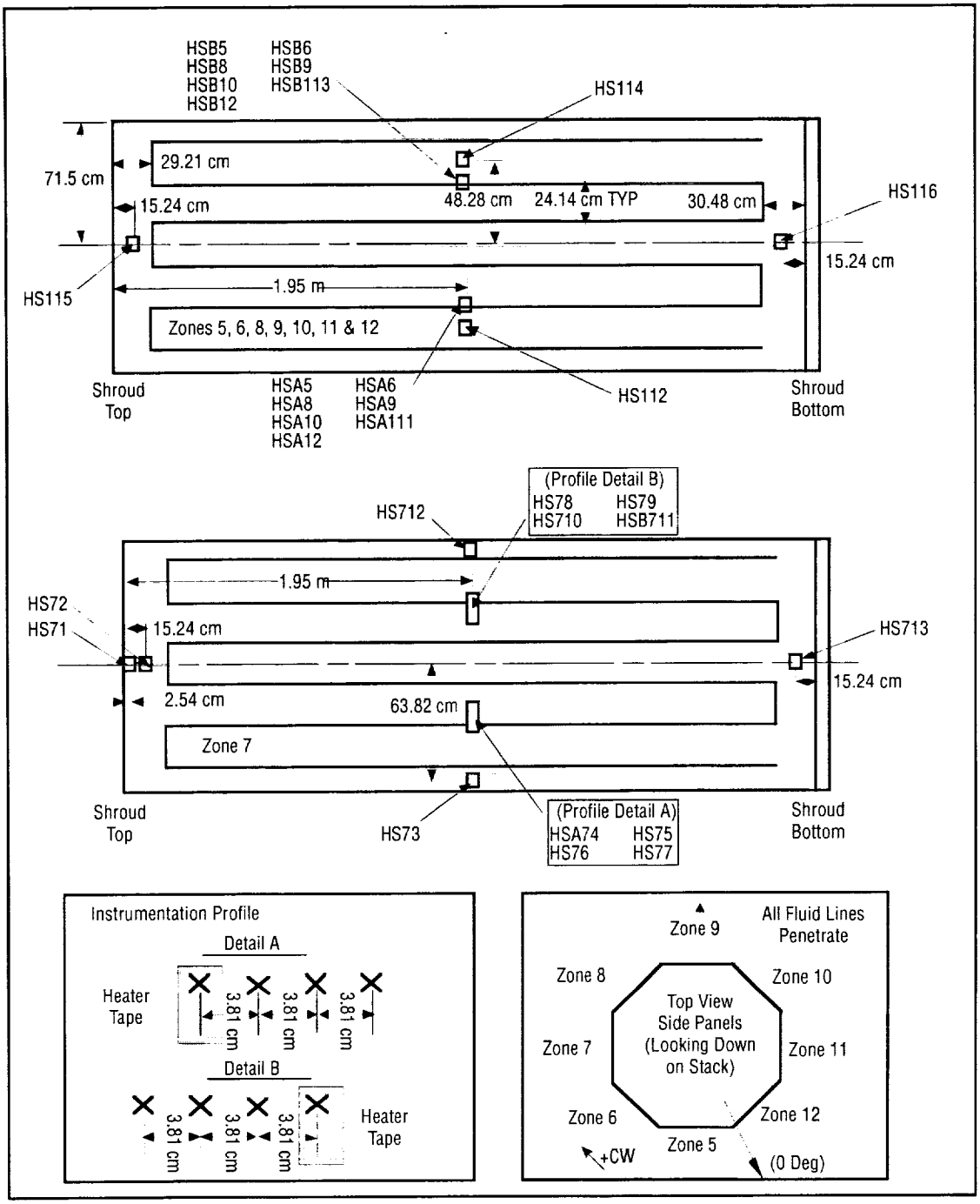

Figure 11.2 MHTB typical side wall environmental shroud panels.

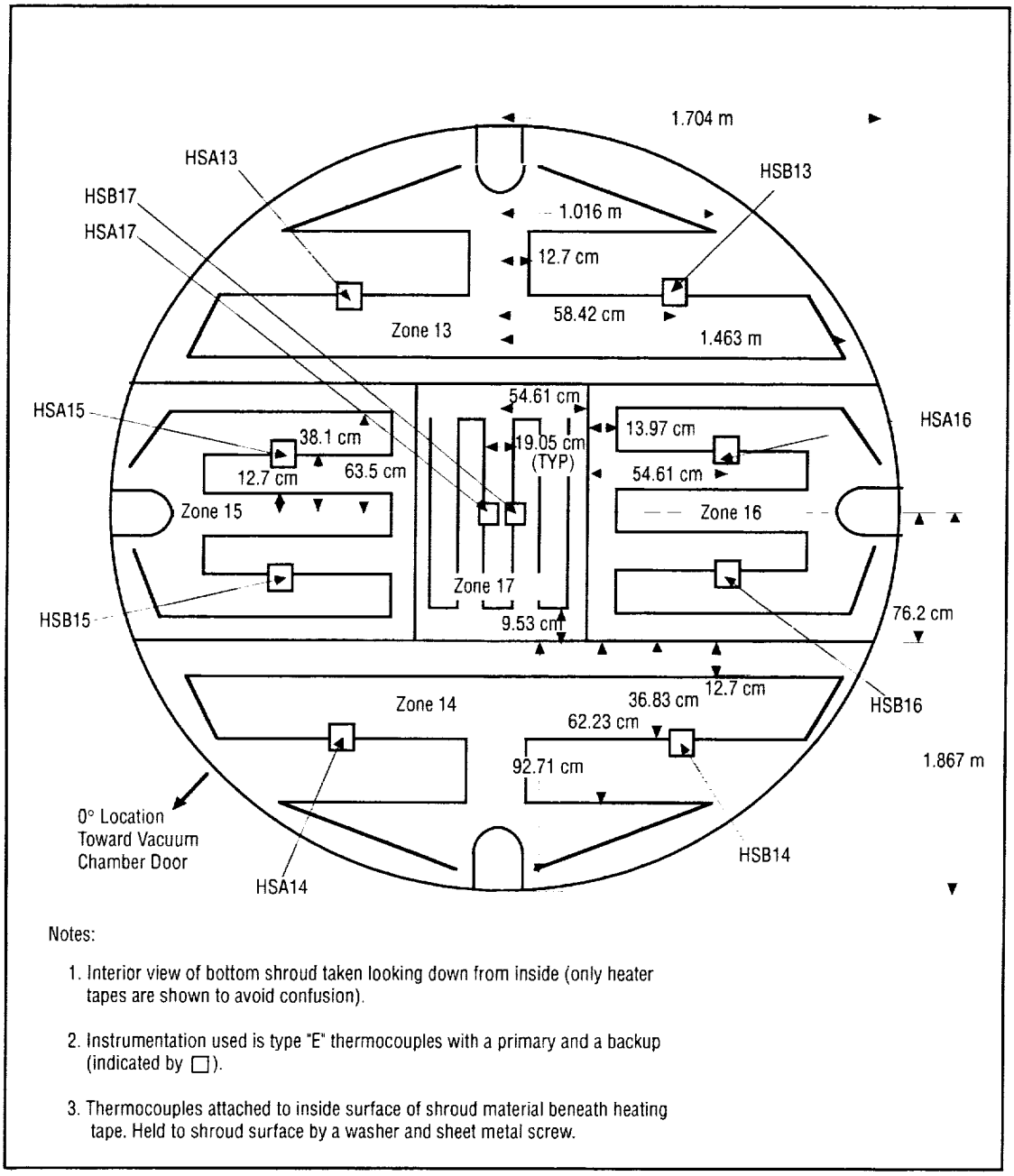

Notes:

1. Interior view of bottom shroud taken looking down from inside (only heater tapes are shown to avoid confusion).
2. Instrumentation used is type "E" thermocouples with a primary and a backup (indicated by □).
3. Thermocouples attached to inside surface of shroud material beneath heating tape. Held to shroud surface by a washer and sheet metal screw.

Figure 11.3 MHTB typical lower environmental shroud panels.

12. Zero-g Thermodynamic Vent System Instrumentation

The second MHTB test phase will require that hardware related to the zero-g TVS be installed both internal and external to the MHTB test tank. Figure 1.1 illustrates the general hardware placement on the test tank while instrumentation placement on the hardware is outlined in figure 12.1. Attached to the lower MHTB tank bulkhead flange (external to the tank) is the vacuum-tight TVS enclosure, which contains the system control valving and recirculation pump. Instrumentation within the enclosure consists of thermocouples (T411, T412, T415, T416, and T417) pressure transducers (P402, DP400, P403, P404, and P405) and a flow meter (F401). Internal to the test tank is the heat exchanger/spray bar and a backpressure orifice. The spray bar is equipped with two silicon diodes (T413 and T414) and the orifice is instrumented with two diodes (T418 and T419) and two pressure transducers (P406 and P407). External to the MHTB tank, but still within the vacuum chamber, are temperature (diode T420) and pressure (P408) measurements on the TVS vent line to quantify the properties of the exiting gas flow. Instrumentation internal to the MHTB test tank will be routed through the 20.32-cm (8-in.) vent flange with the other internal instrumentation. The instrumentation within the TVS enclosure shall be routed through two Deutsche feedthroughs and two thermocouple pullthroughs. All thermocouples utilize an infinity meter for signal conditioning. The TVS enclosure shall be equipped externally with three thermocouples (T421, T422, and T423) mounted on the top, bottom, and side of the enclosure, respectively. The enclosure internal pressure will be measured by two pressure transducers (P409 and P410).

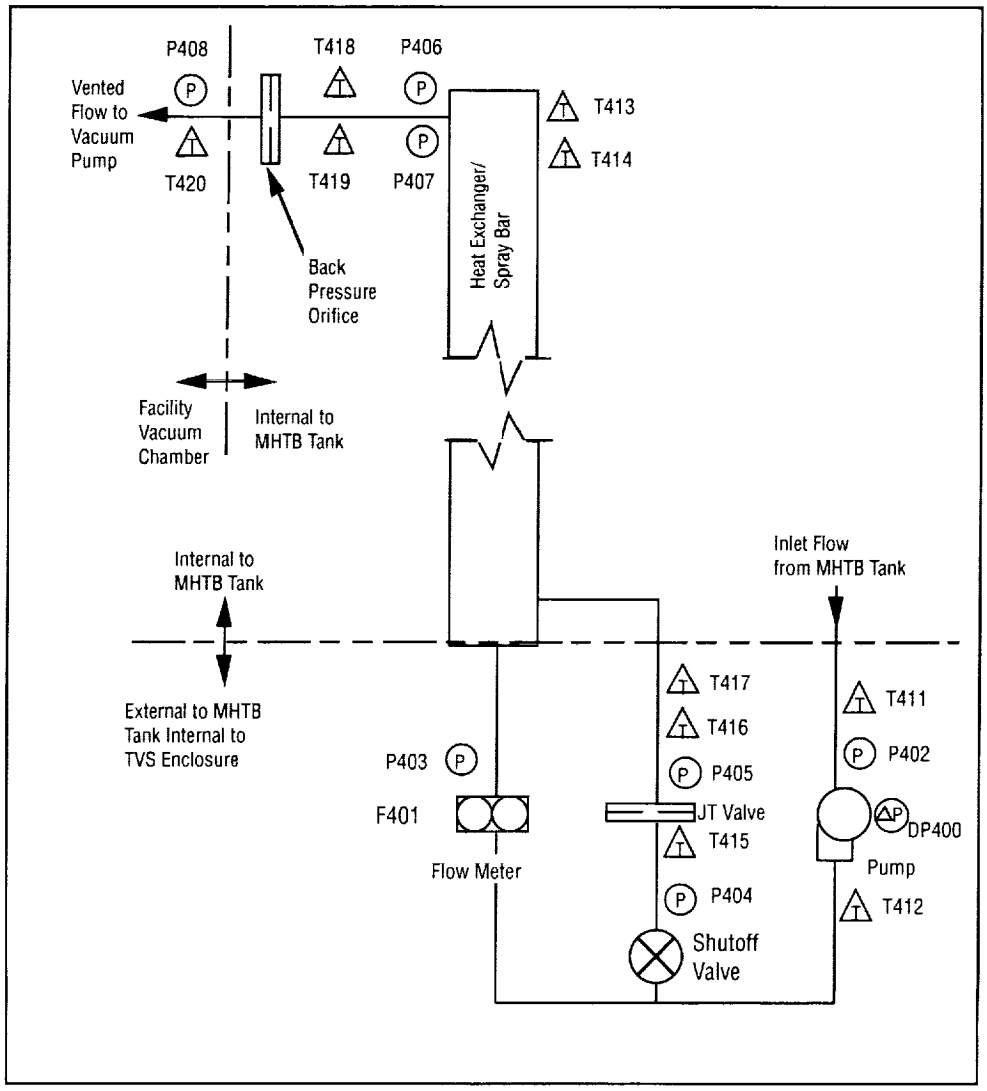

Figure 12.1 MHTB TVS instrumentation layout.

APPENDIX C—MEASURED INSULATION TEMPERATURE PROFILES

The steady-state ground hold temperatures averaged for all testing (program average) are presented in table C.1 for the SOFI exterior surface and MLI layers. High and low values for each position or layer are also presented. Table C.2 presents the insulation ground hold temperatures averaged for each test series. Ground hold temperatures for test P9502 were very close to the program averages. Test P9601 temperatures were slightly lower than the program averages, whereas test P9602B temperatures were slightly higher.

Similarly, the steady-state program and test averages for the orbit hold insulation temperatures, without heat guards, are tabulated in tables C.3 and C.4, respectively, for each of the three warm boundary conditions tested (164, 235, and 305 K). The test average variations from test to test were small, with the maximum variations occurring on sheet 1 (adjacent to SOFI). The test average deviations from the program averages were generally less than 3 K with the 305 K boundary. The P9601 inside surface temperatures (sheet 1) did tend to be colder.

Table C.1 MHTB program TCS average SOFI/MLI ground hold temperatures.

SOFI Temperature (K)		MLI Temperature (K)			
		Sheet 1	Sheet 10	Sheet 25	Sheet 45
Average	173	179	198	227	266
High Value	225	232	252	268	274
Low Value	119	118	131	215	257

Table C.2 Test average SOFI/MLI ground hold temperatures.

Test No.	SOFI Temperature (K)	MLI Temperature (K)			
		Sheet 1	Sheet 10	Sheet 25	Sheet 45
P9502	174	181	201	230	271
P9601	166	172	192	221	260
P9602B	180	185	202	230	267

Table C.3 MHTB program TCS average SOFI/MLI orbit hold temperatures (no heat guards).

		SOFI Temperature (K)	MLI Temperature (K)			
			Sheet 1	Sheet 10	Sheet 25	Sheet 45
305	Average	30	75	174	238	288
	High Value	46	102	188	251	291
	Low Value	23	50	150	223	284
235	Average	29	56	121	180	224
	High Value	42	63	134	187	226
	Low Value	23	49	108	174	221
164	Average	24	43	82	122	156
	High Value	44	54	94	128	157
	Low Value	21	28	71	111	155

Table C.4 Test average SOFI/MLI orbit hold temperatures (without heat guards).

Test No.	Hot Boundary Temperature (K)	SOFI Temperature (K)	MLI Temperature (K)			
			Sheet 1	Sheet 10	Sheet 25	Sheet 45
P9502	305	27	77	176	238	289
	164	26	40	85	124	156
P9601	305	29	70	173	236	287
	305	29	74	173	237	289
	164	23	38	80	120	156
P9602B	235	29	57	125	181	225
	305	34	78	173	241	290

Insulation temperature profiles for each of seven profile positions, are graphically presented for each warm boundary condition in figures C.1 through C.3.

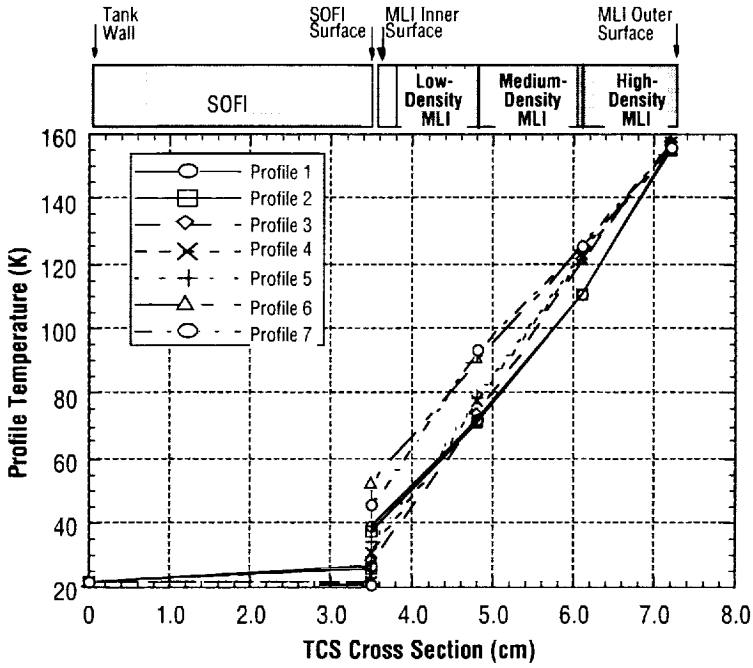

Figure C.1 Test P9601 orbit hold TCS temperature profiles with hot boundary at 164 K.

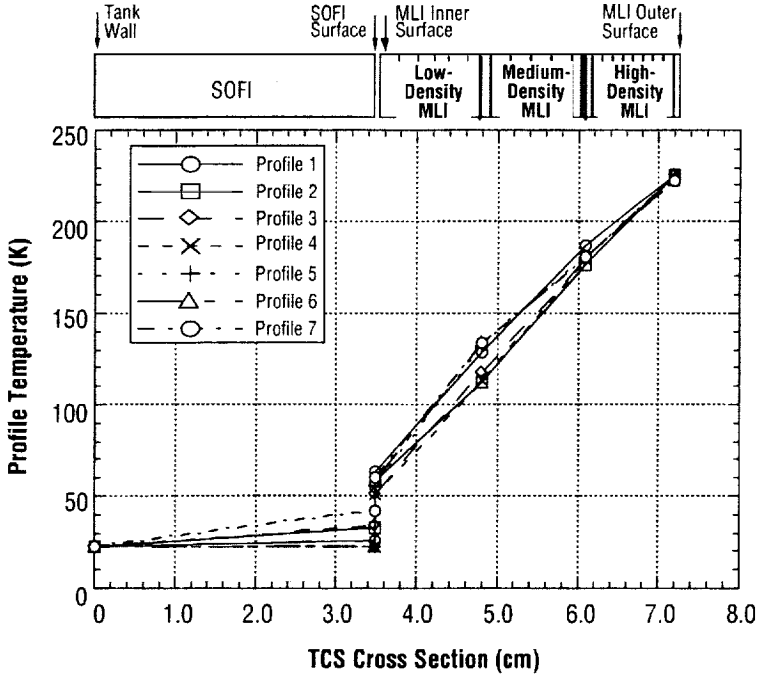

Figure C.2 Test average SOFI/MLI ground hold temperatures with hot boundary at 235 K.

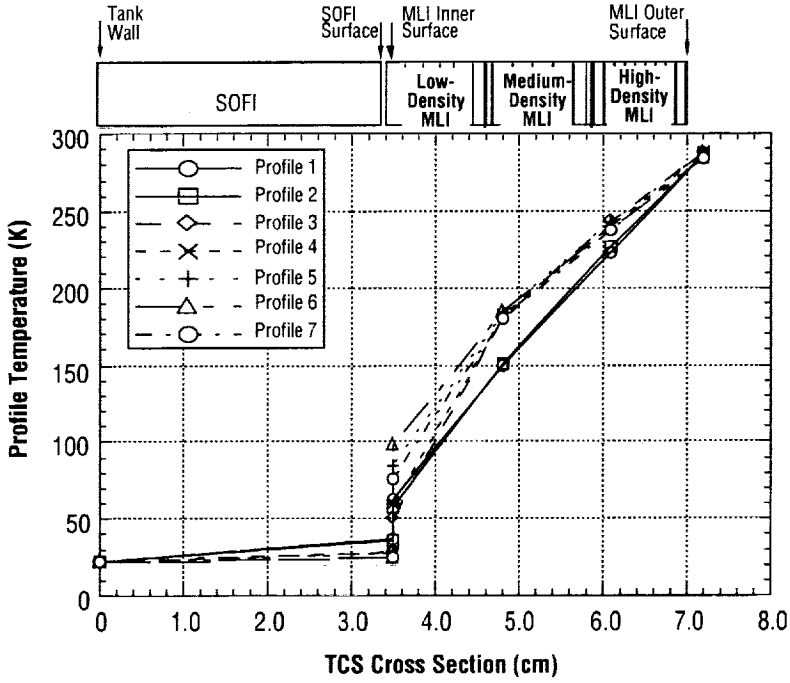

Figure C.3 Test P9601 orbit hold TCS temperature profiles with hot boundary at 305 K.

REFERENCES

1. Fox, E.C.; et al.: Multipurpose Hydrogen Test Bed—System Definition and Insulated Tank Development, Final Report, Martin Marietta Astronautics, NAS8–39201, July 1993.

2. Ozisik, M.N: Heat Transfer—A Basic Approach, McGraw-Hill Book Company, New York, NY, 1985.

3. Cillimore, B.A.; et al.: Systems Improved Numerical Differencing Analyzer and Fluid Integrator, Version 2.2, MCR 86–594, Martin Marietta, NAS9–17448, 1988.

4. Keller, C.W.; et al.: Thermal Performance of Multilayer Insulations, Final Report, Lockheed Missiles and Space Co., NAS3–14377, 1974.

5. Fredrickson, G.O.: Investigation of High-Performance Insulation Application Problems, Final Report, McDonnell Douglas Astronautics Company—West, NAS8–21400, MDC G4722, August 1973.

6. Kramer, E.W.; et al.: "Evaluation of Propellant Tank Insulation Concepts for Low-Thrust Chemical Propulsion Systems, Final Report," Boeing Aerospace Company, NAS8–2284, *NASA CR–168320*, March 1984.

REPORT DOCUMENTATION PAGE

Form Approved
OMB No. 0704-0188

1. AGENCY USE ONLY *(Leave Blank)*	2. REPORT DATE	3. REPORT TYPE AND DATES COVERED
	June 2001	Technical Memorandum

4. TITLE AND SUBTITLE

Large-Scale Liquid Hydrogen Testing of Variable Density Multilayer Insulation With a Foam Substrate

5. FUNDING NUMBERS

6. AUTHORS

J.J Martin and L. Hastings

7. PERFORMING ORGANIZATION NAMES(S) AND ADDRESS(ES)

George C. Marshall Space Flight Center
Marshall Space Flight Center, AL 35812

8. PERFORMING ORGANIZATION REPORT NUMBER

M–1020

9. SPONSORING/MONITORING AGENCY NAME(S) AND ADDRESS(ES)

National Aeronautics and Space Administration
Washington, DC 20546–0001

10. SPONSORING/MONITORING AGENCY REPORT NUMBER

NASA/TM—2001–211089

11. SUPPLEMENTARY NOTES

Prepared by Vehicle and Systems Development Department, Space Transportation Directorate

12a. DISTRIBUTION/AVAILABILITY STATEMENT

Unclassified–Unlimited
Subject Category 24
Nonstandard Distribution

12b. DISTRIBUTION CODE

13. ABSTRACT *(Maximum 200 words)*

The multipurpose hydrogen test bed (MHTB), with an 18-m^3 liquid hydrogen tank, was used to evaluate a combination foam/multilayer combination insulation (MLI) concept. The foam element (Isofoam SS–1171) insulates during ground hold/ascent flight, and allowed a dry nitrogen purge as opposed to the more complex/heavy helium purge subsystem normally required. The 45-layer MLI was designed for an on-orbit storage period of 45 days. Unique MLI features include a variable layer density, larger but fewer double-aluminized Mylar perforations for ascent to orbit venting, and a commercially established roll-wrap installation process that reduced assembly man-hours and resulted in a roust, virtually seamless MLI. Insulation performance was measured during three test series. The spray-on foam insulation (SOFI) successfully prevented purge gas liquefaction within the MLI and resulted in the expected ground hold heat leak of 63 W/m^2. The orbit hold tests resulted in heat leaks of 0.085 and 0.22 W/m^2 with warm boundary temperatures of 164 and 305 K, respectively. Compared to the best previously measured performance with a traditional MLI system, a 41-percent heat leak reduction with 25 fewer MLI layers was achieved. The MHTB MLI heat leak is half that calculated for a constant layer density MLI.

14. SUBJECT TERMS

orbital cryogenic fluid management, cryogenic storage, cryogenic insulation, multilayer insulation

15. NUMBER OF PAGES

88

16. PRICE CODE

17. SECURITY CLASSIFICATION OF REPORT	18. SECURITY CLASSIFICATION OF THIS PAGE	19. SECURITY CLASSIFICATION OF ABSTRACT	20. LIMITATION OF ABSTRACT
Unclassified	Unclassified	Unclassified	Unlimited

NSN 7540-01-280-5500

Standard Form 298 (Rev. 2-89)
Prescribed by ANSI Std. 239-18
298-102